LU TP 16-10
June 2016

Strongly First Order Phase Transitions and The Possibility of Electroweak Baryogenesis in General Two-Higgs-Doublet Models

Nils Hermansson Truedsson

Department of Astronomy and Theoretical Physics, Lund University

Master Thesis Supervised by Johan Rathsman

LUND
UNIVERSITY

Abstract

The possibility to have a strongly first order electroweak phase transition, which is one of the Sakharov conditions for electroweak baryogenesis together with $\mathcal{CP}$ violation and baryon number violation, in general Two-Higgs-Doublet Models (2HDMs) is here investigated. Different kinds of $\mathbb{Z}_2$ breaking beyond standard assumptions are studied, in particular by allowing it to be completely broken as well as by assuming it to be only approximately preserved in the Yukawa sector. Throughout the study a 1-loop thermally corrected effective potential is used.

Parameter space scans are performed for several kinds of 2HDMs and experimental constraints from Higgs physics, flavour physics, electroweak physics and searches for electric dipole moments of the electron, neutron, mercury and radium are imposed. Also theoretical constraints are taken into account, in particular tree level unitarity, perturbativity and positivity as well as demanding that the tree level minimum of the potential is global. As a starting point $\mathcal{CP}$ conserving models are considered, but after that also $\mathcal{CP}$ violating models (which are relevant for electroweak baryogenesis) are investigated.

It is found that a reasonable amount of points satisfy all imposed constraints for both $\mathcal{CP}$ conserving and $\mathcal{CP}$ violating models, and that the average strength of a phase transition increases when $\mathcal{CP}$ violation is added, as favoured by the Sakharov conditions. The $\mathcal{CP}$ violating models with only soft $\mathbb{Z}_2$ breaking are seen to more easily satisfy the imposed constraints than those with a completely broken $\mathbb{Z}_2$ symmetry. In the models with only an approximate $\mathbb{Z}_2$ symmetry in the Yukawa sector no difference can be seen when non-diagonal perturbations, as compared to the case of only having diagonal ones, are allowed. It is observed that the electroweak constraints in general require small squared mass differences between the scalar particles, and that the constraints from electric dipole moment searches are the most constraining ones. Finally, it is found that low $\tan\beta$ is generally preferred by all imposed constraints, thus making the picture consistent, and, as is known from the generation of a baryon asymmetry, low $\tan\beta$ is also favoured since the asymmetry $n_B \sim \cot^2\beta$. Hence it is concluded that there indeed is hope for 2HDMs to explain the observed baryon asymmetry of the Universe through electroweak baryogenesis.

Populärvetenskaplig beskrivning

Vad har egentligen kokande vatten, Higgspartikeln och det faktum att någonting snarare än ingenting existerar gemensamt? Jo, om vi tittar ut i universum och jämför mängden vanlig materia, d.v.s. materia bestående av partiklar så som protoner och neutroner, med mängden s.k. antimateria (materiens nemesis i den bemärkelse att dessa förgör varandra vid kontakt och som med god anledning därför har fått prefixet anti-), visar det sig att det väsentligen inte finns någon antimateria alls. För gemene man är detta väldigt rogivande, ty annars skulle den värld vi känner sannerligen inte kunna existera, men för en partikelfysiker med antagandet att det inte fanns någon materie-antimaterieasymmetri vid universums skapelse i Stora Smällen, så sticker detta i ögonen eftersom experiment vid t.ex. partikelacceleratorn LHC i Schweiz visar att det bildas lika stora delar materia som antimateria vid en partikelkollision (skapelsen av partiklar i en sådan kollision kan ses som skapelsen av partiklar efter Stora Smällen). Det är därför väldigt underligt, men likväl intressant, hur materie-antimatieasymmetrin i fråga faktiskt har uppkommit.

Sedan upptäckten av denna asymmetri har flertalet möjliga lösningar föreslagits och en särskilt populär sådan är s.k. elektrosvag baryogenes. Ordet elektrosvag härrör från det faktum att mekanismen i fråga är relaterad till det symmetribrott som i partikelfysikens Standardmodell sker vid den elektrosvaga energiskalan (d.v.s. vid temperaturer av storleksordningen 100 GeV, eller, i mer vardagliga enheter, 1000 miljarder grader Celsius) när Higgspartikeln ger massa till de partiklar som i dagens universum är massiva, och det är just denna fasövergång, den s.k. elektrosvaga fasövergången, som studeras i detta arbete. Speciellt så måste denna fasövergång ha en viss egenskap som också kokande vatten har, nämligen att den sker genom att det i rumtiden bildas bubblor (jämför det kokande vattnet i kastrullen på spisen där det bildas bubblor av vattenånga) i vilka massiva partiklar kan existera. Det andra ordet, baryogenes, är mer lättförståeligt och innebär helt enkelt skapelsen av baryonasymmetrin (baryoner är just dessa partiklar, uppbyggda av tre kvarkar, som utgör grunden för den vanliga materien).

Det bör nämnas att Standardmodellen trots dess annars så stora framgång inte kan förklara den observerade asymmetrin i fråga och att det därför krävs någon typ av ny fysik som ännu inte har observerats, men det är just med anledning av dess framgång som det ofta föreslås nya modeller där mycket är sig likt men någon liten detalj är annorlunda. De s.k. två-Higgsdublettmodellerna, ofta benämnda 2HDMs, är just sådana minimalt utvidgade modeller vars största fysikaliska konsekvens är existensen av inte bara en utan fem Higgspartiklar, varav tre är oladdade och resterande två har laddning. Med i skrivande stund enbart en experimentellt hittad Higgspartikel finns det många parametervärden i 2HDMs att skruva på, så att man därför måste undersöka fasövergången i fråga för ett ofantligt stort antal punkter och med hjälp av experimentella och teoretiska begränsningar utvärdera hur bra dessa är, detta för att i slutändan kunna avgöra huruvida 2HDMs, under antagandet att elektrosvag baryogenes är korrekt, är goda kandidater för att förklara den något oväntade, men ack så viktiga, baryonasymmetri som finns i det synliga universum.

Contents

Contents **3**

1 Introduction **6**

2 Theoretical background **8**
2.1 Cosmology and electroweak baryogenesis 8
2.1.1 Electroweak baryogenesis 8
2.2 Two-Higgs-Doublet Models 10
2.2.1 Tree level potential 11
2.2.2 Tadpole equations 12
2.2.3 The scalar particles and their masses 13
2.2.4 Yukawa sector 16
2.2.5 The effective potential 18

3 Theoretical and experimental constraints **20**
3.1 Theoretical constraints 20
3.1.1 Positivity 20
3.1.2 Unitarity 21
3.1.3 Perturbativity 22
3.1.4 Global minimum at tree level 22
3.2 Experimental constraints 22
3.2.1 Oblique parameters 23
3.2.2 Higgs physics 23
3.2.3 Flavour physics 24
3.2.4 Electric dipole moments 24

4 Programs **25**
4.1 `Vevacious` 25
4.2 `2HDMC` 26
4.3 `HiggsBounds` 27
4.4 `HiggsSignals` 27
4.5 `ParamGen` and `ParamGenComplex` 28

5 Results **29**
5.1 $\mathcal{CP}$ conserving systems 29
5.1.1 Hybrid basis 29
5.1.2 Flavour diagonal $\mathbb{Z}_2$ breaking models 30
5.1.3 Flavour non-diagonal $\mathbb{Z}_2$ breaking models 38
5.2 $\mathcal{CP}$ violating systems 40
5.2.1 The masses and $\mathcal{CP}$ violation 40
5.2.2 Flavour diagonal explicitly $\mathcal{CP}$ violating 2HDMs 42

6 Summary and conclusions **53**

A Spontaneous symmetry breaking **55**

B Tadpole equations for general 2HDMs **57**

C Relations between potential parameters in the general basis and those in the Higgs bases **58**

D Scalar masses in $\mathcal{CP}$ violating 2HDMs **59**

E Oblique parameters **60**

F Electric dipole moments **62**

References **63**

List of Acronyms

Below is a list of the acronyms introduced in this study.

Acronym	**Full Meaning**
2HDM	Two-Higgs-Doublet Model
BAU	Baryon Asymmetry of the Universe
BSM	Beyond Standard Model
CKM	Cabibbo-Kobayashi-Maskawa
CL	Confidence Level
CMBR	Cosmic Microwave Background Radiation
$\overline{DR}'$	Dimensional Reduction
EDM	Electric Dipole Moment
EM	Electromagnetism
EWBG	Electroweak Baryogenesis
EWPT	Electroweak Phase Transition
EWSB	Electroweak Symmetry Breaking
FCNC	Flavour Changing Neutral Current
LHC	Large Hadron Collider
PDG	Particle Data Group
SLHA	Supersymmetry Les Houches Accord
SM	Standard Model
SSB	Spontaneous Symmetry Breaking
VEV	Vacuum Expectation Value

1 Introduction

The Standard Model (SM) of particle physics attempts to describe the observable Universe in terms of three of the four fundamental forces in Nature, namely, the weak force, the strong force and the electromagnetic force, and experiments indicate that it manages to do so very well. Despite this success, there are phenomena in nature which it fails to explain, some common examples being the observed matter/antimatter asymmetry of the Universe and the mysterious dark matter.

The above mentioned asymmetry concerns the fact that in the present Universe there is a vast abundance of baryons as compared to antibaryons [1], which in light of, e.g., particle processes at the Large Hadron Collider (LHC), where matter and antimatter are produced in equal amounts, is rather peculiar. In the perturbative regime the SM treats matter and antimatter symmetrically as well, so there is also a problem from the theoretical perspective[1]. Thus, a reasonable question to ask is what is required from a particle physics model to be able to generate an asymmetry such as that observed. It turns out that the following conditions, called the Sakharov conditions, necessarily must be satisfied [2]:

The model must contain

1. $\mathcal{C}$ *and* $\mathcal{CP}$ *violation,*
2. *Baryon number violation,*
3. *Processes in thermal inequilibrium.*

Even though these in principle could be met by the SM it turns out that it actually does not contain enough $\mathcal{CP}$ violation. Moreover, in the framework of so-called electroweak baryogenesis (EWBG) which will be introduced below, the third condition demands a strongly first order phase transition[2], something which would require the SM Higgs boson to have a mass $m_h \lesssim m_W$, where $m_W \approx 80\,\text{GeV}$ is the mass of the W boson [2]. Experiments at the LHC have measured $m_h \approx 125\,\text{GeV}$ [3] and so it can be concluded that the SM for at least two reasons cannot generate the observed baryon asymmetry of the Universe (BAU).

Because of these limitations, there is clearly strong observational evidence of the need to go beyond the SM. However, as the SM has been very successful it is clear that any new model must incorporate many of its predictions and traits. In the so-called Two-Higgs-Doublet Models (2HDMs) an additional hypercharged scalar $\text{SU}(2)_L$ doublet is added to the SM, thus yielding, e.g., new sources of $\mathcal{CP}$ violation and hence possibly an explanation of the BAU through EWBG. Essentially, EWBG is intimately related to the EWPT, i.e., the spontaneous symmetry breaking (SSB) occurring at the electroweak scale ($\sim 100\,\text{GeV}$)

[1] Of course, this assumes that there was no net baryon asymmetry at the creation of the Universe.

[2] The phase transition in question, called the electroweak phase transition (EWPT), is the process where particles obtain masses via interactions with the Higgs field (the so-called Higgs mechanism) and the electroweak symmetry is broken. This phase transition will be defined more properly below.

due to the scalar fields acquiring non-zero vacuum expectation values (VEVs). This phase transition is defined by (in terms of the symmetry group $\mathrm{SU}(3)_C \times \mathrm{SU}(2)_L \times \mathrm{U}(1)_Y$ of the SM, where C refers to colour, L to left and Y to hypercharge) $\mathrm{SU}(2)_L \times \mathrm{U}(1)_Y \longrightarrow \mathrm{U}(1)_{EM}$, where $\mathrm{U}(1)_{EM}$ is the gauge group of electromagnetism, occurring at some temperature near the electroweak scale. Now, the additional sources of $\mathcal{CP}$ violation in 2HDMs come from the possibility of having a relative complex phase between the VEVs (so-called spontaneous $\mathcal{CP}$ violation) as well as complex phases on certain potential parameters (so-called explicit $\mathcal{CP}$ violation). As a side note, there are alternatives to EWBG, where one example is so-called leptogenesis (see, e.g., [1]) but the fact that EWBG is thought to occur at the electroweak scale, i.e., at energies accessible at colliders, makes it easier to falsify and thus has attracted much interest.

Of course, adding an extra scalar doublet as that above to the SM has several other consequences than just the mentioned additional sources of $\mathcal{CP}$ violation and the possibility of having processes in thermal inequilibrium satisfying experimental bounds. For instance, one direct physical consequence is the existence of not only one but five Higgs-like particles [4]. Obviously, with the discovery of a neutral scalar Higgs boson at the LHC in 2012 the question remains which of the neutral scalars in the 2HDM it would correspond to. Each conceivable scenario has its own phenomenological implications and so it is important to take this into consideration in analyses by comparing with existing experimental limits.

In this study, the goal is to investigate the EWPT in general 2HDMs and to evaluate, with the help of experimental as well as theoretical constraints, the possibility of explaining the BAU through EWBG in such models. There is a certain symmetry, called the $\mathbb{Z}_2$ symmetry, often employed to avoid so-called flavour changing neutral currents which are heavily constrained by experiments, but as these phenomena have not been ruled out completely some freedom remains to not demand such a symmetry. Furthermore, many previous investigations of the EWPT have relied on simplifications such as $\mathcal{CP}$ conservation[3] (see, e.g., [2]), but the goal here is to make less simplifications in order to obtain a more realistic result. In particular, the types of 2HDMs investigated in this study are

1. $\mathbb{Z}_2$ breaking and $\mathcal{CP}$ conserving
2. $\mathbb{Z}_2$ breaking and $\mathcal{CP}$ violating

The structure of this thesis is as follows: In Sec. 2 the theoretical background of 2HDMs, cosmological phase transitions, EWBG and other relevant concepts are presented. After this, in Sec. 3, the theoretical and experimental constraints and limits used are introduced. In Sec. 4 there is a brief review of the programs used and written to do the numerical studies as well as, for the programs already existing before, the corresponding alterations needed for the studies in question. In Sec. 5 results are presented and analyzed, after which a summary and some conclusions of the study are given in Sec. 6. Acknowledgments are given directly after that, and more technical details related to the study have been relegated to appendices following the acknowledgments.

[3]Note that this is in contradiction with one of the Sakharov conditions.

2 Theoretical background

In this section, the main theoretical concepts and tools needed to understand EWBG in 2HDMs are presented. It is assumed that the reader has knowledge of the SM, but the most important concepts for this study will briefly be reviewed here.

2.1 Cosmology and electroweak baryogenesis

The so-called Hot Big Bang theory tries to explain the creation and evolution of the Universe and in the light of observations does so quite well (although not without problems in certain cases). This theory states that, following closely the material in [1], in the beginning of time the Universe was hot and dense, but as time passed the Universe expanded, cooled off and became less dense. During this evolution certain cosmic epochs arose, of which a few are worth mentioning (in reverse time order)[4]

- *Recombination*: The transition to neutral gas from a plasma consisting of baryons, electrons and photons. It is light from this epoch that today can be seen in the cosmic microwave background radiation (CMBR), since after the transition in question photons could no longer scatter with electrons in the neutral gas. ($T \sim 0.1$ eV)
- *Nucleosynthesis*: The transition to nuclei from a plasma consisting of protons and neutrons. ($T \sim 1$ MeV)
- *QCD transition*: The transition to hadronic matter from a quark-gluon plasma in which the color charged particles could move as individual particles. ($T \sim 100$ MeV)
- *Electroweak transition*: The transition to massive particles from a state with massless particles, occuring when $\mathrm{SU}(2)_L \times \mathrm{U}(1)_Y \to \mathrm{U}(1)_{EM}$, as explained below. ($T \sim 100$ GeV)

As was remarked in Sec. 1, the last of these phase transitions, namely the EWPT, is of central importance to EWBG. Henceforth denote the critical temperature, i.e., the temperature at which the EWPT occurs, as T_C.

2.1.1 Electroweak baryogenesis

Here the basic concepts of EWBG are presented, starting with the EWPT and then going on to the three most important steps in the generation of a baryon asymmetry. For the sake of discussion assume that there is a Higgs VEV, v, and that the model in question satisfies the three Sakharov conditions enumerated in Sec. 1.

[4]Throughout this thesis the reduced Planck constant and the Boltzmann constant are set to unity, i.e., $\hbar = k_B = 1$. Note that in these conventions temperature T and energy E have the same units.

The electroweak phase transition

For temperatures $T > T_C$, the symmetry group of the SM is $G_{SM} = \mathrm{SU}(3)_C \times \mathrm{SU}(2)_L \times \mathrm{U}(1)_Y$. The subgroup $\mathrm{SU}(2)_L \times \mathrm{U}(1)_Y$ defines the so-called electroweak symmetry[5] of the SM. At $T = T_C$, this symmetry is broken down to $\mathrm{U}(1)_{EM}$ by means of spontaneous symmetry breaking (for a review of spontaneous symmetry breaking, see App. A). In mathematical terms,

$$\mathrm{SU}(3)_C \times \mathrm{SU}(2)_L \times \mathrm{U}(1)_Y \supset \mathrm{SU}(2)_L \times \mathrm{U}(1)_Y \longrightarrow \mathrm{U}(1)_{EM} \tag{2.1}$$

EWBG requires the EWPT to be strongly first order, this in order to avoid any so-called baryon wash-out through which an obtained baryon asymmetry is erased. The strength of the phase transition can be characterized by the parameter [5]

$$\zeta = \frac{\Delta v_C}{T_C} \tag{2.2}$$

where Δv_C is the difference between the VEV just below the critical temperature and the VEV just above the critical temperature[6]. As a rule of thumb from lattice simulations [6], the transition is strongly first order if $\zeta \gtrsim 1$. A first order phase transition is such that bubbles of the new phase nucleate in the old phase[7], and so if the phase transition in question is characterized by the transition of the VEV of the Higgs field from being zero to being non-zero, the situation can be depicted as in fig. 1. There, bubbles of $v \neq 0$, i.e., broken electroweak symmetry, nucleate and can either expand or implode, this depending on bubble properties at the time of nucleation. In-between bubbles $v = 0$ and the electroweak symmetry is unbroken, and it is just outside the bubble walls that the EWBG starts:

Step 1 of EWBG: Scattering with walls

Particles in the surrounding symmetric plasma may scatter with the bubble walls. From $\mathcal{CP}$ violation, these processes can create asymmetries in number densities between particles and antiparticles.

Step 2 of EWBG: Sphaleron transitions

So-called sphalerons are unstable solutions of the field equations, and since they are non-perturbative cannot be seen in Feynman diagrams. Furthermore, they have the property of allowing systems with zero net baryon charge to reach states with non-zero net baryon charge, and conversely, so that baryon number is violated. This is called the 't Hooft effect [1]. From the asymmetries in number densities between particles and antiparticles generated in Step 1, an excess of e.g., baryons can be created, i.e., if the Universe from the

[5]It might be that at even higher energies also the strong force is unified with the electroweak force, so that some other symmetry group breaks down to G_{SM} at some critical temperature $T'_C > T_C$. This would mean that the three forces described in the SM are in fact the same at high enough energies.

[6]Note that ζ measures the jump in VEV at the critical temperature, hence its usefulness.

[7]This is exactly what happens when water starts boiling.

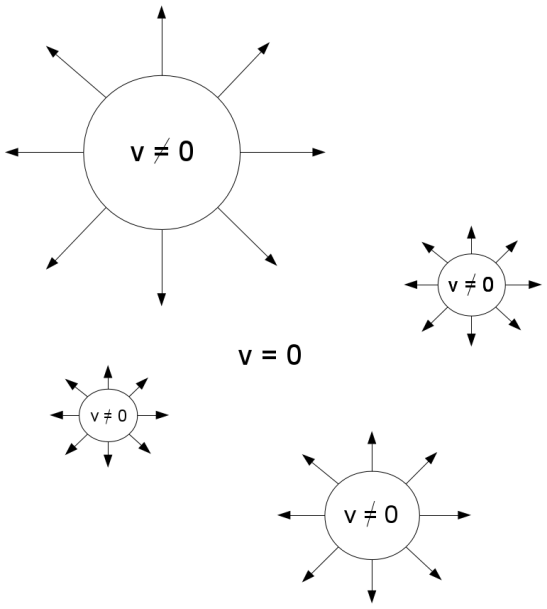

Figure 1: Bubbles of broken phase nucleate and start expanding.

beginning had zero net baryon charge, sphaleron transitions in the symmetric phase could have produced a small baryon asymmetry.

Step 3 of EWBG: Avoiding baryon wash–out

Now, a small baryon asymmetry created as explained above could equally well be washed out by the reversed process, but if some of the created baryons are swept up into one of the bubbles, inside which sphaleron transitions are exponentially suppressed [5], a net baryon charge of the Universe can be obtained as the bubbles expand and eventually cover all of spacetime. This is how the BAU can be explained in terms of EWBG.

2.2 Two-Higgs-Doublet Models

In the light of EWBG as presented above, it can be shown that the SM alone has too little $\mathcal{CP}$ violation and a too high Higgs mass [5]. This means that there is need for beyond SM (BSM) physics. However, with the success of the SM the new physics must necessarily reproduce the experimentally verified results of the SM. The so-called two-Higgs-doublet models (2HDMs) are effective field theories and minimal extensions of the standard model with not one, as in the SM, but two complex scalar doublets.

To study the EWPT there is need for the temperature dependent so-called effective potential introduced in Sec. 2.2.5, as it is at the global minimum of this function that the scalar fields can acquire non-zero VEVs, thus breaking the electroweak symmetry. Before getting

there, however, the implications of adding a second scalar doublet and hence differences from the SM must be considered in more detail.

Since most of the material in this section can be found in, e.g., [4], references are only used for that which cannot.

2.2.1 Tree level potential

Define the two hypercharged $SU(2)_L$ doublets $\Phi_i(x) = \left(\Phi_i^+(x),\, \Phi^0(x)\right)^T$ for $i \in \{1,\, 2\}$ with hypercharges $+1/2$. The fields can be rotated according to $\Phi_i \to \Phi_i' = U_{ij}\Phi_j$ where $U_{ij} \in U(2)$. Having defined the fields, the most general, gauge invariant and renormalizable tree level potential can be written

$$\begin{aligned} V_{\text{tree}}\left(\Phi_1, \Phi_2\right) \;=\; & m_{11}^2 \Phi_1^\dagger \Phi_1 + m_{22}^2 \Phi_2^\dagger \Phi_2 - \left(m_{12}^2 \Phi_1^\dagger \Phi_2 + \text{H.C.}\right) + \frac{1}{2}\lambda_1 \left(\Phi_1^\dagger \Phi_1\right)^2 + \\ & + \frac{1}{2}\lambda_2 \left(\Phi_2^\dagger \Phi_2\right)^2 + \lambda_3 \left(\Phi_1^\dagger \Phi_1\right)\left(\Phi_2^\dagger \Phi_2\right) + \lambda_4 \left(\Phi_1^\dagger \Phi_2\right)\left(\Phi_2^\dagger \Phi_1\right) + \\ & + \left(\frac{1}{2}\lambda_5 \left(\Phi_1^\dagger \Phi_2\right)^2 + \left[\lambda_6 \left(\Phi_1^\dagger \Phi_1\right) + \lambda_7 \left(\Phi_2^\dagger \Phi_2\right)\right]\left(\Phi_1^\dagger \Phi_2\right) + \text{H.C.}\right) \end{aligned} \tag{2.3}$$

where m_{11}^2, m_{22}^2, λ_1, λ_2, λ_3, $\lambda_4 \in \mathbb{R}$ and λ_5, λ_6, λ_7, $m_{12}^2 \in \mathbb{C}$. The fact that the four latter parameters may be complex is a source for so-called *explicit* $\mathcal{CP}$ violation.

Now, the two fields can both acquire VEVs, v_1 and v_2, respectively, which can be complex. Then, bearing in mind that[8] $\sqrt{|v_1|^2 + |v_2|^2} = v$, where $v \approx 246$ GeV is the SM VEV, the two VEVs can be written $|v_1| = v\cos\beta$ and $|v_2| = v\sin\beta$. Therefore, at the minimum[9]

$$\langle \Phi_1 \rangle = \frac{v}{\sqrt{2}} \begin{pmatrix} 0 \\ e^{i\xi_1}\cos\beta \end{pmatrix}, \quad \langle \Phi_2 \rangle = \frac{v}{\sqrt{2}} \begin{pmatrix} 0 \\ e^{i\xi_2}\sin\beta \end{pmatrix} \tag{2.4}$$

where $\beta \in [0,\, \pi/2]$ and phases $e^{i\xi_i}$ have been included to capture the fact that the VEVs can be complex. Note that the existence of these phases gives another source for $\mathcal{CP}$ violation, so-called *spontaneous* $\mathcal{CP}$ violation[10].

Now expand around the minimum, i.e., let

$$\langle \Phi_i \rangle \longrightarrow \langle \Phi_i \rangle + \frac{1}{\sqrt{2}} \begin{pmatrix} \varphi_i^+ \\ \eta_i + i\chi_i \end{pmatrix} = \frac{1}{\sqrt{2}} \begin{pmatrix} \varphi_i^+ \\ v_i + \eta_i + i\chi_i \end{pmatrix} = \frac{1}{\sqrt{2}} \begin{pmatrix} \varphi_i^+ \\ v_{iR} + iv_{iI} + \eta_i + i\chi_i \end{pmatrix} \tag{2.5}$$

[8] The reason this is required comes from the masses m_W and m_Z of the vector bosons being proportional to $\sqrt{|v_1|^2 + |v_2|^2}$ in the same way as they are proportional to v in the SM.

[9] In principle, one could also allow the upper components of the doublets to be non-zero, but this scenario is not considered as it corresponds to breaking electrical charge conservation and thus giving photons mass.

[10] Note that it would be sufficient to introduce only one *relative* phase between the two VEVs, but for later convenience two phases are allowed.

where η_i and χ_i are real scalar fields, and v_{iR} and and v_{iI} are the real and imaginary parts of v_i, respectively. Putting this into Eq. (2.3) gives the mass matrices for the scalar particles (a more detailed discussion of the masses can be found in Sec. 2.2.3).

There is a special family of bases called the Higgs bases in which only one of the two doublets, now called H_1 and H_2, respectively, acquires a VEV. The doublets in the Higgs bases can be written as linear combinations of Φ_1 and Φ_2 according to

$$\begin{pmatrix} H_1 \\ H_2 \end{pmatrix} = \begin{pmatrix} e^{i(\gamma+\xi_1)}\cos\beta & e^{i(\gamma+\xi_2)}\sin\beta \\ -e^{-i(\gamma+\xi_2)}\sin\beta & e^{-i(\gamma+\xi_1)}\cos\beta \end{pmatrix} \begin{pmatrix} \Phi_1 \\ \Phi_2 \end{pmatrix} \tag{2.6}$$

where $\gamma \in [0, \pi]$ defines which particular Higgs basis is chosen [7]. Obviously, under this basis change the tree level potential is also transformed (although retaining its general form) such that

$$\begin{aligned} V_{\text{tree}}(H_1, H_2) \;=\; & M_{11}^2 H_1^\dagger H_1 + M_{22}^2 H_2^\dagger H_2 - \left(M_{12}^2 H_1^\dagger H_2 + \text{H.C.}\right) + \frac{1}{2}\Lambda_1 \left(H_1^\dagger H_1\right)^2 + \\ & + \frac{1}{2}\Lambda_2 \left(H_2^\dagger H_2\right)^2 + \Lambda_3 \left(H_1^\dagger H_1\right)\left(H_2^\dagger H_2\right) + \Lambda_4 \left(H_1^\dagger H_2\right)\left(H_2^\dagger H_1\right) + \\ & + \left(\frac{1}{2}\Lambda_5 \left(H_1^\dagger H_2\right)^2 + \left[\Lambda_6 \left(H_1^\dagger H_1\right) + \Lambda_7 \left(H_2^\dagger H_2\right)\right]\left(H_1^\dagger H_2\right) + \text{H.C.}\right) \end{aligned} \tag{2.7}$$

where now M_{11}^2, M_{22}^2, Λ_1, Λ_2, Λ_3, $\Lambda_4 \in \mathbb{R}$ and Λ_5, Λ_6, Λ_7, $M_{12}^2 \in \mathbb{C}$. These new parameters are given in terms of the old ones in App. C. Note that there is a corresponding expansion as that in Eq. (2.5) for the Higgs bases (see Eq. (2.14)).

As will be shown, this basis is convenient to use when finding the masses of the particles in the most general $\mathcal{CP}$ violating case. Yet another basis, the so-called Hybrid basis, is convenient for parameter space studies in the $\mathcal{CP}$ conserving case and introduced in Sec. 5.1.1.

2.2.2 Tadpole equations

Before going on to find the masses of the scalar particles, the so-called tadpole equations are needed. In essence, the tadpole equations are nothing but minimization conditions for the tree level potential, i.e., for $\mathbf{\Phi} = (\Phi_1, \Phi_2)$,

$$\left.\frac{\partial V_{\text{tree}}}{\partial \mathbf{\Phi}}\right|_{\mathbf{\Phi}=(\langle\Phi_1\rangle, \langle\Phi_2\rangle)} = 0 \tag{2.8}$$

These can be used to demand that a minimum of the tree level potential indeed occurs at $v \approx 246$ GeV. It should be noted, however, that since V_{tree} is a polynomial of degree four in terms of the scalar fields, there may be several minima not necessarily degenerate. Unless the minima with $v \approx 246$ GeV are global (in the sense that any minima at this distance with the same depths are simultaneously global) there is a possibility to tunnel to

a deeper one. Such a transition could possibly result in a quite different Universe, so that the current state of the Universe is metastable (and hence dubbed a panic vacuum) [8]. As will be mentioned in Sec. 3, there exists a condition, whose simplicity to check depends on the particular kind of 2HDM dealt with, for determining whether or not the minimum with $v \approx 246$ GeV is the global minimum at tree level or not.

Now, decomposing Φ_1 and Φ_2 according to (cf. Eq. (2.5))

$$\Phi_1 = \frac{1}{\sqrt{2}} \begin{pmatrix} \varphi_1 + i\varphi_2 \\ \varphi_3 + i\varphi_4 \end{pmatrix}, \quad \Phi_2 = \frac{1}{\sqrt{2}} \begin{pmatrix} \varphi_5 + i\varphi_6 \\ \varphi_7 + i\varphi_8 \end{pmatrix} \tag{2.9}$$

where $\varphi_1, \ldots, \varphi_8$ are real scalar fields, gives Eq. (2.8) as

$$\left. \frac{\partial V_{\text{tree}}}{\partial \varphi_i} \right|_{\varphi_3 + i\varphi_4 = v_1,\, \varphi_7 + i\varphi_8 = v_2,\, \varphi_j = 0\, \forall j \notin \{3,4,7,8\}} = 0, \quad \forall i \in \{1, 2, \ldots, 8\} \tag{2.10}$$

which is what here will be referred to as the tadpole equations. Using these decreases the dimensionality of the parameter space. The equations in question are presented in App. B, but can be solved to give the below equations [9]:

$$\Im\left(m_{12}^2\right) = |v_1|\,|v_2|\, e^{i\xi}\, \Im\left[\frac{1}{2}\lambda_5 e^{-2i\xi} + \cot\beta\, \lambda_6 e^{-i\xi} + \tan\beta\, \lambda_7 e^{-i\xi}\right] \tag{2.11}$$

$$m_{11}^2 = \lambda_1 |v_1|^2 + \lambda_{345} |v_2|^2 - 2\tilde{\nu} |v_2|^2 + \tan\beta\, \Re\left(3 |v_1|^2 \lambda_6 + |v_2|^2 \lambda_7\right) \tag{2.12}$$

$$m_{22}^2 = \lambda_2 |v_2|^2 + \lambda_{345} |v_1|^2 - 2\tilde{\nu} |v_1|^2 + \cot\beta\, \Re\left(|v_1|^2 \lambda_6 + 3 |v_2|^2 \lambda_7\right) \tag{2.13}$$

where $\lambda_{345} = \lambda_3 + \lambda_4 + \Re(\lambda_5)$. Note, however, that $\Re\left(m_{12}^2\right)$ is still a free parameter, and in the case $\xi = 0$ the parameter $\nu = \frac{\Re\left(m_{12}^2\right)}{2v_1 v_2}$ is often introduced to simplify calculations (as, e.g., in the phenomenological basis presented in Sec. 5.2.2).

2.2.3 The scalar particles and their masses

From the eight degrees of freedom in the scalar fields three give rise to Goldstone modes, G^0 and $G^\pm$ (these giving mass to $W^\pm$ and Z), and five give rise to actual physical Higgs states. Eq. (2.5) can be written in the Higgs bases for doublets H_i as [7]

$$H_1 = \frac{e^{i\gamma}}{\sqrt{2}} \begin{pmatrix} \sqrt{2}\, G^+ \\ v + \tilde{h}_1^0 + i\, G^0 \end{pmatrix}, \quad H_2 = \frac{e^{-i\gamma}}{\sqrt{2}} \begin{pmatrix} \sqrt{2}\, H^+ \\ \tilde{h}_2^0 + i\, \tilde{h}_3^0 \end{pmatrix} \tag{2.14}$$

where γ is the angle defining the Higgs basis and the $\tilde{h}_j^0$ are neutral fields mixing to yield the physical particles. The masses of these particles are obtained by inserting the above equation (or Eq. (2.5)) into Eq. (2.7) (or Eq. (2.3)) and expanding. Below, the physical

particles and their masses are reviewed for both the $\mathcal{CP}$ violating and the $\mathcal{CP}$ conserving case.

$\mathcal{CP}$ violating models

In the general case with all possible sources of $\mathcal{CP}$ violation the situation is quite complicated. It is presumably because of this complexity that many analyses assume $\mathcal{CP}$ conservation or make some other simplifying assumptions, where an example is to only include one kind of $\mathcal{CP}$ violation. For now, no such simplifications are made and all results below are completely general. In particular, the neutral scalars will all mix with each other which can be seen from the squared mass matrix obtained when using the expansion in Eq. (2.14), in the tree level potential. The mass matrix in question, $\mathcal{M}_4^2$, in the Higgs basis corresponding to[11] $\gamma = 0$, is now a 4×4 matrix and given by

$$\mathcal{M}_4^2 = \left(\begin{array}{ccc|c} v^2\Lambda_1 & v^2\Re\left(\Lambda_6\right) & -v^2\Im\left(\Lambda_6\right) & 0 \\ v^2\Re\left(\Lambda_6\right) & M_{22}^2 + \frac{1}{2}v^2\left[\Lambda_3 + \Lambda_4 + \Re\left(\Lambda_5\right)\right] & -\frac{1}{2}v^2\Im\left(\Lambda_5\right) & 0 \\ -v^2\Im\left(\Lambda_6\right) & -\frac{1}{2}v^2\Im\left(\Lambda_5\right) & M_{22}^2 + \frac{1}{2}v^2\left[\Lambda_3 + \Lambda_4 - \Re\left(\Lambda_5\right)\right] & 0 \\ \hline 0 & 0 & 0 & 0 \end{array}\right) \tag{2.15}$$

As can be seen from the horizontal and vertical lines, this is a block diagonal matrix with four eigenvalues, of which one is $m_{G^0}^2 = 0$ (as it should according to Goldstone's theorem which is mentioned in App. A). To find the masses of the three physical states, h_1, h_2 and h_3, say, it is sufficient to look at the 3×3 upper left matrix, i.e.,

$$\tilde{\mathcal{M}}_3^2 = \left(\begin{array}{ccc} v^2\Lambda_1 & v^2\Re\left(\Lambda_6\right) & -v^2\Im\left(\Lambda_6\right) \\ v^2\Re\left(\Lambda_6\right) & M_{22}^2 + \frac{1}{2}v^2\left[\Lambda_3 + \Lambda_4 + \Re\left(\Lambda_5\right)\right] & -\frac{1}{2}v^2\Im\left(\Lambda_5\right) \\ -v^2\Im\left(\Lambda_6\right) & -\frac{1}{2}v^2\Im\left(\Lambda_5\right) & M_{22}^2 + \frac{1}{2}v^2\left[\Lambda_3 + \Lambda_4 - \Re\left(\Lambda_5\right)\right] \end{array}\right) \tag{2.16}$$

The eigenvalues of this are quite lengthy and hence given in App. D. The eigenvectors (i.e., the physical fields) are even longer and are thus left out completely. What should be noted though, is that it is possible to define a rotation matrix R_3 diagonalizing $\tilde{\mathcal{M}}^2$ such that $R_3\,\tilde{\mathcal{M}}^2\,R_3^{\mathrm{T}} = \mathrm{diag}\left(m_{h_1}^2, m_{h_2}^2, m_{h_3}^2\right)$, where $m_{h_i}^2$ is the squared mass[12] of field h_i [10]. Furthermore, this rotation matrix may be parametrized in terms of three angles, α_1, α_2 and α_3, with $c_i = \cos\alpha_i$ and $s_i = \sin\alpha_i$, as [11]

$$R_3 = \left(\begin{array}{ccc} c_1c_2 & s_1c_2 & s_2 \\ -\left(c_1s_2s_3 + s_1c_3\right) & c_1c_3 - s_1s_2s_3 & c_2s_3 \\ -c_1s_2c_3 + s_1s_3 & -\left(c_1s_3 + s_1s_2c_3\right) & c_2c_3 \end{array}\right) \tag{2.17}$$

where $\alpha_1 \in (-\pi/2, \pi/2]$, $\alpha_2 \in (-\pi/2, \pi/2]$ and $\alpha_3 \in [0, \pi/2]$ are the so-called *mixing angles*. This means that the neutral scalars indeed do mix, which, as will be seen below, is a generalization of the $\mathcal{CP}$ conserving case where there is only one mixing angle, α_1,

[11] The reason for choosing $\gamma = 0$ is to have $G^0 = \Im\left(H_1^0\right)$ (cf. Eq. (2.14)), where $\Im$ denotes imaginary part (and $\Re$ would denote real part).

[12] Here, by convention $m_{h_1} \leq m_{h_2} \leq m_{h_3}$.

and the other two are identically zero. In that case, the upper left 2×2 matrix in R_3 diagonalizes the 2×2 mass matrix of the two mixing neutral scalars.

The mass matrix for the charged fields is the 2×2 matrix

$$\mathcal{M}^2_{\text{charged}} = \begin{pmatrix} 0 & 0 \\ 0 & M_{22}^2 + \frac{1}{2}v^2\Lambda_3 \end{pmatrix} \tag{2.18}$$

The eigenvalues of this matrix are $m^2_{G^\pm} = 0$ and $m^2_{H^\pm} = M_{22}^2 + \frac{1}{2}v^2\Lambda_3$. By inspection, the eigenvectors yield $G^\pm = H_1^\pm$ and $H^\pm = H_2^\pm$.

$\mathcal{CP}$ conserving models

If there is no $\mathcal{CP}$ violation, many calculations are much simplified. In particular, the mass matrix for the neutral scalars in $\mathcal{CP}$ conserving 2HDMs is, as these 2HDMs are just a special case when compared to $\mathcal{CP}$ violating ones, again given by Eq. (2.16), but note that this simplifies to

$$\tilde{\mathcal{M}}_3^2\Big|_{\Lambda_i \in \mathbb{R},\, \forall i} = \left(\begin{array}{cc|c} v^2\Lambda_1 & v^2\Lambda_6 & 0 \\ v^2\Lambda_6 & M_{22}^2 + \frac{1}{2}v^2\left[\Lambda_3 + \Lambda_4 + \Lambda_5\right] & 0 \\ \hline 0 & 0 & M_{22}^2 + \frac{1}{2}v^2\left[\Lambda_3 + \Lambda_4 - \Lambda_5\right] \end{array}\right) \tag{2.19}$$

which is block diagonal. This means that there is one scalar particle not mixing with the others.

The physical scalar states are easily found and, expressed in terms of the fields in Eq. (2.14), are given by

- $\mathcal{CP}$ even neutrals: $h = \tilde{h}_1^0 \sin(\beta - \alpha) + \tilde{h}_2^0 \cos(\beta - \alpha)$ and $H = \tilde{h}_1^0 \cos(\beta - \alpha) - \tilde{h}_2^0 \sin(\beta - \alpha)$, for angle $\beta - \alpha = \alpha_1$ defined in Eq. (2.17), with $m_h \leq m_H$
- $\mathcal{CP}$ odd neutral: $A = \tilde{h}_3^0$
- Charged Higgs bosons: $H^\pm$

As can be seen, it is the pseudoscalar A that cannot mix with the other neutral particles. Now, the masses for charged scalar and the pseudoscalar are given by [7] (for their expressions in the general basis, see e.g., [12])

$$\begin{aligned} m^2_{H^\pm} &= M_{22}^2 + \tfrac{1}{2}v^2\Lambda_3 \\ m_A^2 &= m^2_{H^\pm} - \tfrac{1}{2}v^2\left(\Lambda_5 - \Lambda_4\right) \end{aligned} \tag{2.20}$$

whereas, due to mixing, the squares of the masses of the two remaining scalars are given as the eigenvalues to the upper left block of Eq. (2.19), i.e., squared mass matrix $\tilde{\mathcal{M}}_2^2$ given by

$$\tilde{\mathcal{M}}_2^2 = \begin{pmatrix} v^2\Lambda_1 & v^2\Lambda_6 \\ v^2\Lambda_6 & M_{22}^2 + \frac{1}{2}v^2\left[\Lambda_3 + \Lambda_4 + \Lambda_5\right] \end{pmatrix} = \begin{pmatrix} v^2\Lambda_1 & v^2\Lambda_6 \\ v^2\Lambda_6 & m_A^2 + v^2\Lambda_5 \end{pmatrix} \tag{2.21}$$

Rotating to the basis in which $\tilde{\mathcal{M}}_2^2$ is diagonal, this by the angle $\alpha_1 = \beta - \alpha$ (which defines[13] α), mixing the neutral scalars h and H as above, gives the masses of the two particles as, with $m_+^2 = m_H^2$ and $m_-^2 = m_h^2$ so that $m_H^2 \geq m_h^2$,

$$m_\pm^2 = \frac{1}{2}\left[m_A^2 + v^2\left(\Lambda_1 + \Lambda_5\right) \pm \sqrt{\left[m_A^2 + v^2\left(\Lambda_5 - \Lambda_1\right)\right]^2 + 4v^4\Lambda_6^2}\right] \tag{2.22}$$

It is one of these two scalars that must correspond to the experimentally verified scalar with mass ≈ 125 GeV.

2.2.4 Yukawa sector

The Yukawa part of the Lagrangian, $\mathcal{L}_{\text{Yuk}}$, gives the interactions between the scalar fields and the fermions, and is therefore very important. The most general form of this Lagrangian is [4]

$$\begin{aligned} -\mathcal{L}_{\text{Yuk}} &= \bar{Q}_L\left(\eta_1^D\Phi_1 + \eta_2^D\Phi_2\right)d_R + \bar{Q}_L\left(\eta_1^U\tilde{\Phi}_1 + \eta_2^U\tilde{\Phi}_2\right)u_R + \\ &\quad + \bar{L}_L\left(\eta_1^L\Phi_1 + \eta_2^L\Phi_2\right)l_R + \text{H.C.} \end{aligned} \tag{2.23}$$

where the Yukawa matrices $\eta_i^F \in \mathbb{C}^{3\times 3}$ are vectors in flavour space, the scalar fields $\tilde{\Phi}_j = -i\sigma_2\,\Phi_j^*$ where $\sigma_2 = \begin{pmatrix} 0 & -i \\ i & 0 \end{pmatrix}$. $\bar{Q}_L$ and $\bar{L}_L$ are quark and lepton doublets, respectively, under $SU(2)_L$, whereas d_R, u_R and l_R are the corresponding singlets under $SU(2)_L$. In the Higgs bases there are six matrices, called κ_0^F and ρ_0^F, given by

$$\begin{pmatrix} \kappa_0 \\ \rho_0 \end{pmatrix}^F = \begin{pmatrix} \cos\beta & \sin\beta \\ -\sin\beta & \cos\beta \end{pmatrix}\begin{pmatrix} \eta_1 \\ \eta_2 \end{pmatrix}^F \tag{2.24}$$

Now rotate to the mass eigenstate basis by bi-diagonalizing κ_0^F with six unitary matrices, commonly referred to as V_L^F and V_R^F, according to $\kappa_0^F \to \kappa^F = V_L^F\kappa_0^F V_R^{F\,\dagger} = \frac{\sqrt{2}}{v}M^F$ where M^F are the mass matrices of the fermions [13]. Under this rotation $\rho_0^F \to \rho^F = V_L^F\rho_0^F V_R^{F\,\dagger}$ and if the ρ^F are non-diagonal there are so-called flavour changing neutral currents (FCNCs), which are heavily constrained by experiments and therefore not wanted. There is a theorem by Glashow and Weinberg saying that if a given fermion couples to only one of the scalar fields, then there will not be any FCNCs present in the theory [14]. A symmetry is therefore often imposed, this defined by $\mathbb{Z}_2 : \Phi_i \mapsto (-1)^{i+1}\Phi_i$ and $\mathbb{Z}_2 : f_R \mapsto \pm f_R$, where f_R is one of the right handed fermions in Eq. (2.23), such that the Lagrangian $\mathcal{L} \mapsto \mathcal{L}$. Now, the combinatorial possibilities of assigning charges for the fields under $\mathbb{Z}_2$ gives rise to four so-called *types*. These are

$$\text{Type I:}\ \left\{f_R \mapsto f_R,\ \forall\, f\right. \implies \left.\left\{\rho^F = \kappa^F\cot\beta,\ \forall\, F\right.\right. \tag{2.25}$$

[13]Note that β does not exist in the Higgs bases, but that the mixing angles there necessarily must depend on it. Thus, one may in the $\mathcal{CP}$ conserving case write $\alpha_1 = \beta - \alpha$ for some angle α.

$$\text{Type II:} \quad \begin{cases} u_R \mapsto u_R \\ d_R \mapsto -d_R \\ l_R \mapsto -l_R \end{cases} \implies \begin{cases} \rho^D = -\kappa^D \tan\beta \\ \rho^U = \kappa^U \cot\beta \\ \rho^L = -\kappa^L \tan\beta \end{cases} \tag{2.26}$$

$$\text{Type X:} \quad \begin{cases} u_R \mapsto u_R \\ d_R \mapsto d_R \\ l_R \mapsto -l_R \end{cases} \implies \begin{cases} \rho^D = \kappa^D \cot\beta \\ \rho^U = \kappa^U \cot\beta \\ \rho^L = -\kappa^L \tan\beta \end{cases} \tag{2.27}$$

$$\text{Type Y:} \quad \begin{cases} u_R \mapsto u_R \\ d_R \mapsto -d_R \\ l_R \mapsto l_R \end{cases} \implies \begin{cases} \rho^D = -\kappa^D \tan\beta \\ \rho^U = \kappa^U \cot\beta \\ \rho^L = \kappa^L \cot\beta \end{cases} \tag{2.28}$$

Note that if the leptons are left out of the analysis, there are only types I and II. Furthermore, the requirement that $\mathcal{L} \mapsto \mathcal{L}$ under $\mathbb{Z}_2$ yields, as can be seen when looking at Eq. (2.3), $m_{12}^2 = \lambda_6 = \lambda_7 = 0$. However, since m_{12}^2 is the coupling for the quadratic combinations of the two fields and λ_6 and λ_7 are those for the quartic ones, it is often assumed that $m_{12}^2 \neq 0$. The $\mathbb{Z}_2$ symmetry is in this case said to be *softly* broken[14].

It should be noted that there also are other ways to suppress FCNCs, two notable being through Yukawa alignment and the Cheng-Sher Ansatz [13]. The first of these assumes that η_1^F and η_2^F, and hence also κ_0^F and ρ_0^F, are proportional to one another, so that both κ_0^F and ρ_0^F are diagonalized simultaneously, thus yielding an absence of FCNCs. Although this approach may sound good, one should remember that such a relation can be violated at another energy scale, thus allowing for contributions to FCNCs in the end either way. As for the Cheng-Sher Ansatz, off-diagonal entries in the ρ^F are allowed, but they must be small enough that experimental constraints are still satisfied. The ansatz has as consequence that each element ij of ρ^F can be written as

$$\rho_{ij}^F = \lambda_{ij}^F \frac{\sqrt{2m_i m_j}}{v} \tag{2.29}$$

where m_i and m_j are fermion masses and $\lambda_{ij}^F \sim \mathcal{O}(1)$. In fact, from experimental limits $\lambda_{ij}^F \lesssim 0.1$ for $i \neq j \neq t$ [13]. Yukawa alignment is not used in this study, but the above consequence of the Cheng-Sher Ansatz is.

Before going on to the effective potential, stopping for a closer look at the diagonalization matrices V_L^F and V_R^F will be useful for Sec. 4. Now, these matrices are in fact related to the Cabibbo–Kobayashi–Maskawa matrix, or, as it is usually abbreviated, the CKM matrix, V_{CKM}, this by $V_{CKM} = V_L^U V_L^{D\,\dagger}$ [13]. Moreover, a flavour basis can be chosen such that

$$\begin{cases} V_L^U = V_R^U = \mathbb{1} \\ V_L^L = V_R^L = \mathbb{1} \\ V_L^D = V_{CKM}^\dagger,\ V_R^D = \mathbb{1} \end{cases} \tag{2.30}$$

[14]The reason why it is said to be softly broken in this case is that at large energies, or, at large field values, the contributions from the quadratic terms (i.e., the mass terms) in the tree level potential are negligible as compared to the quartic terms.

thus yielding

$$\begin{cases} \kappa_0^U = \kappa^U = \frac{\sqrt{2}}{v} M^U \\ \rho_0^U = \rho^U \\ \kappa_0^L = \kappa^L = \frac{\sqrt{2}}{v} M^L \\ \rho_0^L = \rho^L \\ \kappa_0^D = V_{CKM}\, \kappa^D = \frac{\sqrt{2}}{v} V_{CKM}\, M^D \\ \rho_0^D = V_{CKM}\, \rho^D \end{cases} \tag{2.31}$$

As can be seen, this only requires V_{CKM} in the down sector so that some calculations can be simplified.

2.2.5 The effective potential

In order to investigate the EWPT there is obviously need for a temperature dependent potential, and since temperature effects formally are a loop effect, there is need to go at least to 1-loop level. The full effective potential at zero temperature can be written, with the ith loop correction denoted by $V_{(i)}$,

$$V\left(\Phi_1, \Phi_2\right) = V_{\text{tree}}\left(\Phi_1, \Phi_2\right) + \sum_{i=1}^{\infty} V_{(i)}\left(\Phi_1, \Phi_2\right) \tag{2.32}$$

This potential can be obtained from the effective action of a generating functional (see e.g., [15]), but, as such a derivation is not really relevant here, it is left out to the interested reader. As is pointed out in [16], the potential in Eq. (2.32) is contained in the full temperature dependent effective potential but very often temperature corrections are added to a truncated version of Eq. (2.32). In this study, a 1-loop thermally corrected effective potential is used. This potential can be shown to have the form [17]

$$\begin{aligned} V\left(\Phi_1, \Phi_2, T\right) &= V_{\text{tree}}\left(\Phi_1, \Phi_2\right) + V_{CT}\left(\Phi_1, \Phi_2\right) + \\ &\quad + V_{(1)}\left(\Phi_1, \Phi_2\right) + V_T\left(\Phi_1, \Phi_2, T\right) \end{aligned} \tag{2.33}$$

$V_{CT(\Phi_1,\Phi_2)}$ consists of counter terms, i.e., terms added so as to absorb infinities when renormalizing. The form of this part of the effective potential is the same as the tree level potential, but with different coefficients. The terms in question can be chosen in several ways, e.g., by requiring invariance of solutions to the tadpole equations when going to 1-loop level [8].

$V_{(1)}\left(\Phi_1, \Phi_2\right)$ is the zero temperature 1-loop correction to V_{tree} given by

$$V_{(1)}\left(\Phi_1, \Phi_2\right) = \sum_i \pm \frac{n_i}{64\pi^2} m_i^4\left(\Phi_1, \Phi_2\right) \left[\ln \frac{m_i^2\left(\Phi_1, \Phi_2\right)}{Q^2} - c_i\right] \tag{2.34}$$

Here, the sum runs over all particles of the theory and the upper sign is for bosons whereas the lower one is for fermions. n_i is the multiplicity and $m_i\left(\Phi_1,\Phi_2\right)$ the mass[15] of particle i, and Q is the renormalization scale. The potential is thus explicitly renormalization scale dependent, as it should since the effective potential is truncated at finite order [8]. Since large contributions from the terms with the logarithms are unsought, Q needs to be chosen cleverly. Note that for small masses m_i (i.e., masses m_i much smaller than Q), the term $m_i^4\,\ln\frac{m_i^2}{Q^2}$ still remains small, whereas it for large masses (i.e., masses m_i much larger than Q) does not. Therefore, Q should be chosen on the order of the largest mass in the model and is chosen to be 1 TeV in this study, this in accordance with conventions in one of the used programs[16], `Vevacious`. The constants c_i depend on the regularization scheme, which here has been chosen as dimensional reduction[17] ($\overline{\text{DR}}'$) so that $c_i = 3/2\ \forall i$ [18].

$V_T\left(\Phi_1,\Phi_2,T\right)$ are the thermal corrections (which can be found from calculating the 1-loop contributions in the temperature dependent effective potential and subtracting $V_{(1)}\left(\Phi_1,\Phi_2\right)$) given by

$$V_T\left(\Phi_1,\Phi_2,T\right) = T^4\sum_i \pm\frac{n_i}{2\pi}\int_0^\infty dx\,x^2\ln\left(1\mp\exp\left[-\sqrt{x^2+m_i^2\left(\Phi_1,\Phi_2\right)/T^2}\right]\right) \quad (2.35)$$

This can be approximated both in the high temperature region and the low temperature region (i.e., when comparing the temperature to the masses) [5]. Denoting the integral for high temperatures and fermionic degrees of freedom as $I_{HT}^f\left(y^2\right)$ (where $y = m_i/T$ has been introduced, and index i neglected, for simplicity) and that for bosonic ones $I_{HT}^b\left(y^2\right)$, the expansions can be written

$$I_{HT}^f\left(y^2\right) = -\frac{7\pi^3}{360} - \frac{\pi}{24}y^2 - \frac{1}{32\pi}y^4\ln\left(\frac{y^2}{a_f}\right) + \mathcal{O}\left(y^5\right) \quad (2.36)$$

and

$$I_{HT}^b\left(y^2\right) = -\frac{\pi^3}{45} - \frac{\pi}{12}y^2 - \frac{1}{6}y^3 - \frac{1}{32\pi}y^4\ln\left(\frac{y^2}{a_b}\right) + \mathcal{O}\left(y^5\right) \quad (2.37)$$

where $\ln a_f \approx 2.6351$ and $\ln a_b \approx 5.4076$.

High temperature means $y \ll 1$. In the low temperature region, i.e., where $y \gg 1$, the two integrals can be written in the same form,

$$I_{LT}^b\left(y^2\right) \approx I_{LT}^f\left(y^2\right) = \left(\frac{y}{2\pi^{5/3}}\right)^{3/2} e^{-y}\left(1+\frac{15}{8y}+\mathcal{O}\left(y^{-2}\right)\right) \quad (2.38)$$

[15] In particular, $m_i^2\left(\Phi_1,\Phi_2\right)$ is given as the ith eigenvalue of the corresponding mass matrix as derived from the potential. These can also get contributions from having a finite temperature, but such effects are not considered in this study.

[16] These programs will be presented in Sec. 4.

[17] In ordinary $\overline{\text{DR}}$, to which $\overline{\text{DR}}'$ is related by a parameter redefinition, both integral measures in loop integrals and dimensions on gauge fields are shifted according to $d = 4 \to 4-2\epsilon$, where d is the number of dimensions [18].

In `Vevacious` the integrals are expanded in this fashion and an extrapolation is made between the two regions in order to obtain continuity.

As was mentioned at the beginning of this section the effective potential in Eq. (2.33) is the key to studying the EWPT, this since it is when the global minimum[18] of this function changes from the origin to one at distance $\sqrt{|v_1|^2 + |v_2|^2} \neq 0$ from the origin that the electroweak symmetry is broken. Therefore, the potential in question needs to be minimized for different temperatures in order to yield a critical VEV and a corresponding critical temperature, thus resulting in a measure of the strength of the phase transition, i.e., ζ. In this study quantities are calculated in the Landau gauge[19] and any calculated VEVs and critical temperatures might have unphysical values whereas their respective ratios $\zeta = \Delta v_C / T_C$ do not [8].

3 Theoretical and experimental constraints

In this section, the experimental and theoretical constraints used in the study are presented. In particular, there are two subsections, one for the former and one for the latter, both containing respective subsections.

3.1 Theoretical constraints

In this section the theoretical constraints used are presented, with one type of constraint in each subsection.

3.1.1 Positivity

To insure that the vacua are stable minima, the tree level potential has to be bounded from below in all field directions, i.e., there can be no direction in which it tends to $-\infty$ [9]. As an example, for a softly broken $\mathbb{Z}_2$ symmetric and $\mathcal{CP}$ violating 2HDM the constraints on the potential parameters are

$$\begin{aligned} &\lambda_1 > 0, && \lambda_2 > 0, \\ &\lambda_3 > -\sqrt{\lambda_1 \lambda_2}, && \lambda_3 + \lambda_4 - |\lambda_5| + \sqrt{\lambda_1 \lambda_2} > 0 \end{aligned} \tag{3.1}$$

[18] Note that this may now have several minima as it depends on two scalar fields, unlike the SM case where there is only one scalar field.

[19] This is an R_ξ gauge corresponding to the limit $\xi \to 0$. The reason for choosing this gauge here is that the program `Vevacious` (see Sec. 4) uses it as well. The reason why in turn `Vevacious` uses it has to do with gauge dependence of paths between vacua (which should be considered when calculating tunneling times). Moreover, the so-called Faddeev-Popov ghosts also decouple in this gauge at 1-loop level [17].

When λ_6 or λ_7 are non-zero there are additional, and a lot more complicated, constraints [19]. These can be handled numerically as in e.g., [20] or [21], where a matrix Λ_E, whose eigenvalues and properties determine whether or not the potential is stable, is defined. In particular, the matrix is given by

$$\Lambda_E = \frac{1}{2}\begin{pmatrix} \frac{1}{2}(\lambda_1+\lambda_2)+\lambda_3 & \Re(\lambda_6+\lambda_7) & -\Im(\lambda_6+\lambda_7) & \frac{1}{2}(\lambda_1-\lambda_2) \\ -\Re(\lambda_6+\lambda_7) & -\lambda_4-\Re(\lambda_5) & \Im(\lambda_5) & -\Re(\lambda_6-\lambda_7) \\ \Im(\lambda_6+\lambda_7) & \Im(\lambda_5) & -\lambda_4+\Re(\lambda_5) & \Im(\lambda_6-\lambda_7) \\ -\frac{1}{2}(\lambda_1-\lambda_2) & -\Re(\lambda_6-\lambda_7) & \Im(\lambda_6-\lambda_7) & -\frac{1}{2}(\lambda_1+\lambda_2)+\lambda_3 \end{pmatrix} \tag{3.2}$$

and if the eigenvalues are denoted by $\tilde{\Lambda}_\mu$, where $\mu \in \{0,\, 1,\, 2,\, 3\}$, then the potential is stable if and only if the eigenvalues are real and satisfy $\tilde{\Lambda}_0 > 0$ and $\tilde{\Lambda}_k < \tilde{\Lambda}_0$ for $k \neq 0$. In order to identify which eigenvalue is $\tilde{\Lambda}_0$, a certain projection operator for each eigenvalue can be defined and for which a specific condition holds for $\tilde{\Lambda}_0$ (see [20]), but these operators are here left out for simplicity.

3.1.2 Unitarity

The scattering matrix S has to be unitary i.e., $S^\dagger S = S S^\dagger = \mathbb{1}$, something which can be ensured by constraints on its eigenvalues [22]. In particular, S can be expanded according to $S = S^{(0)} + \epsilon S^{(1)} + \ldots$, where $S^{(0)} = \mathbb{1}$ is the zeroth order contribution, $S^{(1)}$ is the first order contribution and so on, and ϵ is some small parameter. As the contributions to S in general are decreasing with order in weakly coupled theories, it is reasonable to require that it be unitary already at tree level (i.e., to order ϵ) [22]. Denoting, for a certain state, the total hypercharge by $Y \in \{0,\, \pm 2\}$ and the total isospin by $\sigma \in \{0,\, 1\}$, which are conserved in Higgs-Higgs scattering, four matrices $S_{(Y,\,\sigma)}$ can be written down as [22]

$$\begin{aligned}
8\pi\, S_{(2,\,1)} &= \begin{pmatrix} \lambda_1 & \lambda_5 & \sqrt{2}\lambda_6 \\ \lambda_5^* & \lambda_2 & \sqrt{2}\lambda_7^* \\ \sqrt{2}\lambda_6^* & \sqrt{2}\lambda_7 & \lambda_3+\lambda_4 \end{pmatrix} \\
8\pi\, S_{(2,\,0)} &= \lambda_3 - \lambda_4 \\
8\pi\, S_{(0,\,1)} &= \begin{pmatrix} \lambda_1 & \lambda_4 & \lambda_6 & \lambda_6^* \\ \lambda_4 & \lambda_2 & \lambda_7 & \lambda_7^* \\ \lambda_6^* & \lambda_7^* & \lambda_3 & \lambda_5^* \\ \lambda_6 & \lambda_7 & \lambda_5 & \lambda_3 \end{pmatrix} \\
8\pi\, S_{(0,\,0)} &= \begin{pmatrix} 3\lambda_1 & 2\lambda_3+\lambda_4 & 3\lambda_6 & 3\lambda_6^* \\ 2\lambda_3+\lambda_4 & 3\lambda_2 & 3\lambda_7 & 3\lambda_7^* \\ 3\lambda_6^* & 3\lambda_7^* & \lambda_3+2\lambda_4 & 3\lambda_5^* \\ 3\lambda_6 & 3\lambda_7 & 3\lambda_5 & \lambda_3+2\lambda_4 \end{pmatrix}
\end{aligned} \tag{3.3}$$

The unitarity condition can then be translated into bounds on the respective eigenvalues l of these matrices. Inspired by the choice in [23], the upper bounds are here chosen so that the eigenvalues must satisfy $|l| \leq 16\pi$.

3.1.3 Perturbativity

As this study is based on perturbative calculations there is obviously good reason to demand perturbativity. Perturbativity can be ensured by demanding that the quartic Higgs couplings $C_{H_iH_jH_kH_l}$, for H_n one of the physical Higgs states, satisfy $\left|C_{H_iH_jH_kH_l}\right| \leq 4\pi$ [23]. The couplings in question can be found in e.g., [24].

3.1.4 Global minimum at tree level

As remarked in Sec. 2.2.2, with a fourth degree polynomial in the fields Φ_1 and Φ_2, the tree level potential in Eq. (2.3) can have several minima. A vacuum that does not correspond to a global minimum is often referred to as a panic vacuum, this as there is a probability of tunneling to one corresponding to a deeper minimum. It is therefore reasonable to check whether or not the minimum with $v \approx 246$ GeV is the global minimum, something which for a softly broken $\mathbb{Z}_2$ symmetric and possibly $\mathcal{CP}$ violating 2HDM is easily checked with the help of the discriminant [20]

$$\tilde{D} = \left[\left(\frac{m_{H^\pm}^2}{v^2} + \frac{\lambda_4}{2}\right)^2 - \frac{|\lambda_5|^2}{4}\right]\left[\frac{m_{H^\pm}^2}{v^2} + \frac{\sqrt{\lambda_1\lambda_2} - \lambda_3}{2}\right] \tag{3.4}$$

such that if $\tilde{D} > 0$ the tree level minimum in question is in fact global. Just as for the positivity constraints, when λ_6, $\lambda_7 \neq 0$ a numerical approach is needed. In such cases, again the eigenvalues of the matrix Λ_E should be used [20]. In particular, the full discriminant (from which $\tilde{D}$ can be derived when $\lambda_6 = \lambda_7 = 0$) is then given by $D = \left(\tilde{\Lambda}_0 - \frac{m_{H^\pm}^2}{v^2}\right)\left(\frac{m_{H^\pm}^2}{v^2} - \tilde{\Lambda}_1\right)\left(\frac{m_{H^\pm}^2}{v^2} - \tilde{\Lambda}_2\right)\left(\frac{m_{H^\pm}^2}{v^2} - \tilde{\Lambda}_3\right)$ and if $D > 0$, the minimum is global. When $D < 0$ the eigenvalues $\tilde{\Lambda}_\mu$ have to be considered: the minimum is gobal only if the potential is stable and $\tilde{\Lambda}_0 < \frac{m_{H^\pm}^2}{v^2}$.

3.2 Experimental constraints

The aim of any physical model is to explain and predict actual phenomena in Nature, so it is hence essential that any such model satisfies already existing experimental limits. In this section the experimental constraints used in this study are briefly presented[20].

[20]The interested reader is encouraged to look further into the referenced articles.

3.2.1 Oblique parameters

As was remarked at the beginning of Sec. 2.2 the SM has had great success as a physics model describing Nature, but as more and more experiments have been performed some shortcomings have been unveiled. To remedy these shortcomings many new models, such as the 2HDMs, have been proposed, but also many have fallen due to not being able to reproduce predictions close enough to those of the SM. Because of this, the so-called oblique parameters have been defined to measure how much a new physics model deviates from the SM, and in particular these parameters are electroweak precision constraints in the sense that they measure how the new physics couples to the electroweak gauge bosons via changes in vacuum polarizations. For a general discussion, see, e.g., [25].

The parameters in question are six in total, S, T, U, V, W and X, and are defined such that they are all zero for the SM. The exact expressions for these parameters are given in App. E. As is noted in [26], noticeable deviations from the SM can occur for 2HDMs but in the case these deviations are small the custodial symmetry[21] is preserved.

In the review article by the Particle Data Group (PDG) [25] there is plotted an ellipse (constructed from experimental data) in the ST-plane[22] corresponding to 90% confidence level (CL), inside which lies the SM value $(S, T) = (0, 0)$. In general it turns out that in this study U is very small, so using this ellipse as a constraint of "goodness" is a reasonable approximation. The ellipse ϵ_{ST} can be parametrized as in [27], but with more recent data[23],

$$\epsilon_{ST} = \left\{ S, T \in \mathbb{R} \;\middle|\; 1 = \left(\frac{S\cos\theta + \tilde{T}\sin\theta}{0.262} \right)^2 + \left(\frac{\tilde{T}\cos\theta - S\sin\theta}{0.063} \right)^2 \right\} \tag{3.5}$$

where $\tilde{T} = T - 0.05$ and $\theta = 0.712$. In particular, it is required of a good point to lie within the ellipse in question.

3.2.2 Higgs physics

Naturally, experimental constraints from searches and discovery of the Higgs particle that was found the LHC are also included. In particular, for a given parameter point this is done by checking model predictions of branching ratios, cross sections and decay widths, and then comparing with experimental data to see if the point is excluded or allowed at 95% CL. Moreover, the "goodness of fit" of a given model to experimental data can be

[21] The custodial symmetry is connected to the tree level relation $\cos\theta_W = \frac{M_W}{M_Z}$, where θ_W is the weak mixing angle.

[22] That is, U has been fixed to zero.

[23] The authors of [27] refer to an older version of [25].

measured in terms of a χ^2 value. This value is calculated for a given point and constrained[24] for a given number, n, say, of degrees of freedom and a p-value (here $p = 0.05$ since 95% CL is considered). The number of degrees of freedom n is the difference between number of observables used and the number of free parameters.

3.2.3 Flavour physics

There are interesting constraints from flavour physics. Two that are used for the $\mathcal{CP}$ conserving models in this study[25] come from $b \to s\gamma$ transitions and the mass difference ΔM_B from $B^0 - \bar{B}^0$ mixing. In [28] the limits are given in the plane spanned by $\tan\beta$ and $m_{H^\pm}$ for $\mathcal{CP}$ conserving models. In the absence of the exact parametrizations of these constraints, in this study a very conservative approach is used. In particular, the most constraining value for a given constraint in the mentioned plane is taken as a uniform limit in the whole plane, so that the allowed region must be rectangular (see e.g., fig. 4b for such a plot, where the upper right rectangle is the allowed region). The precise limits used here are: $\log^{10}(\tan\beta) > \log^{10}(3) \approx 0.477$ coming from both ΔM_B and $b \to s\gamma$ (type I) and $\log^{10}(\tan\beta) > 0$ coming from ΔM_B and $m_{H^\pm} > 350$ GeV coming from $b \to s\gamma$ (type II). Other than simplifying matters there is good reason to use this approach: the limits in [28] were found for $\mathbb{Z}_2$ symmetric Yukawa sectors so that for any slightly perturbed such systems the limits in question should be somewhat changed in the plane, but not so much that the qualitative picture changes (clearly, this is an assumption and should thus be considered as such). Of course, points lying very close to the limits can still be excluded but if there is a substantial amount of points situated a bit away from the limits, then they are most likely allowed.

3.2.4 Electric dipole moments

$\mathcal{CP}$ violation can be constrained by measurements of electric dipole moments (EDMs) of e.g., electrons and neutrons [29], since 2HDMs can give rise to non-zero EDMs. The most severe constraints on the electron EDM comes from the experiments performed by the ACME collaboration, in which electric fields are used to measure energy shifts in the ThO spectrum so that there are resulting asymmetric charge distributions along the spins of electrons [30]. In [29], constraints of electron, neutron, mercury and radium EDMs for flavour conserving explicitly $\mathcal{CP}$ violating softly broken $\mathbb{Z}_2$ symmetric 2HDMs of type I and type II, are presented in the plane spanned by $|\sin\alpha_b|$ and $\tan\beta$ (α_b is related to the mixing angles α_1, α_2 and α_3 introduced in Sec. 2.2.3, as is explained in Sec. 5.2.2).

[24] For a plot of these constraints for different p and n see e.g., [25]. They can be calculated to good precision by some programs with support for statistics, and, in this study, they were calculated using the function `chi2inv(`p`,` n`)` available in `MATLAB`.

[25] Since flavour physics constraints only were found for $\mathcal{CP}$ conserving models no such constraints are used for the $\mathcal{CP}$ violating models studied.

These constraints are in this study used in a similar manner as the constraints from flavour physics, and it is required that $|\sin \alpha_b| < 0.005$. For a brief review of how EDMs arise, see App. F.

4 Programs

In this section the programs used are briefly reviewed. For those that have required modifications there is also some explanation of what has been done.

4.1 `Vevacious`

`Vevacious` (see [8]) takes the tree level potential for a given model and calculates all the tree level minima. It does this with a method called homotopy continuation, which is guaranteed to find *all* the tree level minima, not only the global one. Then the program takes these minima and uses them as starting points for a gradient based minimization of the zero temperature 1-loop potential (see Sec. 2.2.5). It is possible to do this for an arbitrary temperature as well, but not without modifications of the source code.

To be able to run the program, a so-called model file defining e.g., the Lagrangian as well as mass matrices and an SLHA file containing numerical parameter values are required[26]. The first of these files can be generated with the help of the `Mathematica` package[27] `SARAH` (see [32]). The second file however, i.e., the SLHA file, needs to be created manually. As was mentioned earlier, the program operates in the Landau gauge and so the calculated VEVs and critical temperatures might not be physical, but the ratio $\zeta = \Delta v_C / T_C$ is.

Modifications

This program in its official form does not calculate $\zeta = v_C/T_C$, and so this had to be added to the code. Furthermore, the program was modified to have the possibility of producing files with data needed to plot an actual phase transition such as that in fig. 3a. These things were done by defining an array of temperatures and for each its values minimizing the temperature dependent potential to see where the phase transition occurs, saving the minima and corresponding temperatures in one data file and the corresponding critical values in another. As for $\mathcal{CP}$ violation, with some alterations the program works if complex potential parameters and complex phases on the VEVs are separated into real and imaginary parts. These alterations include making sure to use absolute values of the potential when finding the minima of the effective potential and changing two-dimensional arrays

[26] An SLHA (or, Supersymmetry Les Houches Accord as is the full name) file contains all the necessary information to define the model, i.e., all the parameter values. The conventions can be found in [31].

[27] This package should be used with caution, as it is not quite so general as it is claimed to be. For instance, it does not always calculate all tadpole equations, thus leaving out valuable information that can simplify calculations.

with VEVs to be four-dimensional, thus consisting of two sets of real and imaginary parts. After discussion with one of the authors of `Vevacious`, it was concluded that the changes can be included in the official release of the program.

4.2 `2HDMC`

`2HDMC` (see [23]) assumes a $\mathcal{CP}$ conserving 2HDM and has essentially everything needed when working with such models, e.g., the possibility for conventional basis changes, choices between the different types and calculation of the oblique parameters.

Modifications

- This program in its original form did not allow the user to break an initial $\mathbb{Z}_2$ symmetry by perturbing the Yukawa matrices in a way relevant for this study and so this had to be added. In order to do this, first assume that a model is of type[28] $l \in \{\text{I, II}\}$ so that $\rho_0^F = a_l^F \kappa_0^F$, where the coefficients a_l^F can be found in Eqs. (2.25) and (2.26). Now let $\rho_0^F = a_l^F \kappa_0^F \to a_l^F \kappa_0^F + \delta_0^F$ so that (cf. the inverse of Eq. (2.24))

$$\begin{aligned} \begin{pmatrix} \eta_1 \\ \eta_2 \end{pmatrix}^F \quad &\longrightarrow \quad \begin{pmatrix} \cos\beta & -\sin\beta \\ \sin\beta & \cos\beta \end{pmatrix} \begin{pmatrix} \kappa_0 \\ a_l\,\kappa_0 + \delta_0 \end{pmatrix}^F = \\ &= \quad \kappa_0^F \begin{pmatrix} \cos\beta - a_l^F \sin\beta \\ \sin\beta + a_l^F \cos\beta \end{pmatrix} + \delta_0^F \begin{pmatrix} -\sin\beta \\ \cos\beta \end{pmatrix} \end{aligned} \tag{4.1}$$

  in which Eq. (2.31) then can be used. This is what is implemented in the program.

Furthermore, methods were implemented for

- calculating the masses for a general $\mathcal{CP}$ violating model with the results from App. D,
- creating an SLHA file in the form required by `Vevacious`, both for violation and conservation of $\mathcal{CP}$,
- calculating the oblique parameters for a completely general $\mathcal{CP}$ violating 2HDM (for explicit expressions of these parameters, see App. E),
- calculating and checking the positivity constraints in Sec. 3.1.1, thus generalizing that already existing to the most general $\mathcal{CP}$ violating models,
- calculating and checking the unitarity constraints in Sec. 3.1.2, thus generalizing that already existing to the most general $\mathcal{CP}$ violating models,
- calculating and checking the perturbativity constraints in Sec. 3.1.3, thus generalizing that already existing to the most general $\mathcal{CP}$ violating models,

[28] The reason for not including types X and Y is that the leptons are so light and hence not expected to contribute much to the phase transition, i.e., when compared to for instance the top quark.

- calculating the discriminants $\tilde{D}$ and D defined in Sec. 3.1.4 (so that a discriminant can be calculated for the most general $\mathcal{CP}$ violating 2HDM),
- calculating the parameters in the Higgs basis corresponding to $\gamma = 0$ in terms of those in the general basis for a general $\mathcal{CP}$ violating 2HDM (this with the equations in App. C),
- calculating the parameters in the general basis in terms of those in the particular $\mathcal{CP}$ violating kinds of models defined in Sec. 5.2.2,
- setting the $h_i ff$, $h_i VV$ and $h_i h_j V$ couplings as in Sec. 5.2.2 (i.e., for $\mathcal{CP}$ violating models),
- calculating the angles α_1, α_2 and α_3 defined in Sec. 2.2.3 given the parameters in the general basis for any explicitly $\mathcal{CP}$ violating 2HDM.

Furthermore, the already existing classes `DecayTable.cpp` and `HBHS.cpp` in the `2HDMC` package were modified to allow the user to include `HiggsBounds` and `HiggsSignals` (see below) when having $\mathcal{CP}$ violating 2HDMs of the kind in Sec. 5.2.2. After discussion with one of the authors of `2HDMC`, it was concluded that some of the changes can be included in the official release of the program.

4.3 `HiggsBounds`

This program takes a given model and calculates predictions in the Higgs sector and checks these against experimental bounds from LEP, LHC and the Tevatron at 95% CL. In general, this program takes as input the Higgs particles' respective masses, branching ratios and cross sections normalized to some reference values. In particular, it identifies which channel is most constraining and uses that exclusively to constrain the model in question. For more information, see [33]. This program together with `HiggsSignals` (see below) are what is used to do that described in Sec. 3.2.2.

4.4 `HiggsSignals`

This program takes a given model and calculates a χ^2 value yielding the "goodness of fit" to experimental data from the LHC and the Tevatron. The calculated value can then be used for a given p value and n degrees of freedom to measure how good a point in parameter space is. The input for this program is the same as that for `HiggsBounds`. For more information, see e.g. [34]. This program together with `HiggsBounds` are what is used to do that described in Sec. 3.2.2.

4.5 ParamGen and ParamGenComplex

These programs were created for the sole purpose of generating points in parameter space (with the help of a random number generator form GSL) which are then sent to Vevacious to calculate ζ, after which experimental constraints are checked with the help of HiggsSignals and HiggsBounds. The whole chain of events is represented in fig. 2 below in the form of a flow chart. There, the dashed black arrow is the first one, indicating that user input is given to ParamGen/ParamGenComplex. Once this input has been received 2HDMC, HiggsBounds and HiggsSignals are called to evaluate[29] a, in ParamGen or ParamGenComplex, randomly generated point and produce an SLHA file, which is then sent to Vevacious. After this, Vevacious, with the help of the model file produced beforehand by SARAH, generates a file with information about the EWPT for the given point, which, as is indicated by the red arrows, ParamGen/ParamGenComplex obtains and then sends to the advanced plotting program ROOT (see [35]) along with other information obtained from the process in the filled black circle. ROOT then creates a file with information stored in a tree structure. This last file can then be used in any convenient way, as indicated by the dashed red arrow and box with dots.

The first of the programs, i.e., ParamGen, assumes $\mathcal{CP}$ conservation whereas the other does not.

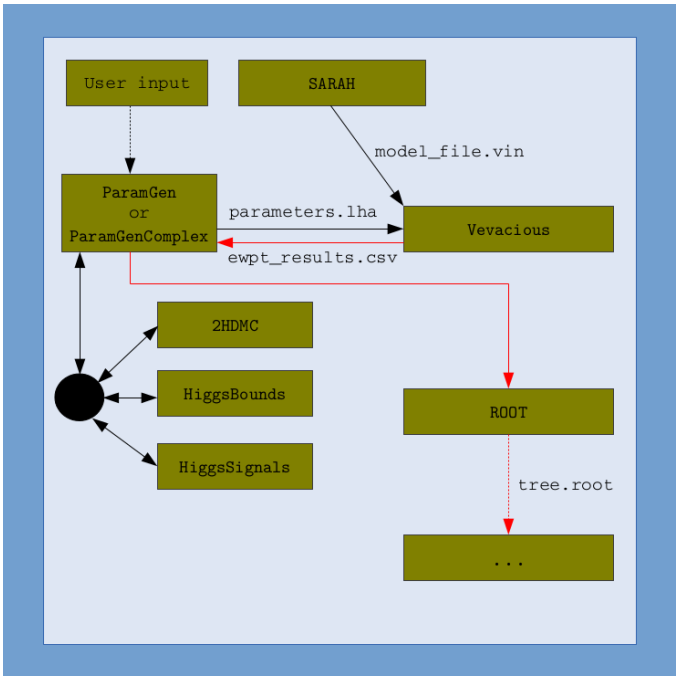

Figure 2: A flow chart representing the process of calculating the quantities of interest, starting from user input and ending with a tree file.

[29]The filled black circle represents the fact that that the three called programs communicate also with each other.

5 Results

In this section the results of the study are presented. Naturally, the section has been divided into two subsections, the first of which deals with $\mathcal{CP}$ conserving models and the second of which deals with $\mathcal{CP}$ violating models. Common for both sections is studies of the parameter space, which are performed in order to see where "good" points exist. The reason why this is interesting to do is the possibility of excluding regions which would otherwise have to be taken into account in further analyses[30]. In particular, this is done for a number of specific kinds of 2HDMs, defined in the respective subsections.

5.1 $\mathcal{CP}$ conserving systems

This section is divided into three subsections. The first of these introduces the mentioned convenient Hybrid basis, which is used for all studies presented in this section. The latter two present results for particular kinds of $\mathbb{Z}_2$ breaking 2HDMs with different Yukawa structures. The different models defined in these two subsections are compared to each other as the results are presented. Unless stated otherwise, all parameters are uniformly distributed.

5.1.1 Hybrid basis

The main problem with the general basis is that it is hard to get an intuitive feeling for what values the parameters can have so that physically relevant points are chosen. Even though the Higgs bases are very useful in some cases, choosing parameters there is just as complicated as when using the general basis. It would be much more convenient to have as parameters masses and couplings for some of the scalar particles. This is one of the reasons the so-called Hybrid basis has been developed (see [36] for a more detailed review).

As the name suggests, this basis is a hybrid in the sense that it uses both phenomenologically important parameters and some of the parameters from the Higgs bases' tree level potential. It assumes a, in the general basis[31], softly broken $\mathbb{Z}_2$ symmetric and $\mathcal{CP}$ conserving 2HDM. As was pointed out in Sec. 1, the discovered Higgs boson h_{SM} just corresponds to one of the neutral scalars in the 2HDM, i.e., in this case, to either h or H. In fact, the vector couplings are

$$g_{hVV} = g_{h_{SM}VV} \sin(\beta - \alpha), \quad g_{HVV} = g_{h_{SM}VV} \cos(\beta - \alpha) \tag{5.1}$$

[30] Having regions of many "good" points would show that a certain model in the regions in question is stable against small perturbations in the parameters, but there is always the possibility that a completely isolated (possibly non-investigated) and hence fine-tuned "good" point could be the correct one.

[31] Note that as the basis change from the general basis to the Higgs bases consists of making linear combinations of the fields, having a $\mathbb{Z}_2$ symmetric potential in the general basis does not necessarily give a $\mathbb{Z}_2$ symmetric potential in the Higgs bases.

where $V \in \{Z,\, W^{\pm}\}$ so that something already is known about either h or H. By convention[32], $\sin(\beta-\alpha) \in [0,1]$ and $\cos(\beta-\alpha) \in [-1,1]$. The Hybrid basis is then given by the parameters

$$m_h,\, m_H,\, \cos(\beta-\alpha),\, \tan\beta,\, \Lambda_4,\, \Lambda_5,\, \Lambda_7 \tag{5.2}$$

where Λ_4, Λ_5 and Λ_7 are quartic couplings from the Higgs basis and should be[33] of $\mathcal{O}(1)$. The other scalar masses are

$$m_A^2 = m_H^2 \sin^2(\beta-\alpha) + m_h^2 \cos^2(\beta-\alpha) - v^2\Lambda_5 \tag{5.3}$$

and

$$m_{H^\pm}^2 = m_A^2 - \frac{1}{2}v^2(\Lambda_4-\Lambda_5) = m_H^2 \sin^2(\beta-\alpha) + m_h^2 \cos^2(\beta-\alpha) - \frac{1}{2}v^2(\Lambda_4+\Lambda_5) \tag{5.4}$$

The Hybrid basis' parameters can be expressed in terms of the general basis' parameters by using the relations in App. C with $\lambda_6 = \lambda_7 = \gamma = \xi = 0$.

5.1.2 Flavour diagonal $\mathbb{Z}_2$ breaking models

Model A

Model A is a 2HDM with an initial type II $\mathbb{Z}_2$ symmetry which is then broken by both allowing λ_6, $\lambda_7 \in (-\pi,\, \pi)$ and perturbing the ρ matrices diagonally (see Eq. (4.1)). In particular, $\rho_{ii} \to \rho_{ii} + \tilde{u}_{ii}\,\rho_{ii}$ for $i \in \{b,\, t\}$ and $\tilde{u}_{ii} \sim \text{unif}(-0.1, 0.1)$, and the reason for only perturbing the tt and bb elements is that the corresponding quarks are the heaviest and hence should contribute most (recall that each term in the effective potential in Eq. (2.34) is weighted with the masses). The parameters Λ_4, Λ_5, $\Lambda_7 \in (-1,\, 1)$. Furthermore, $\tan\beta \in (1/2,\, e^4)$ (where $e^4 \approx 54.6$), is distributed logarithmically. h is here taken to be the discovered scalar with a mass of 125 GeV and $m_H \in (125, 800)$ (with implicit unit GeV). The above intervals within which to generate parameters have been chosen for reasons of perturbativity and unitarity. Here, roughly 10^5 points are used.

For illustration, first consider some examples of the phase diagram of a model such as Model A. In fig. 3a the electroweak phase transition is plotted for a certain parameter point where the scalar masses are $m_h = 125$ GeV (by definition), $m_H = 768$ GeV, $m_A = 534$ GeV and $m_{H^\pm} = 518$ GeV. In particular, $v_C \approx 430$ GeV and $T_C \approx 430$ GeV and hence $\zeta \approx 1.0$ and the transition is strongly first order. Note that v increases to about 500 GeV as the temperature goes to zero, and although this is far from the tree level minimum at roughly 246 GeV one should remember that the calculation is done in the Landau gauge and hence

[32]Note that this is not the internal convention used by `2HDMC`, something which has to be remembered when using the Hybrid basis there.

[33]This choice is for reasons of perturbativity and unitarity. Also, these parameters parametrize squared mass differences between the physical particles (as can be seen from e.g., Eq. (2.20)).

only the ratio ζ is physical (as was remarked in Sec. 4.1). As opposed to this very nice behaviour, there are a lot of points resulting in EWPTs as that shown in fig. 3b where the transition in question is more of a continuous process. The strength of the transition for the corresponding point is $\zeta \sim 10^{-4}$ and hence very far from what is sought. In fig. 3c another very interesting behaviour of the EWPT occurs, where there is a jump between two non-zero minima at roughly $T = 350$ GeV. The reason for this comes from having two scalar fields, something which yields a richer vacuum structure (this possibility was already noted in Sec. 2.2.2). Also this transition is strongly first order.

In fig. 3d the distribution of ζ is plotted for roughly 10^4 points, and as can be seen there is a clear peak around $\zeta = 0.7$ and then essentially monotonically decreasing behaviour as ζ increases. Note that the vast majority of points have very small ζ, however.

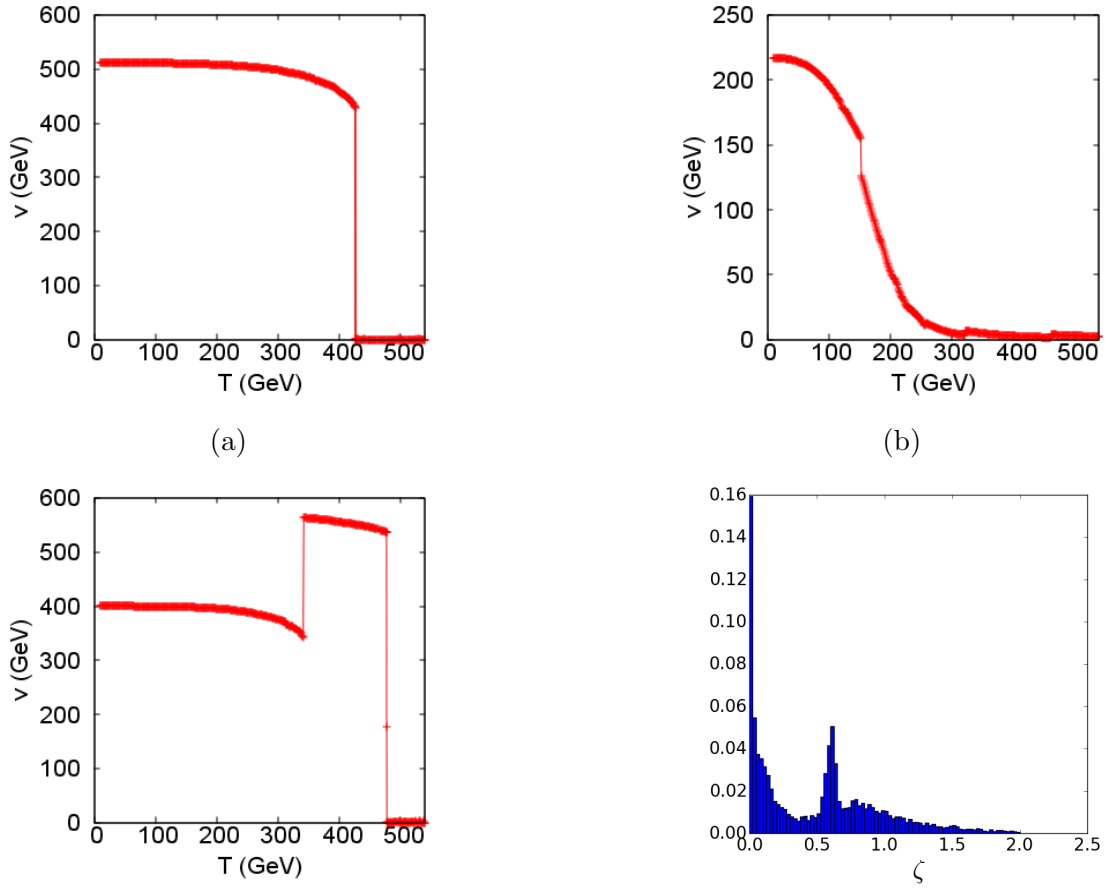

Figure 3: Examples and properties of the EWPT in a $\mathcal{CP}$ conserving 2HDM: (a) A strongly first order phase transition. (b) A very weak, or, second order, phase transition. (c) A strongly first order phase transition, where the rich vacuum structure of the 2HDMs is exposed. (d) The distribution of ζ.

Now consider the parameter space of the model, this in order to see the dependence on some of the parameters. In fig. 4a the two-dimensional section of parameter space spanned by $\tan\beta$ and $c_{\beta-\alpha} = \cos(\beta-\alpha)$ is plotted. The colour convention (and order of plotting) is as follows:

- *Black points:* Satisfy only positivity.
- *Yellow points:* Satisfy positivity, unitarity and perturbativity (for simplicity, call this set of constraints PUP).
- *Green points:* Satisfy PUP and $\zeta \gtrsim 1$ (for simplicity, call this latter constraint PT)
- *Blue points:* Satisfy PUP and constraints from Higgs searches and measurements (for simplicity, call these two latter constraints HP).
- *Red points:* Satisfy PUP, PT, HP, the discriminant condition and the condition to be within the 90% CL ellipse ϵ_{ST} in the ST-plane (for simplicity, call these two latter constraints D and OBL, respectively).

The above colour convention is used in all the other parameter space plots in this section as well. As can be seen in the figure in question, there is a substantial amount of red points (which, except for flavour physics constraints, are "good" points) centered around $c_{\beta-\alpha} = 0$. This is expected as (cf. Eq. (5.1)) it was assumed that $h = h_{SM}$ and so it must hold that $s_{\beta-\alpha} = \sin(\beta-\alpha) \approx 1$ for $g_{hVV} \approx g_{h_{SM}VV}$ where $V \in \{Z, W^{\pm}\}$. However, despite this expected behaviour there are points all the way out to $|c_{\beta-\alpha}| \approx 0.5$, something which can be understood as a result from the many additional phenomenological consequences due to the extra scalars. Note that $\tan\beta \lesssim 10$ are favoured for non-black points in general, and that there is a horizontal band of green (and also red) points around $\tan\beta = 1$, i.e., with strong phase transitions.

The flavour physics constraints are displayed in fig. 4b (the black points have been excluded for clarity). The allowed region is the upper right rectangle, and as can be seen a substantial amount of red points lie within the area in question, thus surviving all the imposed constraints. However, as was noted in Sec. 3.2.3, although the limits are conservative the fact that the Yukawa sector is not $\mathbb{Z}_2$ symmetric should in principle "smear" them out and points close to the limits could be either excluded or allowed. It should be noted, however, that there indeed is a quite good amount of points not close to the limits in question and so should satisfy the flavour constraints.

In fig. 4c the ST-plane is plotted together with the ellipse ϵ_{ST} corresponding to 90% CL. As can be seen, there is a large number of points satisfying both HP and PT constraints outside ϵ_{ST} but a reasonable amount of points still reside within it. All in all, this shows that 2HDMs of this kind can have a neutral scalar with mass 125 GeV as well as satisfy certain theoretical and experimental constraints all the while having a sufficiently strong first order phase transition. This is of course very nice but as far as EWBG is concerned not much can be said, this since the vital $\mathcal{CP}$ violation is absent.

It is of course interesting to see how the strength of the phase transition, i.e., ζ, depends on the parameters λ_6 and λ_7 breaking the $\mathbb{Z}_2$ symmetry maximally, as well as on $\tan\beta$, which fixes the position of the minimum in the v_1v_2-plane, the perturbations in the Yukawa sector and the scalar masses. First consider the dependence on λ_6 and λ_7. In fig. 4e no clear correlation can be seen between strength of the EWPT and λ_6 and the same conclusion can be drawn from fig. 4f for the dependence on λ_7. Moreover, as these plots suggest, there are not many "good" points when $|\lambda_{6,7}| \gtrsim 2$ and so the choice to have $\lambda_{6,7} \in (-\pi, \pi)$ is not so arbitrary[34] (a similar reasoning holds for $|\Lambda_{4,5,7}| \gtrsim 1$).

Next consider the correlation between ζ and $\tan\beta$. In fig. 4d the number of points satisfying a strong phase transition decreases rapidly as $\tan\beta$ increases, with only a handful of allowed (i.e., with $\zeta \gtrsim 1$) points for $\tan\beta \gtrsim 10$, of which even less are "good". So, it would seem that for these kinds of models parameter space scans can be restricted to $\tan\beta \in (\sim 1, \sim 10)$ and $\lambda_{6,7} \in (-\pi, \pi)$ with good reason. This last result shows some discrepancy with a favoured large $\tan\beta$ to explain the mass difference between the top and the bottom quark (for more information, see e.g., [37]), but then again having a large $\tan\beta$ could be interpreted as a hierarchy problem for the scalar VEVs instead. It should also be noted that the 2HDMs might not have the final answer to every problem of the SM, but as every supersymmetric model requires a Higgs sector at least as complicated as that of the 2HDM a lot can be learned from these studies.

Finally consider how ζ depends on the scalar masses as well as ρ_{bb} and ρ_{tt}. In figs. 5a-5c, it can be seen that PT prefers scalar masses $\lesssim 400$ GeV but the other constraints require $m_{H^\pm}$, m_H, $m_A \gtrsim 400$ GeV. As can be seen in figs. 5d and 5e, ζ is clearly independent of the perturbations in the Yukawa sector. This is actually expected, as ρ (which is not related to the masses) on this level does not enter into the effective potential (see Sec. 2.2.5). Note, however, that it was not unnecessary to include the perturbations in question, since they can affect the experimental constraints.

[34] Simulations with $\lambda_{6,7} \in (-4\pi, 4\pi)$ showed exactly this, but the corresponding plots are here not included.

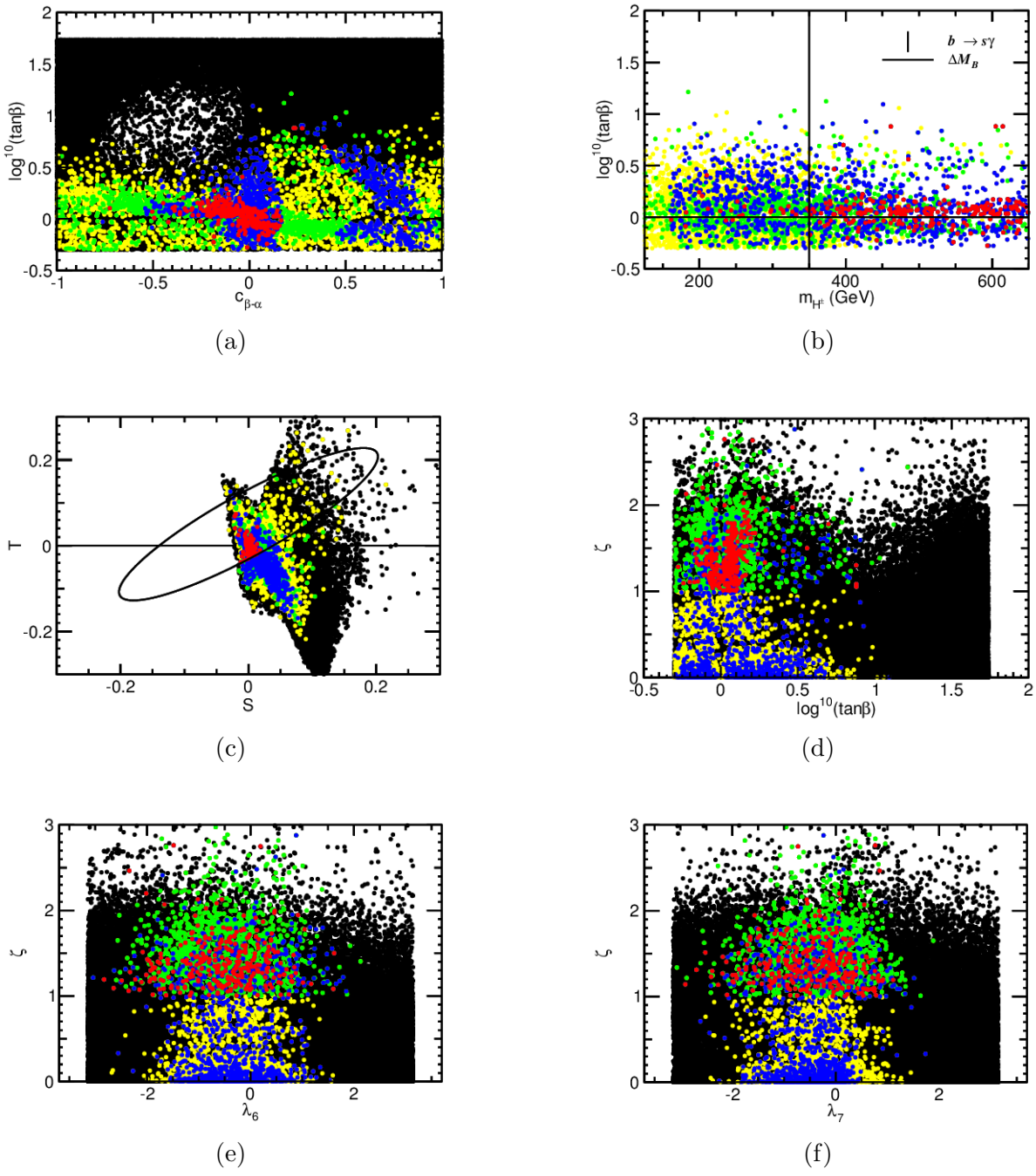

Figure 4: A collection of figures for Model A: (a)–(b) The section of parameter space spanned by (a) $\tan\beta$ and $c_{\beta-\alpha} = \cos(\beta-\alpha)$, and (b) $\tan\beta$ and $m_{H^\pm}$. (c) The ellipse ϵ_{ST} in the ST-plane. (d)–(f) The strength of the EWPT, ζ, as a function of (d) $\tan\beta$, (e) λ_6 and (f) λ_7.

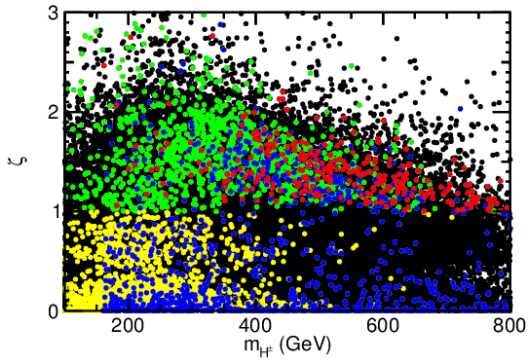

(a)

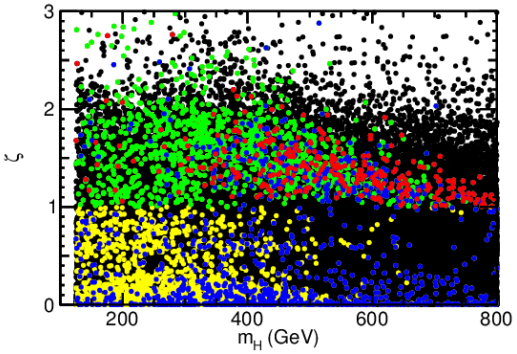

(b)

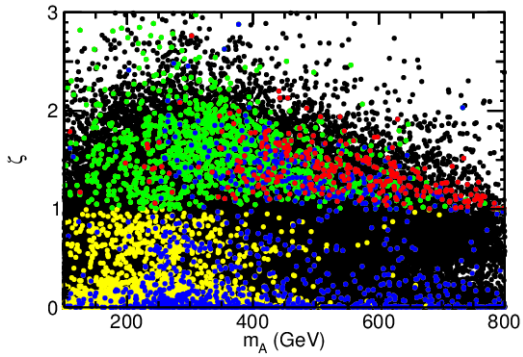

(c)

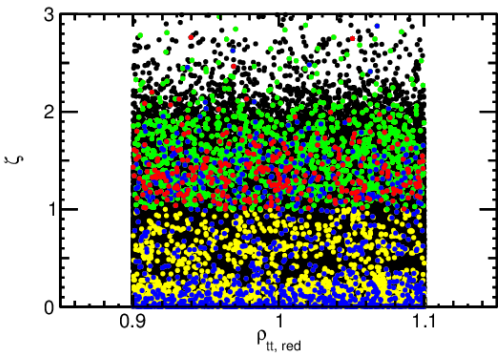

(d)

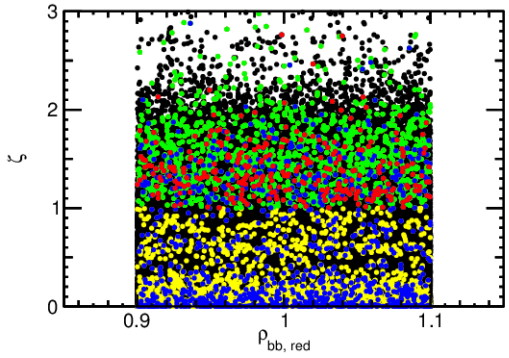

(e)

Figure 5: A collection of figures for Model A: The strength of the EWPT, ζ, as a function of (a) $m_{H^\pm}$, (b) m_H, (c) m_A, (d) the relative difference in ρ_{tt} defined as $\rho_{tt,red}$, the ratio between perturbed and unperturbed ρ_{tt}, (e) the relative difference in ρ_{bb} defined as $\rho_{bb,red}$, the ratio between perturbed and unperturbed ρ_{bb}.

Model B

Here, everything is exactly the same as in Model A except for the initial symmetry in the Yukawa sector, here instead being type I. The qualitative behaviour of the phase transitions is the same as in Model A, so such plots are here not included. Looking at fig. 6a, it can be seen that there is a substantial amount of red points, these again centered around $c_{\beta-\alpha} = 0$, which, as was remarked for Model A, is just as expected. Again there is a band of green points around $\tan\beta = 1$ and $\tan\beta \lesssim 10$ are favoured. What can be noted however, is that the triangular area not allowed for $c_{\beta-\alpha} \gtrsim 0.2$ in Model A is in fact allowed for Model B. Such behaviour is not so unexpected because some differences should occur since the initial symmetries are different.

Looking at the constraints from flavour physics, i.e., in fig. 6b, there is a quite decent amount of "good" points in the allowed region (the upper rectangle). However, there are not as many as for Model A and one thing that can be noted is the requirement for higher $\tan\beta$. This is of course good with respect to the mentioned quark mass hierarchy, but as the number of points surviving as $\tan\beta$ increases decreases there is clearly tension between PT and the flavour physics constraints, which thus can be seen as a problem for type I models. Furthermore, as is remarked in [2], the baryon asymmetry is suppressed with $\cot^2\beta$ (remember that this is not really relevant for $\mathcal{CP}$ conserving models, however). Therefore, in the remainder of this section only Type II models will be considered. Again, the limits are not exact as the Yukawa sector $\mathbb{Z}_2$ symmetry is broken.

The ST-plane in fig. 7a is quite similar to the corresponding one in Model A and no qualitative difference can be seen. The dependence of ζ on $\tan\beta$, λ_6, λ_7, $m_{H^\pm}$, m_H, m_A and the Yukawa perturbations, as shown in figs. 7b-8, is also qualitatively the same as for Model A. To summarize, Model B, just as Model A, allows for a substantial amount of "good" points, but requires larger $\tan\beta$ values than Model A due to flavour physics constraints.

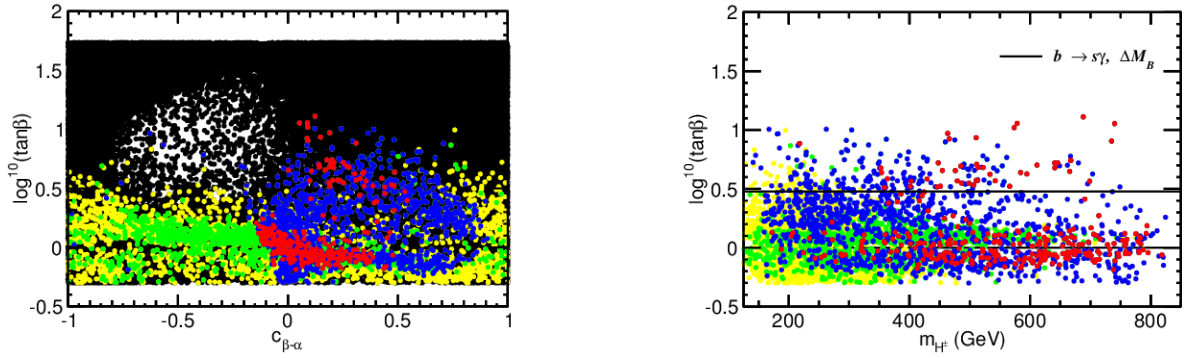

(a) (b)

Figure 6: A collection of figures for Model B: The section of parameter space spanned by (a) $\tan\beta$ and $c_{\beta-\alpha} = \cos(\beta-\alpha)$, and (b) $\tan\beta$ and $m_{H^\pm}$.

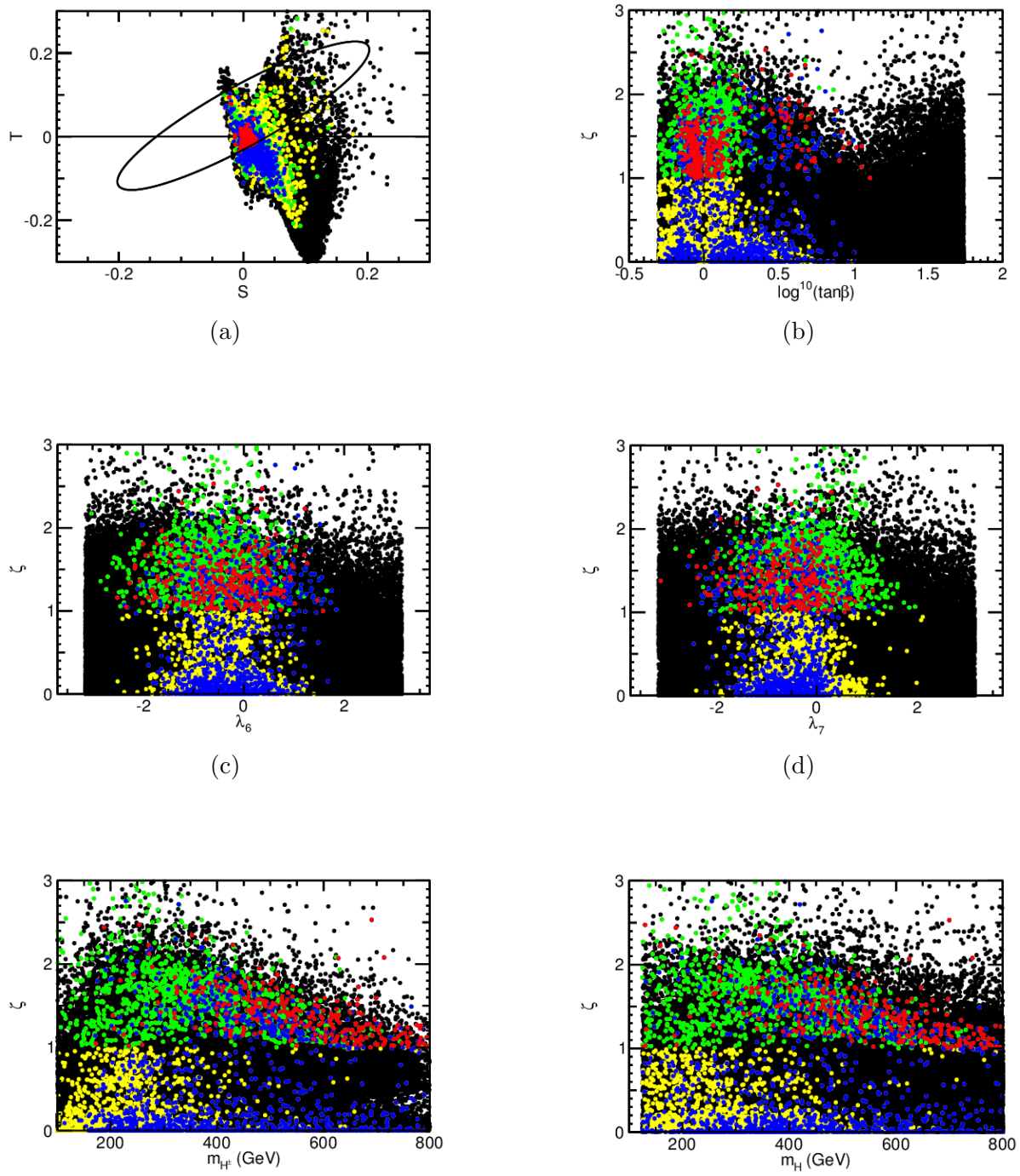

Figure 7: A collection of figures for Model B: (a) The ellipse ϵ_{ST} in the ST-plane. (b)–(f) The strength of the EWPT, ζ, as a function of (b) $\tan\beta$, (c) λ_6, (d) λ_7, (e) $m_{H^\pm}$ and (f) m_H.

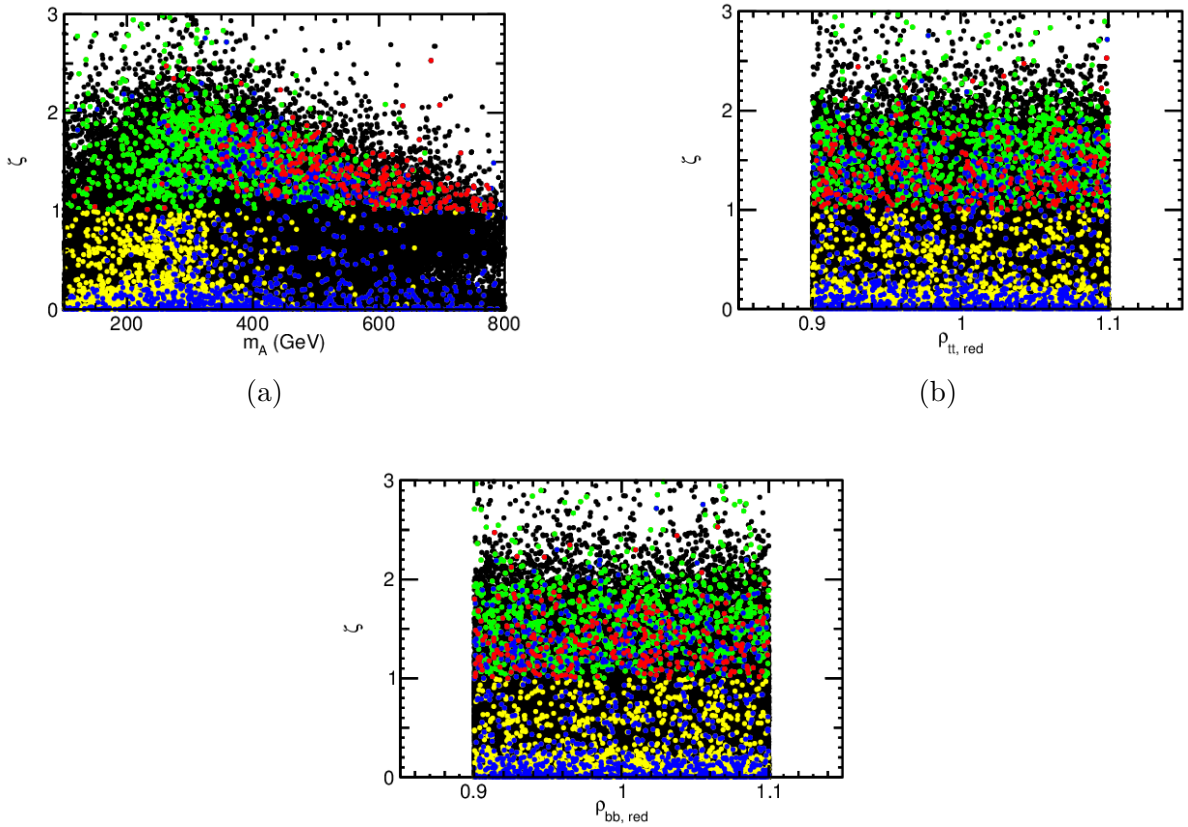

Figure 8: A collection of figures for Model B: The strength of the EWPT, ζ, as a function of (a) m_A, (b) the relative difference in ρ_{tt} defined as $\rho_{tt,red}$, the ratio between perturbed and unperturbed ρ_{tt}, and (c) the relative difference in ρ_{bb} defined as $\rho_{bb,red}$, the ratio between perturbed and unperturbed ρ_{bb}.

5.1.3 Flavour non-diagonal $\mathbb{Z}_2$ breaking models

The kinds of models dealt with here are generalizations of Model A and Model B defined above. Now, because of the problem with favouring of higher $\tan\beta$ in Type I models, as with Model B, only a generalization of Model A, the so-called Model A', is here presented. However, as is mentioned below, a Model B' was also studied.

Model A'

As before for Model A, here a study of roughly 10^5 points for a 2HDM with an initial type II symmetry which is then broken by both allowing λ_6, $\lambda_7 \in (-\pi, \pi)$ and perturbing the ρ matrices non-diagonally (see Eq. (4.1)) is presented. In particular, for $\tilde{u}_{ij} \sim \text{unif}\,(-0.1, 0.1)$, $\rho_{ii} \to \rho_{ii} + \tilde{u}_{ii}\,\rho_{ii}$ for $i \in \{b,\, t\}$ and $\rho_{ji} = \rho_{ij} = 0 \to \tilde{u}_{ij}\,\tilde{\lambda}_{ij}\frac{\sqrt{2m_i m_j}}{v} \equiv \lambda_{ij}\frac{\sqrt{2m_i m_j}}{v}$ for $i \neq j$ and $i,\, j \in \{c,\, t\}$. The reason for only perturbing the t, c and b elements is the same as for

Model A but here including c as well. Note that this choice of perturbations is inspired[35] by the Cheng-Sher ansatz and the experimental constraints mentioned under Eq. (2.29). Everything else, including the colour conventions in the plots below, is the same as for Model A.

As can be seen when comparing figs. 9a-10b to figs. 4a-4d, essentially nothing is different between Model A and Model A'. Perhaps the chosen perturbations were too small to make a difference, this as the experimental limits should exclude points with too large non-diagonal elements. Furthermore, as can be seen in fig. 10c, ζ is clearly independent of the Yukawa perturbations in the ct and tc sector. The same is true for the bb and tt sectors (not shown here).

Similar studies were performed for Model B', i.e., a Model B with perturbations in the ct and tc sectors, and it was found that nothing changed as compared to Model B either.

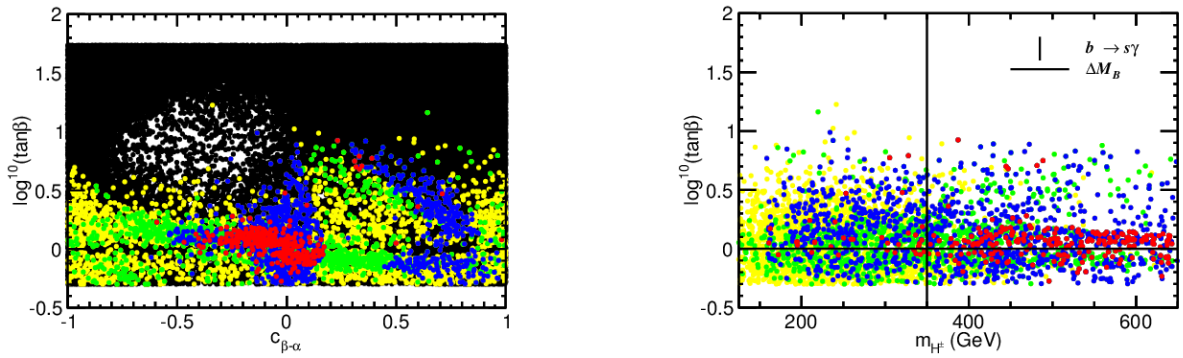

(a) (b)

Figure 9: A collection of figures for Model A': The section of parameter space spanned by (a) $\tan\beta$ and $c_{\beta-\alpha} = \cos(\beta-\alpha)$, and (b) $\tan\beta$ and $m_{H^\pm}$.

[35] Although there are no limits on λ_{ct} or λ_{tc} in [13] it is reasonable to believe that λ_{ct} and λ_{tc} should be constrained in the same way as the other λ_{ij}.

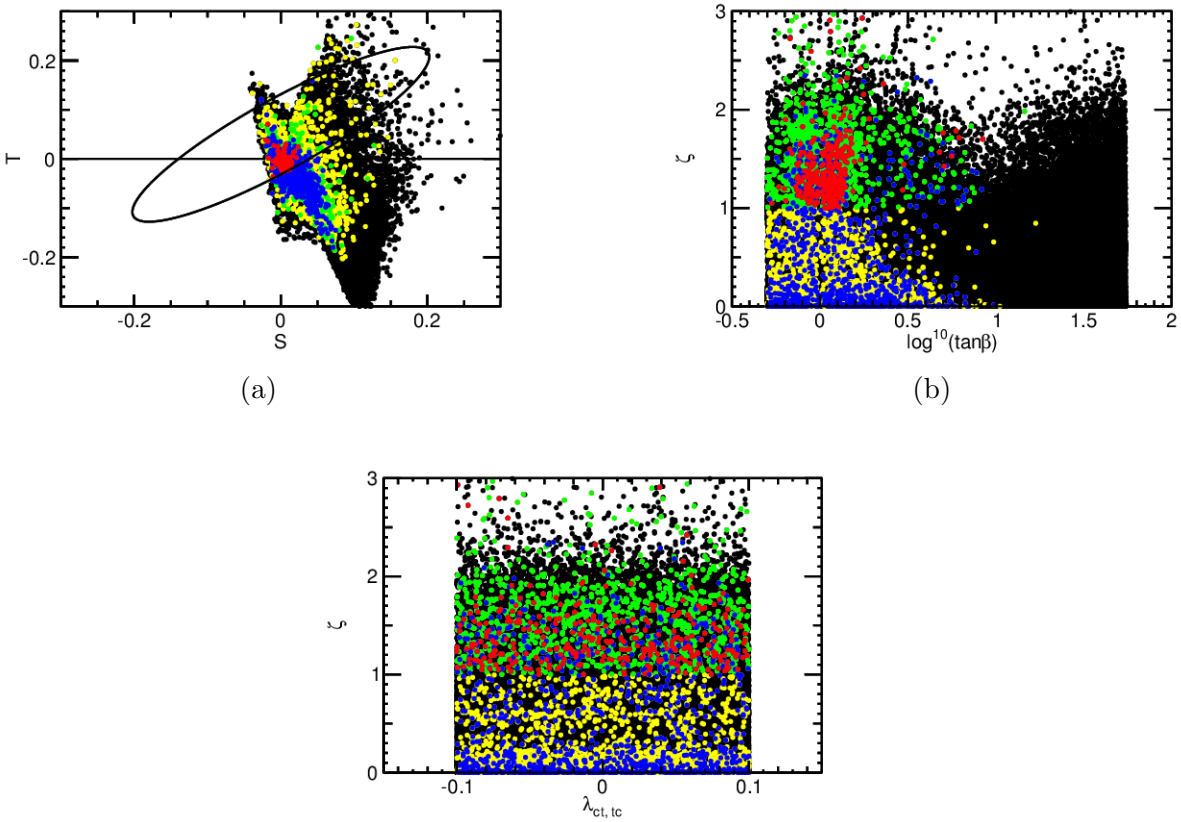

(a) (b) (c)

Figure 10: A collection of figures for Model A': (a) The ellipse ϵ_{ST} in the ST-plane. (b)–(c) The strength of the EWPT, ζ, as a function of (b) $\tan\beta$ and (c) $\lambda_{ct,tc}$.

5.2 $\mathcal{CP}$ violating systems

This section is divided into two subsections. Each of these presents results from certain kinds of $\mathcal{CP}$ violating 2HDMs and comparisons between the different ones are made continuously as the results are presented. Again, unless otherwise stated all parameters generated for the parameter space scans are uniformly distributed.

5.2.1 The masses and $\mathcal{CP}$ violation

It is clear from the rotation matrix in Eq. (2.17) that the masses will depend on the $\mathcal{CP}$ violating mixing angles (i.e., the angles parametrizing how the neutral scalars mix). However, it is not clear how large the effects are. Below, an illustrative example showing this for a spontaneously $\mathcal{CP}$ violating 2HDM is presented.

Consider a parameter space point[36] from the $\mathcal{CP}$ conserving case with initial type II symmetry and non-diagonal perturbations according to the Cheng-Sher Ansatz, where $m_h = 125$ GeV and the other scalar masses are $m_A = 104$ GeV, $m_H = 627$ GeV and $m_{H^\pm} = 140$ GeV. Next introduce spontaneous $\mathcal{CP}$ violation, i.e., allow non-zero complex phases so that $v_j = |v_j| e^{i\xi_j}$, and let the angles vary in ξ_1, $\xi_2 \in (0, \pi)$. In particular, as one Higgs mass has been found to be ≈ 125 GeV one of the neutral scalar masses, m_{h_i}, say, should lie close to 125 GeV. Here, 10^5 points are used in the particular phase interval and it is required that at least one $m_{h_i} \in (120, 130)$ (with implicit unit GeV). The colour conventions in figs. 11a and 11b is as follows:

- *Black points:* No m_{h_j} exists in the interval in question,
- *Green points:* At least one m_{h_j} exists in the interval in question,

As can be seen, in fig. 11a there are three green bands of allowed points. First of all, this shows that it is sufficient to look at the difference $\Delta\xi = \xi_2 - \xi_1$ as the two outer bands lie symetrically around the line $\xi_1 = \xi_2$. The reason why there are three can be more easily understood by comparing with another parameter point. Therefore consider a parameter space point with the remaining scalar masses as $m_A = 571$ GeV, $m_H = 636$ GeV and $m_{H^\pm} = 551$ GeV. In fig. 11b, corresponding to the second parameter space point, there is only one band. Looking at the two respective initial sets of scalar masses of the two points it is clear that there is one major difference: for the first parameter point A and h have a very small mass difference whereas there are no such small neutral scalar mass differences for point two. Thus, for the first parameter point in the two outer bands A and h have switched roles so that $m_A \overset{\Delta\xi\neq 0}{\longrightarrow} m_{h_i} \in (120, 130)$. No such transition occurs for the second parameter point and therefore there is only one band. This simple example shows that the $\mathcal{CP}$ violating phases do affect the masses severely and that it is not possible to take a point from the $\mathcal{CP}$ conserving case and simply add $\mathcal{CP}$ violating phases whilst not expecting any major consequences. Hence, a proper parameter space study is required also for $\mathcal{CP}$ violating 2HDMs. Because of the low amount of available material concerning 2HDMs with both explicit and spontaneous $\mathcal{CP}$ violation, only 2HDMs with explicit $\mathcal{CP}$ violation are investigated below.

[36]The points chosen in this section are chosen because of mass differences between the neutral scalars, a valid choice as other properties such as how well they satisfy the constraints in Sec. 3 do not come into the equations of the masses (see App. D).

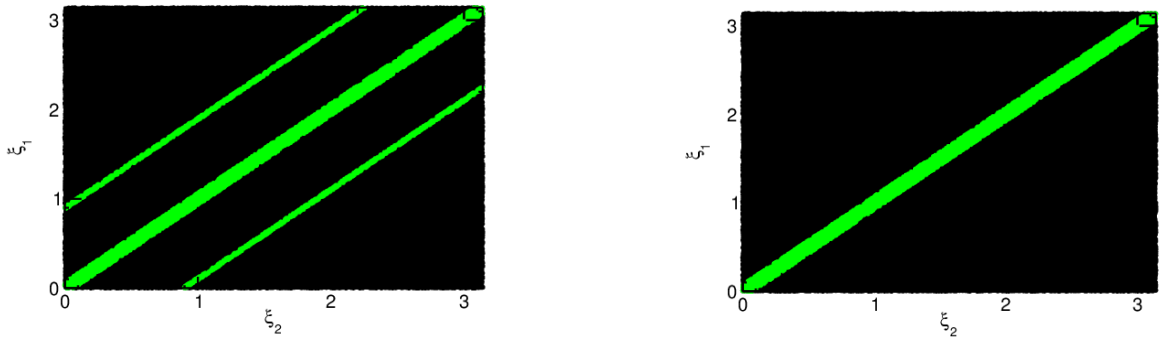

(a) (b)

Figure 11: The mass dependence on spontaneous $\mathcal{CP}$ violation, as seen in the $\xi_1\xi_2$-plane: A parameter space point with (a) small initial mass difference between h and A, and (b) large initial mass difference between h and A.

5.2.2 Flavour diagonal explicitly $\mathcal{CP}$ violating 2HDMs

In this section, results from studies of explicitly $\mathcal{CP}$ violating flavour diagonal 2HDMs are presented in respective subsections. Before going on to the results however, a basis useful for choosing phenomenologically relevant parameter space points is presented.

Phenomenological basis of parameters for explicitly $\mathcal{CP}$ violating softly $\mathbb{Z}_2$ breaking 2HDMs

In [29] a basis of use to parameter scans for explicitly $\mathcal{CP}$ violating softly $\mathbb{Z}_2$ breaking 2HDMs is presented. In particular, a parametrization is there presented which takes as input phenomenologically relevant parameters and translates these into the parameters of the general basis. To obtain the relations between the two bases the squared mass matrix in the general basis,

$$\mathcal{M}^2_{gen} = v^2 \begin{pmatrix} \lambda_1 c_\beta^2 + \nu s_\beta^2 & (\lambda_{345} - \nu)\, c_\beta s_\beta & -\frac{1}{2} s_\beta \Im(\lambda_5) \\ (\lambda_{345} - \nu)\, c_\beta s_\beta & \lambda_2 s_\beta^2 + \nu c_\beta^2 & -\frac{1}{2} c_\beta \Im(\lambda_5) \\ -\frac{1}{2} s_\beta \Im(\lambda_5) & -\frac{1}{2} c_\beta \Im(\lambda_5) & -\Re(\lambda_5) + \nu \end{pmatrix} \tag{5.5}$$

where $\nu = \frac{\Re(m_{12}^2)}{2v_1 v_2}$ and $\lambda_{345} = \lambda_3 + \lambda_4 - \Re(\lambda_5)$, is used (as a sidenote, this is a symmetric 3×3 matrix and so has six independent elements). A rotation matrix, R, of the same form as R_3 in Eq. (2.17) but for angles α, α_b and α_c, is then defined so that $\text{diag}\left(m_{h_1}^2, m_{h_2}^2, m_{h_3}^2\right) = R\,\mathcal{M}^2_{gen} R^{\mathrm{T}}$. This last equation can be rewritten as $\mathcal{M}^2_{gen} = R^{\mathrm{T}} \text{diag}\left(m_{h_1}^2, m_{h_2}^2, m_{h_3}^2\right) R$ which is a linear system of equations from which the general basis parameters can be solved for in terms of the nine parameters m_{h_1}, m_{h_2}, m_{h_3}, $m_{H^\pm}$, ν, $\tan\beta$, α, α_b and α_c. The results for the parameters λ_i are

$$\lambda_1 = \frac{m_{h_1}^2 \sin^2\alpha \cos^2\alpha_b + m_{h_2}^2 R_{21}^2 + m_{h_3}^2 R_{31}^2}{v^2 \cos^2\beta} \tag{5.6}$$

$$\lambda_2 = \frac{m_{h_1}^2 \cos^2\alpha \cos^2\alpha_b + m_{h_2}^2 R_{22}^2 + m_{h_3}^2 R_{32}^2}{v^2 \sin^2\beta} \tag{5.7}$$

$$\Re\left(\lambda_5\right) = \nu - \frac{m_{h_1}^2 \sin^2\alpha_b + \cos^2\alpha_b \left(m_{h_2}^2 \sin^2\alpha_c + m_{h_3}^2 \cos^2\alpha_c\right)}{v^2} \tag{5.8}$$

$$\lambda_4 = 2\nu - \Re\left(\lambda_5\right) - \frac{2m_{H^\pm}^2}{v^2} \tag{5.9}$$

$$\lambda_3 = \nu - \frac{m_{h_1}^2 \sin\alpha \cos\alpha \cos^2\alpha_b - m_{h_2}^2 R_{21} R_{22} - m_{h_3}^2 R_{31} R_{32}}{v_1 v_2} - \lambda_4 - \Re\left(\lambda_5\right) \tag{5.10}$$

$$\begin{aligned} \Im\left(\lambda_5\right) \;=\; & \frac{2\cos\alpha_b}{v^2 \sin\beta}\Big[\left(m_{h_2}^2 - m_{h_3}^2\right) \cos\alpha \sin\alpha_c \cos\alpha_c + \\ & + \left(m_{h_1}^2 - m_{h_2}^2 \sin^2\alpha_c - m_{h_3}^2 \cos^2\alpha_c\right) \sin\alpha \sin\alpha_b \Big] \end{aligned} \tag{5.11}$$

However, as can be seen in the equation

$$\tan\beta = \frac{\left(m_{h_2}^2 - m_{h_3}^2\right) \cos\alpha_c \sin\alpha_c + \left(m_{h_1}^2 - m_{h_2}^2 \sin^2\alpha_c - m_{h_3}^2 \cos^2\alpha_c\right) \tan\alpha \sin\alpha_b}{\left(m_{h_2}^2 - m_{h_3}^2\right) \tan\alpha \cos\alpha_c \sin\alpha_c - \left(m_{h_1}^2 - m_{h_2}^2 \sin^2\alpha_c - m_{h_3}^2 \cos^2\alpha_c\right) \sin\alpha_b} \tag{5.12}$$

$\tan\beta$ is not necessarily a free parameter any longer (i.e., unless one of the other parameters in the equation is solved for in terms of $\tan\beta$ and the remaining ones). Furthermore, since one of the neutral scalars should have a mass of ≈ 125 GeV there are effectively only seven $(9 - 2 = 7)$ free parameters in the phenomenological basis.

Next consider the couplings of the neutral scalars to fermions (for the flavor diagonal case) and gauge bosons. These can be parametrized as [29]

$$\mathcal{L}_{hff} + \mathcal{L}_{hVV} = -\frac{m_f}{v} h_j \left(c_{f,j} \bar{f} f + \tilde{c}_{f,j} \bar{f} i\gamma_5 f\right) + a_j h_j \left(\frac{2m_W^2}{v} W_\mu W^\mu + \frac{m_Z^2}{v} Z_\mu Z^\mu\right) \tag{5.13}$$

where (the rest of the relevant couplings, e.g., the hhV couplings, can be found in [24])

	$c_{t,j}$	$c_{b,j}$	$\tilde{c}_{t,j}$	$\tilde{c}_{t,j}$	a_j
Type I:	$R_{j2}/\sin\beta$	$R_{j2}/\sin\beta$	$-R_{j3}\cot\beta$	$R_{j3}\cot\beta$	$R_{i2}\sin\beta + R_{i1}\cos\beta$
Type II:	$R_{j2}/\sin\beta$	$R_{j1}/\cos\beta$	$-R_{j3}\cot\beta$	$-R_{j3}\tan\beta$	$R_{j2}\sin\beta + R_{j1}\cos\beta$

(5.14)

In [29], besides introducing the above important relations between phenomenological parameters and potential parameters as well as a useful parametrization of couplings, experimental constraints on the mixing angles with respect to EDM searches for the electron, neutron, mercury and radium are presented. These limits can be summarized as $|\sin\alpha_b| \leq 0.005$. As is mentioned in Sec. 3.2.4, it is this limit that is used in this study.

Model C

Model C is a type II flavour diagonal softly $\mathbb{Z}_2$ breaking and explicitly $\mathcal{CP}$ violating 2HDM. Since there is $\mathcal{CP}$ violation, the tadpole equations give a relation between the imaginary parts of m_{12}^2 and λ_5 and the first parametrization presented in the previous subsection can be used. However, as is remarked there, this will limit $\tan\beta$ quite severely. In particular, α, α_b, $\alpha_c \in (-\pi/2, \pi/2)$, $\nu \in (-5, 5)$, $m_{h_1} = 125$ GeV, $m_{h_2} \in (125, 900)$ and $m_{h_3} \in (m_{h_2}, 900)$, where the two last ones have implicit unit GeV. The reason for choosing these intervals is that they are phenomenologically relevant, as is discussed in e.g., [29]. Roughly 10^5 points are here used.

As can be seen in figs. 12a-13a, when comparing to figs. 3a-3c, the kinds of phase transitions are the same for $\mathcal{CP}$ violating and $\mathcal{CP}$ conserving models. In fig. 13a there is a narrow peak around $T = 450$ GeV where the potential ends up in its former minimum and this is surely due to numerical effects as the potential might be very flat around the phase transition jump in question and hence can end up in either minimum. Now, the distribution of ζ in fig. 13b is clearly different from that in fig. 3d, with the peak shifted somewhat to the right (corresponding to in general stronger phase transitions) and an increased width. The effect that a lot fewer points have very small ζ for $\mathcal{CP}$ violating models is not really comparable to the $\mathcal{CP}$ conserving case, as in the latter a much larger interval was used for $\tan\beta$ and it was seen that strong phase transitions favour small $\tan\beta$ (also, here λ_6, $\lambda_7 = 0$). However, this nevertheless shows that the strength of the phase transition depends on $\mathcal{CP}$ violation, so that the Sakharov condition demanding $\mathcal{CP}$ violation actually makes it easier to have a strong enough phase transition, as is required by one of the other two Sakharov conditions.

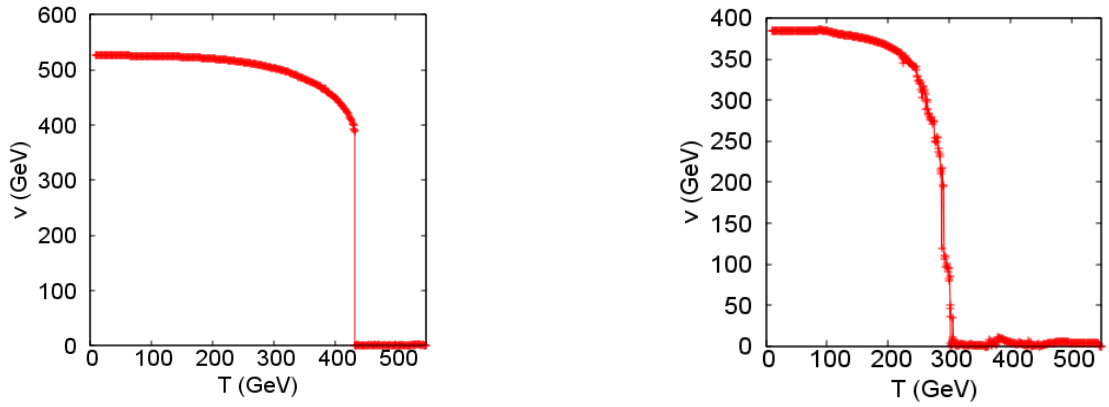

(a) (b)

Figure 12: Examples and properties of phase transitions in a $\mathcal{CP}$ violating 2HDM: (a) A strongly first order electroweak phase transition. (b) A very weak electroweak phase transition.

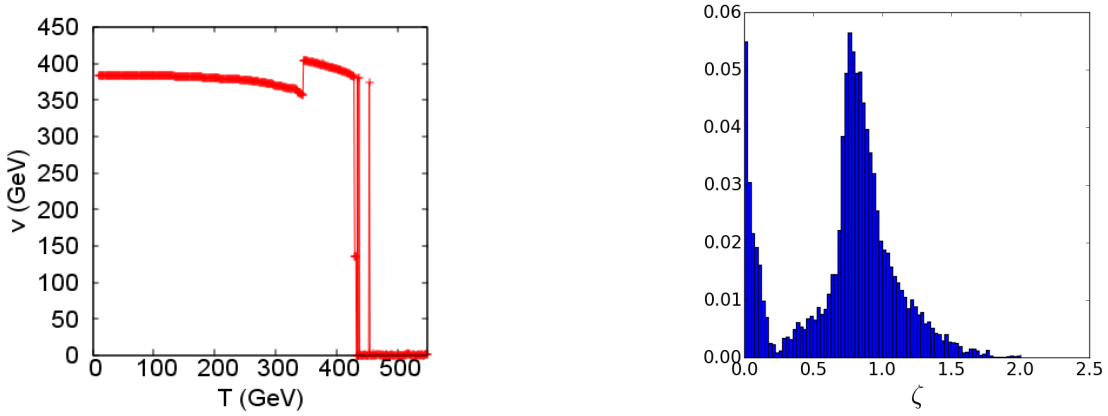

(a) (b)

Figure 13: Examples and properties of phase transitions in a $\mathcal{CP}$ violating 2HDM: (a) A strongly first order electroweak phase transition, where the rich vacuum structure of the 2HDMs is exposed. (b) The distribution of ζ.

Just as for the $\mathcal{CP}$ conserving case it is interesting to look at sections of the parameter space. The colour convention (and order of plotting) used in figs. 14a-14d is the same as for the $\mathcal{CP}$ conserving models, except for the colour red which is redefined as

- *Red points:* Satisfy PUP, PT, HP, the discriminant condition, the condition to be within the 90% CL ellipse ϵ_{ST} in the ST-plane and the angle EDM requirement $|\sin\alpha_b| < 0.005$ from [29] (for simplicity, call these three latter constraints D, OBL and EDMC, respectively).

As can be seen in figs. 14a-14d, there are *no* red points at all, i.e., not a single point surviving all the constraints imposed. The reason for this can be understood on several levels. First and foremost, the $\mathcal{CP}$ violating angles are distributed on a very large interval when comparing to EDMC, i.e., $|\sin\alpha_b| < 0.005$. Hence it might be that the angle α_b is not sampled well enough in the interesting region with only $\sim 10^5$ points.

Also, as can be noted when comparing fig. 14d with e.g., fig. 4c, T is not so restricted to the ellipse anymore. This is not so unexpected from the chosen intervals if the parameter T is analyzed more in detail. Consider Eq. (E.6) but for the moment ignore the terms dependent on m_Z and m_W. Then, using $\sum_{i=1}^{3}\tilde{R}_{ki}=1$ for any k as $\tilde{R}=R_3^T$ (see Eq. (2.17)) is a rotation matrix, T can be rewritten as

$$\begin{aligned} T \;\propto\; & \sum_{j=1}^{3}\left(1-\tilde{R}_{1j}^2\right)F\left(m_{H^\pm}^2,\,m_{h_j}^2\right)-\tilde{R}_{11}^2F\left(m_{h_2}^2,\,m_{h_3}^2\right)-\tilde{R}_{12}^2F\left(m_{h_3}^2,\,m_{h_1}^2\right)-\tilde{R}_{13}^2F\left(m_{h_1}^2,\,m_{h_2}^2\right) \\ = \;& \tilde{R}_{11}^2\left[F\left(m_{H^\pm}^2,\,m_{h_2}^2\right)+F\left(m_{H^\pm}^2,\,m_{h_3}^2\right)-F\left(m_{h_2}^2,\,m_{h_3}^2\right)\right]+ \\ & +\tilde{R}_{12}^2\left[F\left(m_{H^\pm}^2,\,m_{h_1}^2\right)+F\left(m_{H^\pm}^2,\,m_{h_3}^2\right)-F\left(m_{h_1}^2,\,m_{h_3}^2\right)\right]+ \\ & +\tilde{R}_{13}^2\left[F\left(m_{H^\pm}^2,\,m_{h_1}^2\right)+F\left(m_{H^\pm}^2,\,m_{h_2}^2\right)-F\left(m_{h_1}^2,\,m_{h_2}^2\right)\right] \end{aligned} \tag{5.15}$$

Since $F(x,\, y) \approx 0$ for $x \approx y$ (see Eq. (E.11)), every term above in T will be small if the squared mass differences between physical particles are small. In the case they are not, the $\mathcal{CP}$ violating angles in $\tilde{R}$ must combine in such a way so as to cancel all or some of the terms in question for T to be small. As is remarked in Sec. 5.1.1, the choice of having $\Lambda_4, \Lambda_5, \Lambda_7 \in (-1,\, 1)$ yields small squared mass differences[37] and so with only one non-zero angle for $\mathcal{CP}$ conserving models T should consequently be small, as it also is and can be seen in e.g., figs. 4c and 7a.

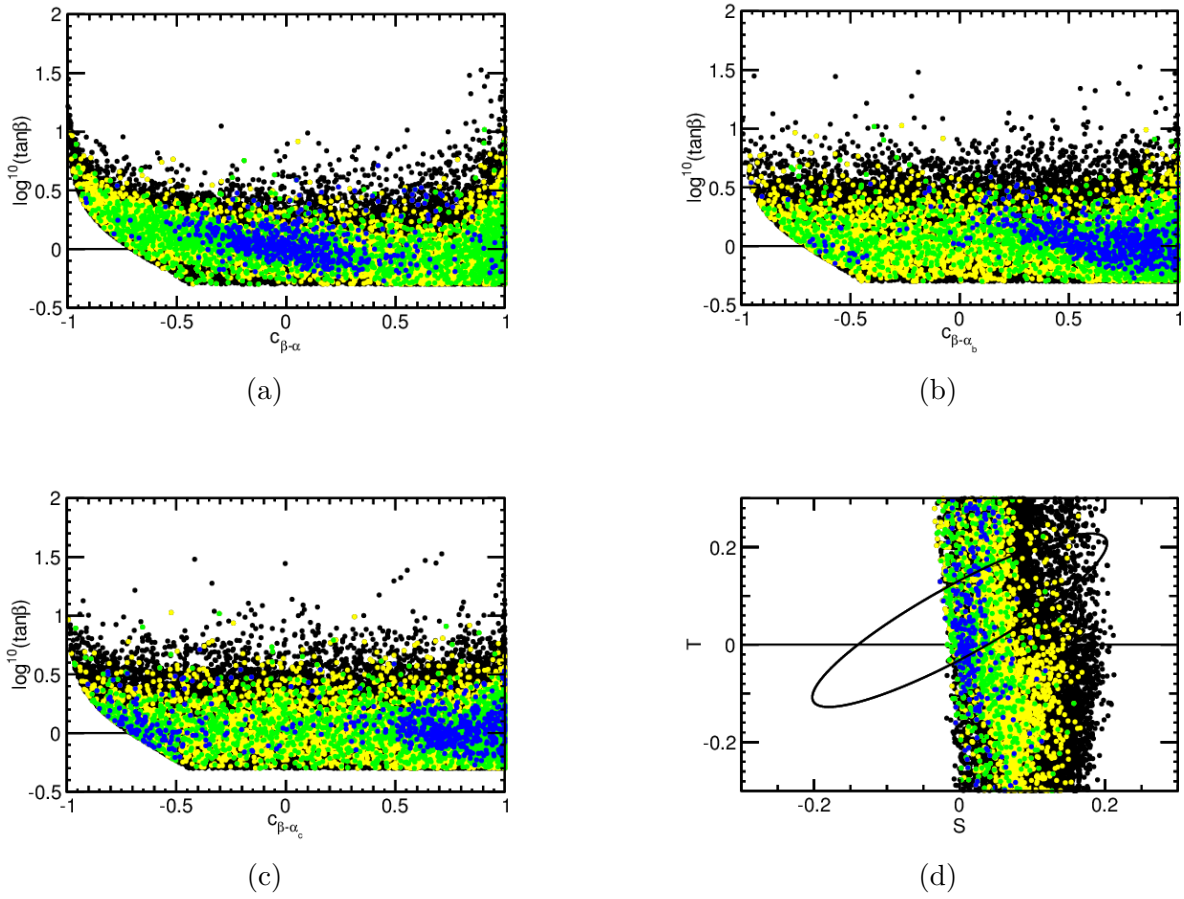

Figure 14: A collection of figures for Model C: (a)–(c) The section of parameter space spanned by (a) $\tan\beta$ and $c_{\beta-\alpha} = \cos(\beta-\alpha)$, (b) $\tan\beta$ and $c_{\beta-\alpha_b} = \cos(\beta-\alpha_b)$, and (c) $\tan\beta$ and $c_{\beta-\alpha_c} = \cos(\beta-\alpha_c)$. (d) The ellipse ϵ_{ST} in the ST-plane.

[37]Note, however, that these do not make mass differences small between h_1 and the other scalars so that the term proportional to $\tilde{R}^2_{13}$ in T generally could give sizeable contributions, but since $\tilde{R}^2_{13} = 0$ for $\mathcal{CP}$ conserving models the term in question vanishes and T remains small.

To illustrate just how restrictive EDMC is in this case, consider figs. 15a-16b, where red points now are allowed to not satisfy EDMC. As the figures show, a reasonable amount of red points do exist. However, as is indicated by fig. 16a, the red points are in fact centered around $\alpha_b = 0$, so that indeed the small α_b region is favoured by also the constraints other than EDMC. For α_c both small and large values are allowed (see fig. 16b), but there seem to be gaps between the allowed regions. This motivates further studies of models where the mixing angles are generated in smaller intervals than those in Model C. Furthermore, since the oblique parameters depend so much on mass differences, there is good reason to choose small squared mass differences just as was done in the $\mathcal{CP}$ conserving models when $\Lambda_4,\ \Lambda_5,\ \Lambda_7 \in (-1, 1)$.

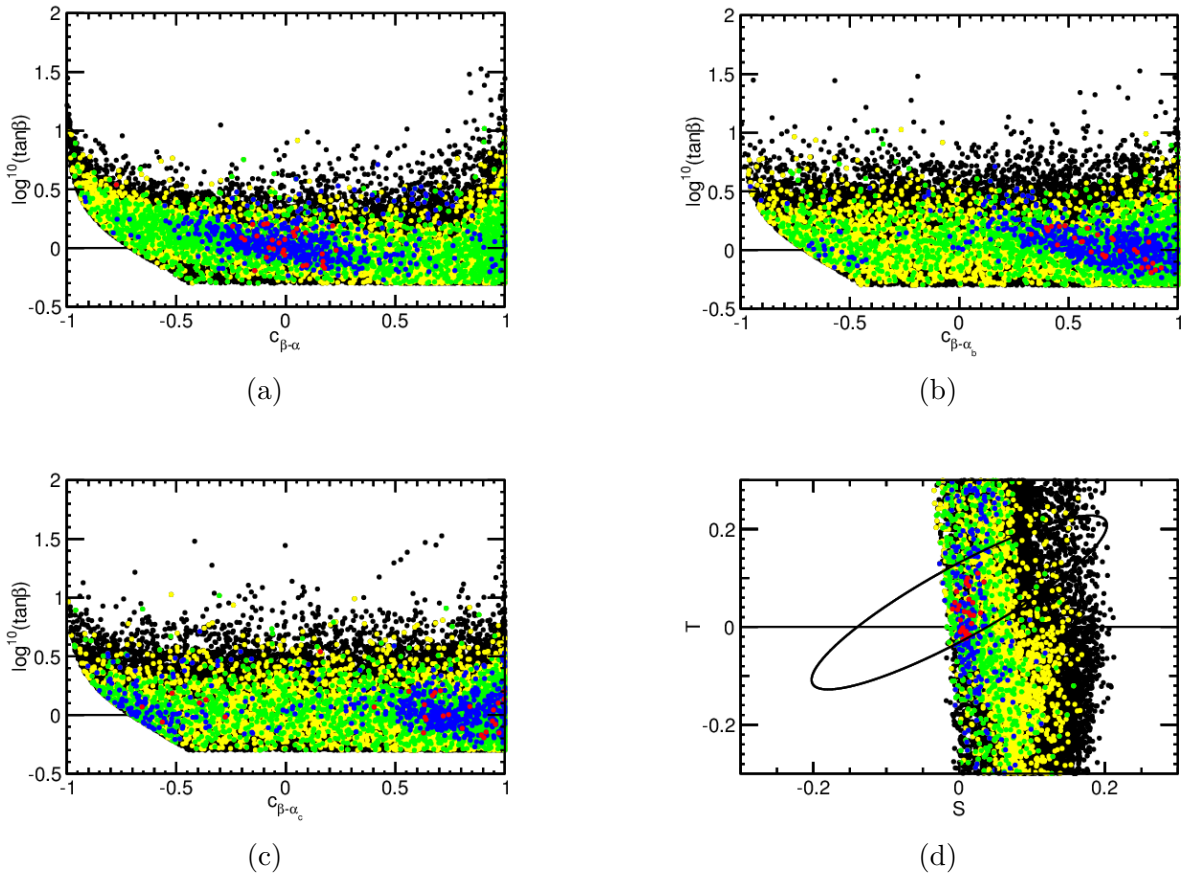

Figure 15: A collection of figures for Model C (without EDMC): (a)–(c) The section of parameter space spanned by (a) $\tan\beta$ and $c_{\beta-\alpha} = \cos(\beta-\alpha)$, (b) $\tan\beta$ and $c_{\beta-\alpha_b} = \cos(\beta-\alpha_b)$, and (c) $\tan\beta$ and $c_{\beta-\alpha_c} = \cos(\beta-\alpha_c)$. (d) The ellipse ϵ_{ST} in the ST-plane.

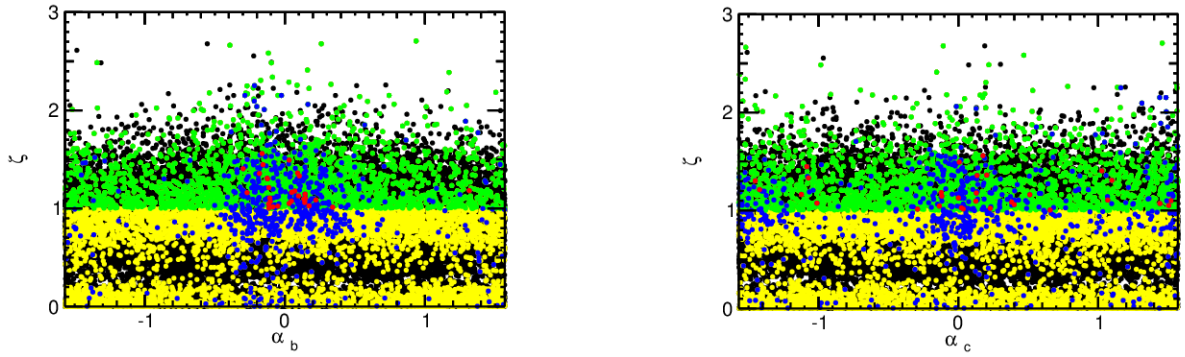

(a) (b)

Figure 16: A collection of figures for Model C (without EDMC): The strength of the EWPT, ζ, as a function of (a) α_b and (b) α_c.

Model C'

Inspired by the results for Model C now consider Model C', a type II flavour diagonal softly $\mathbb{Z}_2$ breaking and explicitly $\mathcal{CP}$ violating 2HDM, i.e., just like Model C, but where the angles α_b, $\alpha_c \in (-0.01, 0.01)$ and masses are chosen so that $m_{h_2} \in (125, 900)$, with implicit unit GeV, $m_{h_3}^2 - m_{h_2}^2 < v^2$ and $\left|m_{H^\pm}^2 - m_{h_2}^2\right| < v^2$. The choice v^2 as an upper bound is quite reasonable as v is a natural scale for the physics in question and corresponds to the choice $|\Lambda_4|, |\Lambda_5| \lesssim 1$ in the $\mathcal{CP}$ conserving case. Again roughly 10^5 points are used.

Sections of the parameter space are shown in figs. 17a-18d, with the same colour convention as in figs. 14a-14d (i.e., where EDMC is included for red points), and as can be seen there is now a large amount of allowed points. As expected from the analysis for Model C, T here has a much smaller range and the oblique parameters in the ST-plane lie in a smaller region (compare fig. 17b with fig. 14d). The dependence on EDMC is shown in fig. 17c where $\sin\alpha_b$ is plotted against $\tan\beta$, and it is seen that the allowed points are uniformly distributed for $\tan\beta$ roughly between 0.5 and 2. There is an analogous plot for $\sin\alpha_c$ in fig. 17d and as no constraint on α_c is imposed in EDMC the allowed points for α_c are more scattered than those for α_b.

Next consider correlations between the strength of the phase transition and some of the parameters. No clear correlation between strength of the phase transition (green points) and α_b or α_c, respectively, can be seen in figs. 17e-17f. In fig. 18a, it is seen that ζ decreases as $\tan\beta$ increases so that, as could be seen already in e.g., fig. 17c, low $\tan\beta$ is favoured once again, just as for generating a baryon asymmetry. As is shown in figs. 18b-18d, the allowed points seem to demand $m_{h_2}, m_{h_3} \gtrsim 300$ GeV and $m_{H^\pm} \gtrsim 400$ GeV but PT favours scalar masses $\lesssim 400$ GeV, similar to the $\mathcal{CP}$ conserving cases. All of the above shows that there indeed are many good points satisfying all the imposed constraints for softly $\mathbb{Z}_2$ breaking explicitly $\mathcal{CP}$ violating 2HDMs, and from the favouring of small $\tan\beta$ this shows that there indeed on this level of the analysis is a possibility to explain the BAU through

EWBG for these kinds of models.

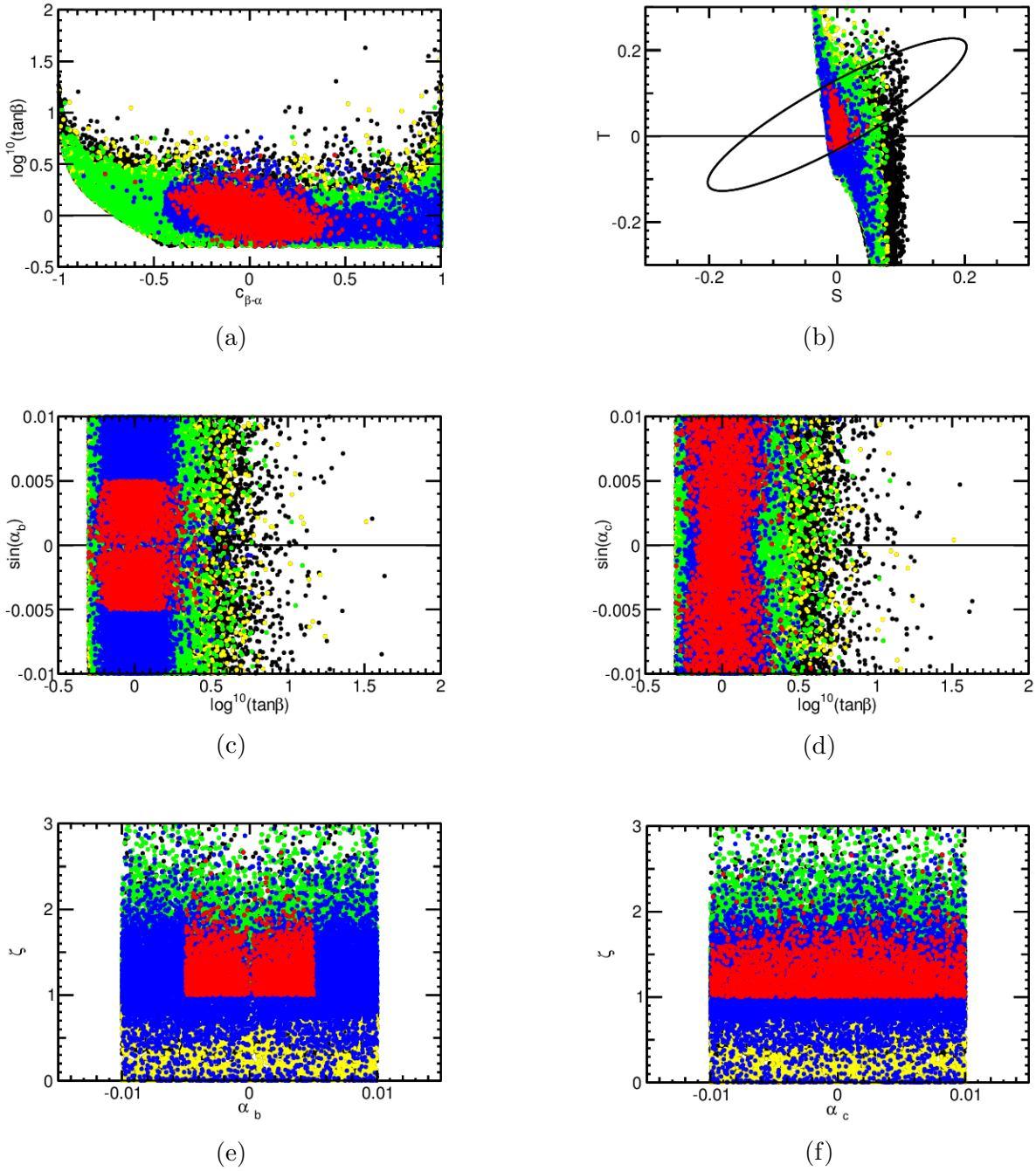

Figure 17: A collection of figures for Model C': (a) The section of parameter space spanned by $\tan\beta$ and $c_{\beta-\alpha} = \cos(\beta-\alpha)$. (b) The ellipse ϵ_{ST} in the ST-plane. (c)–(d) The section of parameter space spanned by (c) $\tan\beta$ and $\sin\alpha_b$, and (d) $\tan\beta$ and $\sin\alpha_c$. (e)–(f) The strength of the EWPT, ζ, as a function of (e) α_b and (f) α_c.

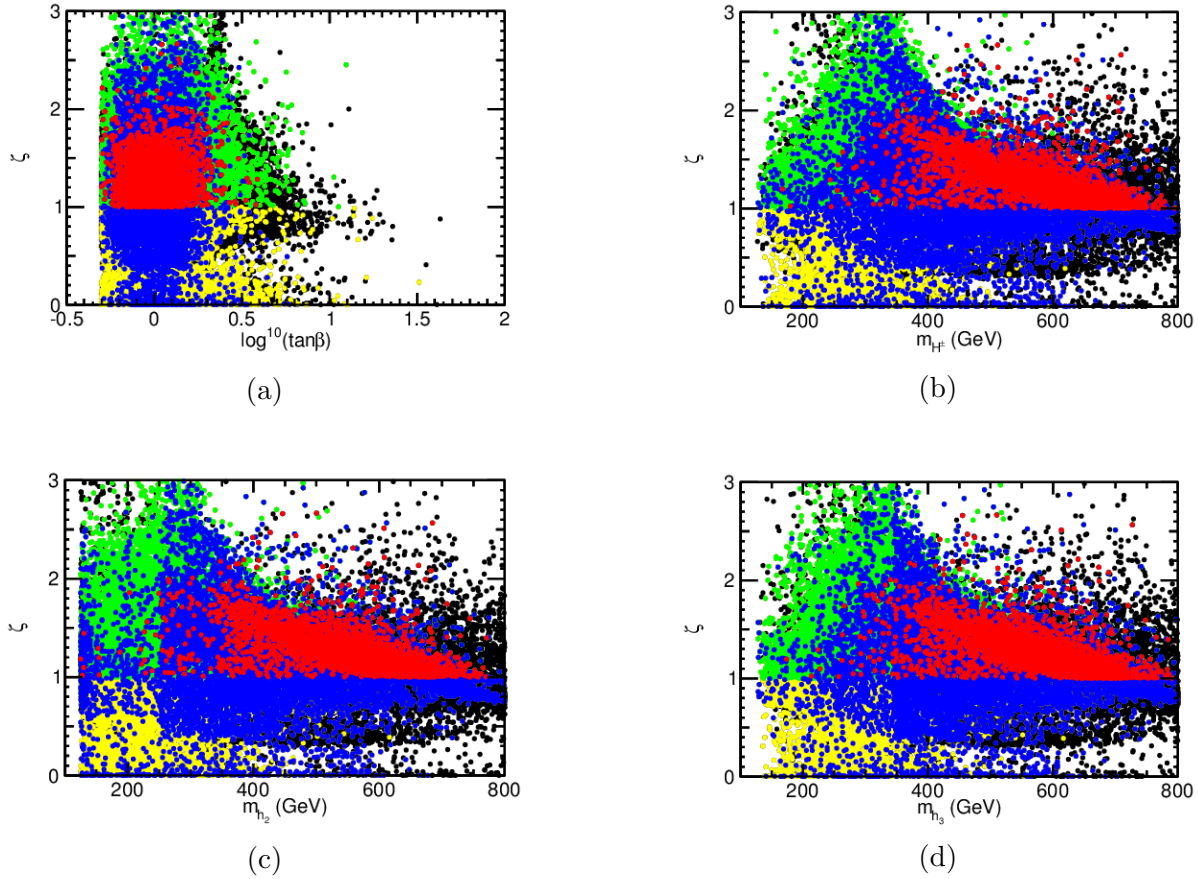

Figure 18: A collection of figures for Model C': The strength of the EWPT, ζ, as a function of (a) $\tan\beta$, (b) $m_{H^\pm}$, (c) m_{h_2} and (d) m_{h_3}.

Phenomenological basis of parameters for explicitly $\mathcal{CP}$ violating $\mathbb{Z}_2$ breaking 2HDMs

Drawing inspiration from the relations between the phenomenological and general bases for explicitly $\mathcal{CP}$ violating softly $\mathbb{Z}_2$ breaking 2HDMs presented earlier, analogous relations were derived by the author for the case of complex λ_6, $\lambda_7 \neq 0$, i.e., for explicitly $\mathcal{CP}$ violating $\mathbb{Z}_2$ breaking 2HDMs. This was done using the mass matrix in the general basis defined in [9], i.e., a generalization of the matrix $\mathcal{M}^2_{gen}$ in Eq. (5.5). In particular, when $\lambda_6, \lambda_7 \neq 0$ it is not possible to obtain an equation for $\tan\beta$ like that in Eq. (5.12) without solving a polynomial equation of degree four. In fact, being able to have $\tan\beta$ as a free parameter and then calculating one of the other parameters in terms of it would be very satisfying, thus yielding freedom to investigate the effects of varying $\tan\beta$ in any non-forbidden interval. This can actually be done when λ_6, $\lambda_7 \neq 0$, assuming that λ_6 and $\Re(\lambda_7)$ are given and $\Im(\lambda_7)$ is calculated in terms of the other parameters.

Now, letting the mass matrix in question, which again is a symmetric 3×3 matrix and

hence consists of six independent elements, be defined by[38] $\mathcal{M}_{11}$, $\mathcal{M}_{12}$, $\mathcal{M}_{13}$, $\mathcal{M}_{22}$, $\mathcal{M}_{23}$ and $\mathcal{M}_{33}$, the relations between the phenomenological and general bases' parameters become (with ν as before and $\tan\beta$ now an independent parameter)

$$\Im\left(\lambda_7\right) = \frac{1}{v^2 s_\beta^2}\left[v^2 c_\beta^2\,\Im\left(\lambda_6\right) + \mathcal{M}_{13}c_\beta - \mathcal{M}_{23}s_\beta\right] \tag{5.16}$$

$$\lambda_1 = \frac{\mathcal{M}_{11}}{v^2 c_\beta^2} - \nu\tan^2\beta + \tan^2\beta\,\Re\left(\frac{3}{2}\lambda_6\cot\beta - \frac{1}{2}\lambda_7\tan\beta\right) \tag{5.17}$$

$$\lambda_2 = \frac{\mathcal{M}_{22}}{v^2 s_\beta^2} - \nu\cot^2\beta + \cot^2\beta\,\Re\left(-\frac{1}{2}\lambda_6\cot\beta + \frac{3}{2}\lambda_7\tan\beta\right) \tag{5.18}$$

$$\Re\left(\lambda_5\right) = \nu - \frac{\mathcal{M}_{33}}{v^2} + \frac{1}{2}\Re\left(\lambda_6\cot\beta + \lambda_7\tan\beta\right) \tag{5.19}$$

$$\lambda_4 = 2\nu - \Re\left(\lambda_5\right) - \Re\left(\lambda_6\cot\beta + \lambda_7\tan\beta\right) - \frac{2m_{H_\pm^2}}{v^2} \tag{5.20}$$

$$\lambda_3 = \nu + \frac{\mathcal{M}_{12}}{v^2 c_\beta s_\beta} - \lambda_4 - \Re\left(\lambda_5\right) - \frac{3}{2}\Re\left(\lambda_6\cot\beta + \lambda_7\tan\beta\right) \tag{5.21}$$

$$\Im\left(\lambda_5\right) = -\frac{\mathcal{M}_{13}c_\beta + \mathcal{M}_{23}s_\beta}{v^2 c_\beta s_\beta} - \Im\left(\lambda_6\cot\beta + \lambda_7\tan\beta\right) \tag{5.22}$$

where $m_{H^\pm}^2 = v^2\left[\nu - \frac{1}{2}\left(\lambda_4 + \Re\left(\lambda_6\cot\beta + \lambda_7\tan\beta\right)\right)\right]$ has been used. Also in this case the limits obtained from EDM searches and the particular parametrization of the couplings as presented in [29] can be used. This is done in Model D defined below.

Model D

Model C and Model C' both assume $\lambda_6, \lambda_7 = 0$ so that the $\mathbb{Z}_2$ symmetry is broken only softly. Having derived also relations between the parameters in the phenomenological basis and those in the general basis when $\lambda_6, \lambda_7 \neq 0$, it is again possible to do parameter space scans in phenomenologically relevant regions. Therefore, consider Model D which is a generalization (with all parameter intervals the same unless otherwise stated) of Model C' with a completely broken $\mathbb{Z}_2$ symmetry. In particular, as was shown above $\tan\beta$ is now a free parameter and is here chosen to be logarithmically distributed in the interval[39]

[38] Here $\mathcal{M}_{ij} = \left(R^{\mathrm{T}}\mathrm{diag}\left(m_{h_1}^2, m_{h_2}^2, m_{h_3}^2\right)R\right)_{ij}$

[39] The choice to not have also larger $\tan\beta$ is for reasons of unitarity and perturbativity.

(1/2, 10). λ_6 and λ_7 are chosen so that $|\lambda_6|, |\Re(\lambda_7)| \in (0, \pi)$, and as was discussed when presenting the phenomenological basis $\Im(\lambda_7)$ is not independent and given by Eq. (5.16). Here, roughly 10^5 points are used and the same colour convention and order of plotting as in Model C' is employed.

As can be seen in figs. 19a-19b, only a small fraction of the points satisfy all of the imposed constraints and in total not many at all even satisfy PUP (it is perturbativity that is most constraining – less than 1% of the points satisfy it). To understand why this occurs consider fig. 20a, where $\log^{10}(\tan\beta)$ is plotted against $\Im(\lambda_7)$. As can be seen, $\Im(\lambda_7)$ ranges from roughly -10 to 10, i.e., $|\Im(\lambda_7)|$ is considerably larger than $|\Re(\lambda_7)|$, while PUP requires it to satisfy $|\Im(\lambda_7)| \lesssim \pi$. Since $\Im(\lambda_7)$ is not a free parameter a possible remedy would be to require $\tan\beta \gtrsim 1$, but as there are many points satisfying PUP for values also smaller than that and the fact that the generation of a baryon asymmetry favours small $\tan\beta$ such a solution is not very attractive. As a side note, the plot also shows that as $\tan\beta$ increases positivity (black points) requires smaller and smaller $|\Im(\lambda_7)|$ as can be expected given the structure of the matrix Λ_E in Eq. (3.2) and that some of the parameters in the general basis, e.g., $\Re(\lambda_5)$ in Eq. (5.19), increase in absolute value as $\tan\beta$ increases, something which clearly affects the eigenvalues of Λ_E from which positivity can be deduced.

In figs. 20b and 20c the strength of the phase transition is plotted against $\Im(\lambda_6)$ and $\Im(\lambda_7)$. No clear correlation can there be seen, but as was also seen in the above analysis PUP (and hence PT) requires $|\Im(\lambda_7)| \lesssim (0, \pi)$. Plotting the absolute value of λ_7 (not displayed here) shows that no points satisfying anything more than positivity exist for $|\lambda_7| \gtrsim \pi$, analogous to Model A in the $\mathcal{CP}$ conserving case.

The above results obviously imply that the possibility for these kinds of models to explain the BAU is limited (at least under the assumption that no isolated and hence in some sense fine-tuned point is the correct one). It can thus be concluded that models like Model C' are preferable to models with a completely broken $\mathbb{Z}_2$ symmetry like Model D, unless $|\Im(\lambda_7)| \lesssim (0, \pi)$.

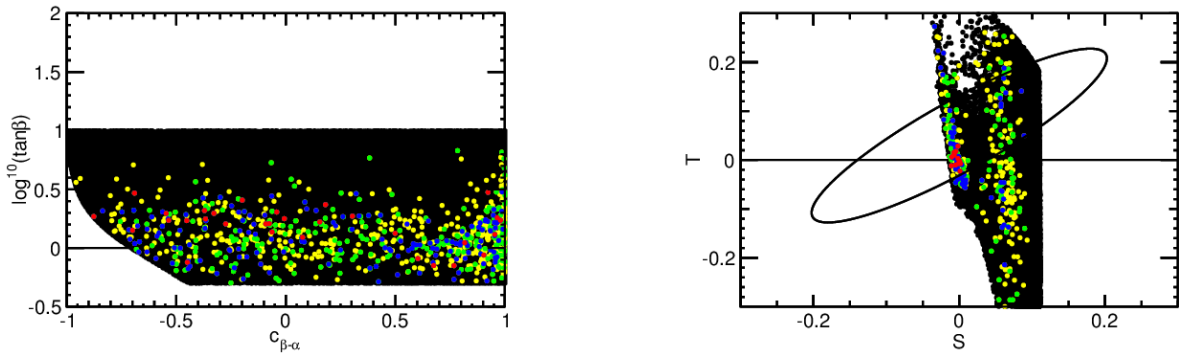

(a) (b)

Figure 19: A collection of figures for Model D: (a) The section of parameter space spanned by $\tan\beta$ and $c_{\beta-\alpha} = \cos(\beta - \alpha)$. (b) The ellipse ϵ_{ST} in the ST-plane.

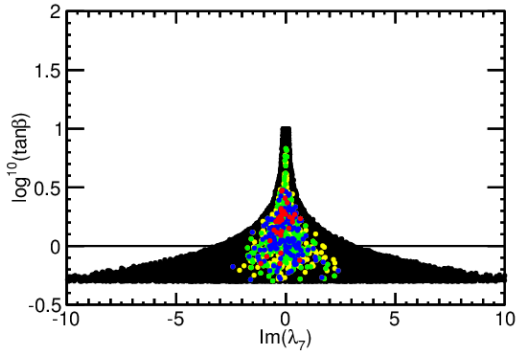

(a)

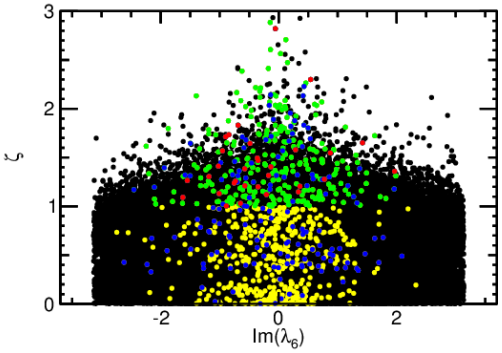

(b)

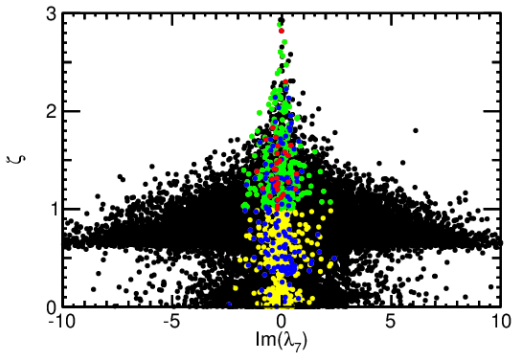

(c)

Figure 20: A collection of figures for Model D: (a) The section of parameter space spanned by $\tan\beta$ and $\Im(\lambda_7)$. (b)–(c) The strength of the EWPT, ζ, as a function of (b) $\Im(\lambda_6)$ and (c) $\Im(\lambda_7)$.

6 Summary and conclusions

In this study the electroweak phase transition in general Two-Higgs-Doublet Models (2HDMs) has been investigated and in particular also the possibility of explaining the observed baryon asymmetry of the Universe (BAU) through electroweak baryogenesis (EWBG). Parameter space scans have been performed for various kinds of 2HDMs where a $\mathbb{Z}_2$ symmetry was either broken completely or softly. As a starting point only $\mathcal{CP}$ conserving 2HDMs were considered, but as these are not really relevant for EWBG, $\mathcal{CP}$ violating models were also considered. In the $\mathcal{CP}$ conserving models perturbations in the Yukawa sector were added so as to break the respective $\mathbb{Z}_2$ symmetries more than by just allowing $\mathbb{Z}_2$ breaking parameters in the tree level potential.

Both experimental and theoretical constraints were imposed on the parameter space points in order to evaluate them, and perhaps most importantly (from the perspective of explain-

ing the baryon asymmetry in question) also the constraint that the electroweak phase transition be strongly first order. The experimental constraints from Higgs physics, electroweak physics, flavour physics as well as searches for electric dipole moments of the electron, neutron, mercury and radium (the last ones only for $\mathcal{CP}$ violating models) were used. The theoretical constraints consisted of perturbativity and stability of the tree level potential, tree level unitarity of the scattering matrices as well as demanding that the tree level minimum is the global one. A one-loop thermally corrected effective potential was used throughout the study.

In both the $\mathcal{CP}$ conserving and $\mathcal{CP}$ violating models the properties of the electroweak phase transition were studied. Both first and second order phase transitions were observed, of which some transitions were seen to occur in several steps (as expected due to having two scalar fields and thus more than one minimum of the potential). Also, it was seen that the distribution of the strength of the phase transition changed as $\mathcal{CP}$ violation was added, this so that the average strength increased.

For the $\mathcal{CP}$ conserving models it was found that small perturbations in the ct and tc Yukawa sectors did not change anything as compared to the case that only perturbations in the bb and tt sector were used. This could be expected as at this level the perturbations do not enter into the effective potential (but in principle they can affect the experimental constraints). The points satisfying all the imposed constraints seem to favour small $\tan\beta$ and m_A, m_H, $m_{H^\pm} \gtrsim 400$ GeV, but strongly first order phase transitions can also be obtained for lower masses. There was a substantial amount of points satisfying all of the imposed constraints for both models with an initial type I and type II symmetry, but the flavour physics constraints required slightly higher values of $\tan\beta$ for type I models, something in discrepancy with the known favouring of small $\tan\beta$ for a generated baryon asymmetry (this favouring is remarked upon in [2]). All in all the investigations showed that the $\mathcal{CP}$ conserving models could satisfy all the imposed constraints, but it should be remembered that for baryogenesis purposes these kinds of models are not really relevant.

For the $\mathcal{CP}$ violating models it was seen that the scalar masses depend on large complex phases between the vacuum expectation values, so that for a parameter space point from the $\mathcal{CP}$ conserving case to which $\mathcal{CP}$ violation is added no neutral scalar particle necessarily needs to have mass 125 GeV anymore. This clearly motivates the need for parameter space scans where one neutral scalar mass is fixed to 125 GeV. Explicitly $\mathcal{CP}$ violating flavour diagonal models (with either hard or soft breaking of the $\mathbb{Z}_2$ symmetry) were then considered in more detail, and it was seen that for arbitrary mass differences the oblique parameters and electric dipole moment searches constrained the number of points satisfying the imposed constraints quite severely. It was seen that the oblique parameters are sensitive to the squared mass differences and $\mathcal{CP}$ violating angles. In the $\mathcal{CP}$ conserving case the oblique parameters were in general smaller, this as the Hybrid basis was used with Λ_4, Λ_5, $\Lambda_7 \in (-1, 1)$ which parametrize squared mass differences. In the case when the $\mathcal{CP}$ violating angles in the general basis as well as the squared mass differences between the two heavier neutral scalars and the charged scalars were chosen to be small, a good

amount of points in the models with only softly broken $\mathbb{Z}_2$ symmetry survived all the imposed constraints. Again, low $\tan\beta$ was favoured. In the completely $\mathbb{Z}_2$ breaking models, however, only a small fraction of the points survived even the theoretical constraints, in particular the perturbativity constraint. Despite this last result, the study clearly shows that there indeed is a possibility for 2HDMs to explain the BAU through EWBG.

As a final remark, there are some interesting extensions and improvements of this study that could be done in the future. First of all, the case when the lightest neutral scalar is less than 125 GeV could be investigated. Furthermore, thermally corrected masses and a more detailed treatment of constraints from flavour physics and electric dipole moment searches could be included, as well as a study of the cosmological implications coming from the property of having several potential minima. Last but not least, it would be very interesting, as well as essential, to study the exact dynamics during the generation and obtaining an estimate of a baryon asymmetry, this in order to settle whether or not 2HDMs and the additional $\mathcal{CP}$ violation (as compared to the Standard Model) actually can generate the BAU while satisfying experimental and theoretical constraints. Having already created parameter scanning tools and a working chain between `2HDMC`, `Vevacious` (which were both generalized to allow for $\mathcal{CP}$ violating models) and `ROOT`, such investigations would be a natural next step.

Acknowledgments

I would here like to thank all those who in some way have helped and supported me during the last year: My supervisor, whose help and guidance along the way has been invaluable. Eliel for the help getting started with `Vevacious`. My fellow students, with whom I shared an office, for the fun during breaks and discussions about physics, mathematics and life in general. Bo for helping with all things practical, both related to and not related to the teaching I have done in his courses, as well as always being encouraging and inspiring. Last but not least I would like my parents, girlfriend and brother (with family) to know that I am deeply grateful for all the kindness and patience, as well as their ability to make non-working hours wonderful and filled with joy.

A Spontaneous symmetry breaking

Spontaneous symmetry breaking (SSB) is a central part in the electroweak symmetry breaking (EWSB) discussed in Sec. 2.1. Therefore, this appendix aims at reviewing the basic ideas behind SSB and their consequences. The discussion closely follows that presented in [15].

Consider a ferromagnet at some temperature such that there is a magnetic field in a certain

direction. The reason it has such a magnetic field is because the spins of the atoms constituting the magnet align. However, if the magnet is heated to high enough temperature the spins of the atoms become randomly distributed, the magnetic field disappears and a rotational symmetry arises. Thus, going in the opposite direction, for some temperature there is a transition such that the rotational symmetry is broken – there is a *spontaneuosly broken* symmetry. Note that this process is equivalent to the EWSB.

To study something more explicit in terms of field theory, consider the linear sigma model which is a scalar field theory with a set of $N \in \mathbb{N}$ real scalar fields, $\{\phi^i(x)\}_{i\in\{1,\,2,\,\ldots,\,N\}}$. The Lagrangian can be written, with the dependence on spacetime coordinate x suppressed and summation over i for repeated indices in squares,

$$\mathcal{L} = \frac{1}{2}\left(\partial_\nu \phi^i\right)^2 + \frac{1}{2}\mu^2\left(\phi^i\right)^2 - \frac{\lambda}{4}\left[\left(\phi^i\right)^2\right]^2 \tag{A.1}$$

where μ and λ are constants. Note that the Lagrangian has an $O(N)$ symmetry (which is global), since for $R_{ij} \in O(N)$, under $\phi^i \longrightarrow R_{ij}\phi^j$, $\mathcal{L}$ is invariant, i.e., $\mathcal{L} \longrightarrow \mathcal{L}$.

The potential part of the Lagrangian is given by the negative of the last two terms in Eq. (A.1), i.e.,

$$V\left(\phi^i\right) = -\frac{1}{2}\mu^2\left(\phi^i\right)^2 + \frac{\lambda}{4}\left[\left(\phi^i\right)^2\right]^2 \tag{A.2}$$

Classically, the minimum to this potential is given by a constant field ϕ^i_{cl} either (i) with distance to the origin given by $\left(\phi^i_{cl}\right)^2 = \frac{\mu^2}{\lambda}$, or (ii) with $\phi^i_{cl} = 0$. The position of the global minimum/minima clearly depends on the parameters μ and λ. Note that in case (i), there is a continuous set of minima on the N-sphere $S^N = \left\{\eta_i \in \mathbb{R},\, i \in \{1,\, 2,\, \ldots,\, N\} \;\middle|\; \sum_i \eta_i^2 = \frac{\mu^2}{\lambda}\right\}$ and for $N = 2$ the so-called Mexican Hat potential is obtained[40].

Now, choose coordinates such that ϕ^i_{cl} lies in one field direction, the Nth, say. Furthermore, let $v = \frac{\mu}{\sqrt{\lambda}}$. Then, it is possible to expand around this minimum so that $\phi^i(x) = \varphi^i(x)$ for $i \leq N-1$ and $\phi^N(x) = v + \sigma(x)$. The Lagrangian in Eq. (A.1) thus becomes, for $k \in \{1,\, 2,\, \ldots,\, N-1\}$,

$$\begin{aligned}\mathcal{L} \;=\; & \frac{1}{2}\left(\partial_\nu \varphi^k\right)^2 + \frac{1}{2}\left(\partial_\nu \sigma\right)^2 - \frac{1}{2}\left(2\mu^2\right)\sigma^2 + \\ & -\sqrt{\lambda}\,\mu\sigma^3 - \sqrt{\lambda}\,\mu\left(\varphi^k\right)^2\sigma - \frac{\lambda}{4}\sigma^4 - \frac{\lambda}{2}\left(\varphi^k\right)^2\sigma^2 - \frac{\lambda}{4}\left[\left(\varphi^k\right)^2\right]^2\end{aligned} \tag{A.3}$$

Note that the fields φ^k have no mass terms whereas the field σ does. Furthermore, there is no longer an $O(N)$ symmetry but an $O(N-1)$ symmetry remains. Thus, the $O(N)$ symmetry has been spontaneously broken to its subgroup $O(N-1)$. This occurred when a particular direction was chosen to contain v.

[40] For a specific choice of parameters μ and λ, that is.

As a side note, the $N-1$ massless fields φ^k appearing as the symmetry was broken correspond to so-called *Goldstone bosons*. Their existence can be inferred from Goldstone's theorem, saying that *for every broken continuous symmetry, a massless particle appears.* A proof of this is left out here, but can easily be found elsewhere.

It should be noted that the above analysis only assumed a global symmetry but when also spontaneous breaking of local symmetries (i.e., gauge symmetries) is allowed the Higgs mechanism can be derived. In particular, for such theories, the Goldstone bosons are "eaten" when giving mass to the gauge bosons and hence disappear from the physical picture.

B Tadpole equations for general 2HDMs

Below the tadpole equations for 2HDMs with both spontaneous and explicit $\mathcal{CP}$ violation are given. In this study they are used to eliminate m_{11}^2, m_{22}^2 and $\Im\left(m_{12}^2\right)$ from the equations, thus yielding a lower-dimensional parameter space to scan through. Note that the v_j are complex, and thus can be divided into real and imaginary parts according to $v_j = v_{jR} + iv_{jI}$. For notational simplicity, the fact that each partial derivative below is evaluated at the point $\varphi_3 + i\varphi_4 = v_1$, $\varphi_7 + i\varphi_8 = v_2$, $\varphi_j = 0\,\forall j \in \{1,\,2,\,5,\,6\}$ is left out.

$$
\begin{aligned}
0 \stackrel{!}{=} \frac{\partial V_{\text{tree}}}{\partial \varphi_3} \quad \propto \quad & 4m_{11}^2 v_{1R} + 2\lambda_1 v_{1I}^2 v_{1R} + 2\lambda_1 v_{1R}^3 - 2im_{12}^2 v_{2I} + i\lambda_6 v_{1I}^2 v_{2I} + 2\lambda_6 v_{1I} v_{1R} v_{2I} + \\
& + 3i\lambda_6 v_{1R}^2 v_{2I} + i\lambda_5 v_{1I} v_{2I}^2 + 2\lambda_3 v_{1R} v_{2I}^2 + 2\lambda_4 v_{1R} v_{2I}^2 - \lambda_5 v_{1R} v_{2I}^2 + i\lambda_7 v_{2I}^3 + \\
& - 2m_{12}^2 v_{2R} + \lambda_6 v_{1I}^2 v_{2R} - 2i\lambda_6 v_{1I} v_{1R} v_{2R} + 3\lambda_6 v_{1R}^2 v_{2R} + 2\lambda_5 v_{1I} v_{2I} v_{2R} + \\
& + 2i\lambda_5 v_{1R} v_{2I} v_{2R} + \lambda_7 v_{2I}^2 v_{2R} - i\lambda_5 v_{1I} v_{2R}^2 + 2\lambda_3 v_{1R} v_{2R}^2 + 2\lambda_4 v_{1R} v_{2R}^2 + \\
& + \lambda_5 v_{1R} v_{2R}^2 + i\lambda_7 v_{2I} v_{2R}^2 + \lambda_7 v_{2R}^3 - i(v_{1I} - iv_{1R})(v_{2I} + iv_{2R})^2 \lambda_5^* + \\
& \left(v_{1I}^2 + 2iv_{1I} v_{1R} + 3v_{1R}^2\right)(-iv_{2I} + v_{2R})\,\lambda_6^* - iv_{2I}^3 \lambda_7^* + v_{2I}^2 v_{2R} \lambda_7^* + \\
& - iv_{2I} v_{2R}^2 \lambda_7^* + v_{2R}^3 \lambda_7^* + 2iv_{2I}\left(m_{12}^2\right)^* - 2v_{2R}\left(m_{12}^2\right)^*
\end{aligned} \tag{B.1}
$$

$$
\begin{aligned}
0 \stackrel{!}{=} \frac{\partial V_{\text{tree}}}{\partial \varphi_4} \quad \propto \quad & 4m_{11}^2 v_{1I} + 2\lambda_1 v_{1I}^3 + 2\lambda_1 v_{1I} v_{1R}^2 - 2m_{12}^2 v_{2I} + 3\lambda_6 v_{1I}^2 v_{2I} + 2i\lambda_6 v_{1I} v_{1R} v_{2I} + \\
& + \lambda_6 v_{1R}^2 v_{2I} + 2\lambda_3 v_{1I} v_{2I}^2 + 2\lambda_4 v_{1I} v_{2I}^2 + \lambda_5 v_{1I} v_{2I}^2 + i\lambda_5 v_{1R} v_{2I}^2 + \lambda_7 v_{2I}^3 + 2im_{12}^2 v_{2R} + \\
& - 3i\lambda_6 v_{1I}^2 v_{2R} + 2\lambda_6 v_{1I} v_{1R} v_{2R} - i\lambda_6 v_{1R}^2 v_{2R} - 2i\lambda_5 v_{1I} v_{2I} v_{2R} + 2\lambda_5 v_{1R} v_{2I} v_{2R} + \\
& - i\lambda_7 v_{2I}^2 v_{2R} + 2\lambda_3 v_{1I} v_{2R}^2 + 2\lambda_4 v_{1I} v_{2R}^2 - \lambda_5 v_{1I} v_{2R}^2 - i\lambda_5 v_{1R} v_{2R}^2 + \lambda_7 v_{2I} v_{2R}^2 + \\
& - i\lambda_7 v_{2R}^3 + (v_{1I} - iv_{1R})(v_{2I} + iv_{2R})^2 \lambda_5^* + \left(3v_{1I}^2 - 2iv_{1I} v_{1R} + v_{1R}^2\right)(v_{2I} + iv_{2R})\,\lambda_6^* + \\
& + v_{2I}^3 \lambda_7^* + iv_{2I}^2 v_{2R} \lambda_7^* + v_{2I} v_{2R}^2 \lambda_7^* + iv_{2R}^3 \lambda_7^* - 2v_{2I}\left(m_{12}^2\right)^* - 2iv_{2R}\left(m_{12}^2\right)^*
\end{aligned} \tag{B.2}
$$

$$
0 \stackrel{!}{=} \frac{\partial V_{\text{tree}}}{\partial \varphi_7} \quad \propto \quad 2im_{12}^2 v_{1I} - i\lambda_6 v_{1I}^3 - 2m_{12}^2 v_{1R} + \lambda_6 v_{1I}^2 v_{1R} - i\lambda_6 v_{1I} v_{1R}^2 + \lambda_6 v_{1R}^3 - i\lambda_5 v_{1I}^2 v_{2I} +
$$

$$
\begin{aligned}
&+2\lambda_5 v_{1I} v_{1R} v_{2I} + i\lambda_5 v_{1R}^2 v_{2I} - i\lambda_7 v_{1I} v_{2I}^2 + \lambda_7 v_{1R} v_{2I}^2 + 4m_{22}^2 v_{2R} + 2\lambda_3 v_{1I}^2 v_{2R} + \\
&+2\lambda_4 v_{1I}^2 v_{2R} - \lambda_5 v_{1I}^2 v_{2R} - 2i\lambda_5 v_{1I} v_{1R} v_{2R} + 2\lambda_3 v_{1R}^2 v_{2R} + 2\lambda_4 v_{1R}^2 v_{2R} + \lambda_5 v_{1R}^2 v_{2R} + \\
&+2\lambda_7 v_{1I} v_{2I} v_{2R} + 2i\lambda_7 v_{1R} v_{2I} v_{2R} + 2\lambda_2 v_{2I}^2 v_{2R} - 3i\lambda_7 v_{1I} v_{2R}^2 + 3\lambda_7 v_{1R} v_{2R}^2 + 2\lambda_2 v_{2R}^3 + \\
&+i\left(v_{1I} - iv_{1R}\right)^2 \left(v_{2I} + iv_{2R}\right) \lambda_5^* + i\left(v_{1I} - iv_{1R}\right)^2 \left(v_{1I} + iv_{1R}\right) \lambda_6^* + iv_{1I} v_{2I}^2 \lambda_7^* + \\
&+v_{1R} v_{2I}^2 \lambda_7^* + 2v_{1I} v_{2I} v_{2R} \lambda_7^* - 2iv_{1R} v_{2I} v_{2R} \lambda_7^* + 3iv_{1I} v_{2R}^2 \lambda_7^* + 3v_{1R} v_{2R}^2 \lambda_7^* + \\
&-2iv_{1I} \left(m_{12}^2\right)^* - 2v_{1R} \left(m_{12}^2\right)^*
\end{aligned} \tag{B.3}
$$

$$
\begin{aligned}
0 \stackrel{!}{=} \frac{\partial V_{\text{tree}}}{\partial \varphi_8} \quad \propto \quad & -2m_{12}^2 v_{1I} + \lambda_6 v_{1I}^3 - 2im_{12}^2 v_{1R} + i\lambda_6 v_{1I}^2 v_{1R} + \lambda_6 v_{1I} v_{1R}^2 + i\lambda_6 v_{1R}^3 + 4m_{22}^2 v_{2I} + \\
&+2\lambda_3 v_{1I}^2 v_{2I} + 2\lambda_4 v_{1I}^2 v_{2I} + \lambda_5 v_{1I}^2 v_{2I} + 2i\lambda_5 v_{1I} v_{1R} v_{2I} + 2\lambda_3 v_{1R}^2 v_{2I} + 2\lambda_4 v_{1R}^2 v_{2I} + \\
&-\lambda_5 v_{1R}^2 v_{2I} + 3\lambda_7 v_{1I} v_{2I}^2 + 3i\lambda_7 v_{1R} v_{2I}^2 + 2\lambda_2 v_{2I}^3 - i\lambda_5 v_{1I}^2 v_{2R} + 2\lambda_5 v_{1I} v_{1R} v_{2R} + \\
&+i\lambda_5 v_{1R}^2 v_{2R} - 2i\lambda_7 v_{1I} v_{2I} v_{2R} + 2\lambda_7 v_{1R} v_{2I} v_{2R} + \lambda_7 v_{1I} v_{2R}^2 + i\lambda_7 v_{1R} v_{2R}^2 + \\
&+2\lambda_2 v_{2I} v_{2R}^2 + (v_{1I} - iv_{1R})^2 (v_{2I} + iv_{2R}) \lambda_5^* + (v_{1I} - iv_{1R})^2 (v_{1I} + iv_{1R}) \lambda_6^* + \\
&+3v_{1I} v_{2I}^2 \lambda_7^* - 3iv_{1R} v_{2I}^2 \lambda_7^* + 2iv_{1I} v_{2I} v_{2R} \lambda_7^* + 2v_{1R} v_{2I} v_{2R} \lambda_7^* + v_{1I} v_{2R}^2 \lambda_7^* + \\
&-iv_{1R} v_{2R}^2 \lambda_7^* - 2v_{1I} \left(m_{12}^2\right)^* + 2iv_{1R} \left(m_{12}^2\right)^*
\end{aligned} \tag{B.4}
$$

These can be solved to yield Eqs. (2.11)-(2.13) in Sec. 2.2.2 [9].

C Relations between potential parameters in the general basis and those in the Higgs bases

In this appendix, the relations between the parameters in the general basis (see, e.g., Eq. (2.3)) and those in the Higgs bases (see, e.g., Eq. (2.7)) are given explicitly. The relations are, with $\xi = \xi_2 - \xi_1$ and $\lambda_{345} = \lambda_3 + \lambda_4 + \Re\left(\lambda_5 e^{2i\xi}\right)$, [7]

$$
\Lambda_1 = \lambda_1 c_\beta^4 + \lambda_2 s_\beta^4 + \frac{1}{2}\lambda_{345} s_{2\beta}^2 + 2s_{2\beta}\left[c_\beta^2 \Re\left(\lambda_6 e^{i\xi}\right) + s_\beta^2 \Re\left(\lambda_7 e^{i\xi}\right)\right] \tag{C.1}
$$

$$
\Lambda_2 = \lambda_1 s_\beta^4 + \lambda_2 c_\beta^4 + \frac{1}{2}\lambda_{345} s_{2\beta}^2 - 2s_{2\beta}\left[s_\beta^2 \Re\left(\lambda_6 e^{i\xi}\right) + c_\beta^2 \Re\left(\lambda_7 e^{i\xi}\right)\right] \tag{C.2}
$$

$$
\Lambda_3 = \frac{1}{4} s_{2\beta}^2 \left(\lambda_1 + \lambda_2 - 2\lambda_{345}\right) + \lambda_3 - s_{2\beta} c_{2\beta} \Re\left[\left(\lambda_6 - \lambda_7\right) e^{i\xi}\right] \tag{C.3}
$$

$$
\Lambda_4 = \frac{1}{4} s_{2\beta}^2 \left(\lambda_1 + \lambda_2 - 2\lambda_{345}\right) + \lambda_4 - s_{2\beta} c_{2\beta} \Re\left[\left(\lambda_6 - \lambda_7\right) e^{i\xi}\right] \tag{C.4}
$$

$$
\begin{aligned}
\Lambda_5 e^{2i(\xi - 2\gamma)} \quad = \quad & \frac{1}{4} s_{2\beta}^2 \left(\lambda_1 + \lambda_2 - 2\lambda_{345}\right) + \Re\left(\lambda_5 e^{2i\xi}\right) + ic_{2\beta} \Im\left(\lambda_5 e^{2i\xi}\right) + \\
& - s_{2\beta} c_{2\beta} \Re\left[\left(\lambda_6 - \lambda_7\right) e^{i\xi}\right] - is_{2\beta} \Re\left[\left(\lambda_6 - \lambda_7\right) e^{i\xi}\right]
\end{aligned} \tag{C.5}
$$

$$\Lambda_6 e^{i(\xi-2\gamma)} = -\frac{1}{2}s_{2\beta}\left[\lambda_1 c_\beta^2 - \lambda_2 s_\beta^2 - \lambda_{345}c_{2\beta} - i\Im\left(\lambda_5 e^{2i\xi}\right)\right] + c_\beta c_{3\beta}\Re\left(\lambda_6 e^{i\xi}\right) + \\ + s_\beta s_{3\beta}\Re\left(\lambda_7 e^{i\xi}\right) + ic_\beta^2\Im\left(\lambda_6 e^{i\xi}\right) + is_\beta^2\Im\left(\lambda_7 e^{i\xi}\right) \quad \text{(C.6)}$$

$$\Lambda_7 e^{i(\xi-2\gamma)} = -\frac{1}{2}s_{2\beta}\left[\lambda_1 s_\beta^2 - \lambda_2 c_\beta^2 + \lambda_{345}c_{2\beta} + i\Im\left(\lambda_5 e^{2i\xi}\right)\right] + s_\beta s_{3\beta}\Re\left(\lambda_6 e^{i\xi}\right) + \\ + c_\beta c_{3\beta}\Re\left(\lambda_7 e^{i\xi}\right) + is_\beta^2\Im\left(\lambda_6 e^{i\xi}\right) + ic_\beta^2\Im\left(\lambda_7 e^{i\xi}\right) \quad \text{(C.7)}$$

$$M_{11}^2 = m_{11}^2 c_\beta^2 + m_{22}^2 s_\beta^2 - \Re\left(m_{12}^2 e^{i\xi}\right) s_{2\beta} \quad \text{(C.8)}$$

$$M_{22}^2 = m_{11}^2 s_\beta^2 + m_{22}^2 c_\beta^2 + \Re\left(m_{12}^2 e^{i\xi}\right) s_{2\beta} \quad \text{(C.9)}$$

$$M_{12}^2 e^{i(\xi-2\gamma)} = \frac{1}{2}\left(m_{11}^2 - m_{22}^2\right) s_{2\beta} + c_{2\beta}\Re\left(m_{12}^2 e^{i\xi}\right) + i\Im\left(m_{12}^2 e^{i\xi}\right) \quad \text{(C.10)}$$

These relations are easily inverted to give the general basis' parameters as functions of the Higgs bases' parameters: simply replace parameters in Eqs. (C.1)-(C.10) as $\Lambda_i \leftrightarrow \lambda_i$, $M_{ij}^2 \leftrightarrow m_{ij}^2$, $\beta \leftrightarrow -\beta$ and $\xi \leftrightarrow \xi - 2\gamma$.

D Scalar masses in $\mathcal{CP}$ violating 2HDMs

The eigenvalues of the 3×3 matrix $\tilde{\mathcal{M}}_3^2$ (see Eq. (2.16)) can be found by solving the characteristic equation $\left|\tilde{\mathcal{M}}_3^2 - m^2\mathbb{1}\right| = 0$, where m^2 is an eigenvalue. This is equivalent to solving a third degree polynomial equation, namely

$$0 = -\left(m^2\right)^3 + \frac{1}{4}\Big[8M_{22}^2 + 4\Lambda_1 v^2 + 4\Lambda_3 v^2 + 4\Lambda_4 v^2\Big]\left(m^2\right)^2 + \frac{1}{4}\Big[-4M_{22}^4 - 8\Lambda_1 M_{22}^2 v^2 + \\ -4\Lambda_3 M_{22}^2 v^2 - 4\Lambda_4 M_{22}^2 v^2 + \Im\left(\Lambda_5\right)^2 v^4 + 4\Im\left(\Lambda_6\right)^2 v^4 - 4\Lambda_1\Lambda_3 v^4 - \Lambda_3^2 v^4 + \\ -4\Lambda_1\Lambda_4 v^4 - 2\Lambda_3\Lambda_4 v^4 - \Lambda_4^2 v^4 + \Re\left(\Lambda_5\right)^2 v^4 + 4\Re\left(\Lambda_6\right)^2 v^4\Big] m^2 + \frac{1}{4}\Big[4\Lambda_1 M_{22}^4 v^2 + \\ -4\Im\left(\Lambda_6\right)^2 M_{22}^2 v^4 + 4\Lambda_1\Lambda_3 M_{22}^2 v^4 + 4\Lambda_1\Lambda_4 M_{22}^2 v^4 - 4M_{22}^2\Re\left(\Lambda_6\right)^2 v^4 - \Im\left(\Lambda_5\right)^2\Lambda_1 v^6 \\ -2\Im\left(\Lambda_6\right)^2\Lambda_3 v^6 + \Lambda_1\Lambda_3^2 v^6 - 2\Im\left(\Lambda_6\right)^2\Lambda_4 v^6 + 2\Lambda_1\Lambda_3\Lambda_4 v^6 + \Lambda_1\Lambda_4^2 v^6 \\ -2\Im\left(\Lambda_6\right)^2\Re\left(\Lambda_5\right) v^6 - \Lambda_1\Re\left(\Lambda_5\right)^2 v^6 + 4\Im\left(\Lambda_5\right)\Im\left(\Lambda_6\right)\Re\left(\Lambda_6\right) v^6 - 2\Lambda_3\Re\left(\Lambda_6\right)^2 v^6 \\ -2\Lambda_4\Re\left(\Lambda_6\right)^2 v^6 + 2\Re\left(\Lambda_5\right)\Re\left(\Lambda_6\right)^2 v^6\Big] \equiv a\left(m^2\right)^3 + b\left(m^2\right)^2 + c\,m^2 + d \quad \text{(D.1)}$$

where coefficients a, b, c and d have been defined. The solutions to this equation are the squared masses of the neutral scalars, $\tilde{m}_1^2$, $\tilde{m}_2^2$ and $\tilde{m}_3^2$ (note that it is not possible to define

an order relation at this stage, so here no reference is made to the ordered masses $m^2_{h_1}$, $m^2_{h_2}$ or $m^2_{h_3}$). The solutions are

$$\tilde{m}_1^2 = -\frac{b}{3a} - \frac{2^{1/3}\left(-b^2+3ac\right)}{3a\left(-2b^3+9abc-27a^2d+\sqrt{4\left(-b^2+3ac\right)^3+\left(-2b^3+9abc-27a^2d\right)^2}\right)^{1/3}} + \\ + \frac{2^{-1/3}\left(-2b^3+9abc-27a^2d+\sqrt{4\left(-b^2+3ac\right)^3+\left(-2b^3+9abc-27a^2d\right)^2}\right)^{1/3}}{3a} \quad \text{(D.2)}$$

$$\tilde{m}_2^2 = -\frac{b}{3a} - \frac{2^{-2/3}\left(1+i\sqrt{3}\right)\left(-b^2+3ac\right)}{3a\left(-2b^3+9abc-27a^2d+\sqrt{4\left(-b^2+3ac\right)^3+\left(-2b^3+9abc-27a^2d\right)^2}\right)^{1/3}} + \\ + \frac{2^{-4/3}\left(-2b^3+9abc-27a^2d+\sqrt{4\left(-b^2+3ac\right)^3+\left(-2b^3+9abc-27a^2d\right)^2}\right)^{1/3}}{3a} \quad \text{(D.3)}$$

$$\tilde{m}_3^2 = -\frac{b}{3a} - \frac{2^{-2/3}\left(1-i\sqrt{3}\right)\left(-b^2+3ac\right)}{3a\left(-2b^3+9abc-27a^2d+\sqrt{4\left(-b^2+3ac\right)^3+\left(-2b^3+9abc-27a^2d\right)^2}\right)^{1/3}} + \\ + \frac{2^{-4/3}\left(-2b^3+9abc-27a^2d+\sqrt{4\left(-b^2+3ac\right)^3+\left(-2b^3+9abc-27a^2d\right)^2}\right)^{1/3}}{3a} \quad \text{(D.4)}$$

From the above expressions, which are already quite lengthy, it is obvious that their corresponding forms in the general basis (which can be found by using the transformations in App. C) will be a lot messier, thus validating the comment about the convenience of the Higgs bases in Sec. 2.2.1.

E Oblique parameters

Here, the exact expressions for the oblique parameters S, T, U, V, W and X are presented. Letting $\tilde{R} = R_3^T$ (i.e., the rotation matrix from Eq. (2.17)), the parameters are given by [4], with the physical neutral Higgs particles' masses $m_{h_i} = m_i$, $m_{h_{SM}} = 125$ GeV is the mass of the SM Higgs boson, $\cos\theta_W = c_W$ and $\sin\theta_W = s_W$,

$$S = \frac{1}{24\pi}\left\{\left(s_W^2-c_W^2\right)^2 G\left(z_+,\, z_+\right) + \tilde{R}_{11}^2 G\left(z_2,\, z_3\right) + \tilde{R}_{12}^2 G\left(z_3,\, z_1\right) + \tilde{R}_{13}^2 G\left(z_1,\, z_2\right) +\right.$$

$$+\sum_{j=1}^{3}\left[\tilde{R}_{1j}^{2}\hat{G}\left(z_{j}\right)+\ln\frac{m_{h_{SM}}^{2}}{m_{H^{\pm}}^{2}}\right]-\hat{G}\left(z_{h_{SM}}\right)-\ln\frac{m_{h_{SM}}^{2}}{m_{H^{\pm}}^{2}}\Bigg\} \tag{E.5}$$

$$\begin{aligned}T &= \frac{1}{16\pi s_{W}^{2}m_{W}^{2}}\Bigg\{\sum_{j=1}^{3}\left(1-\tilde{R}_{1j}^{2}\right)F\left(m_{H^{\pm}}^{2},\, m_{j}^{2}\right)-\tilde{R}_{11}^{2}F\left(m_{2}^{2},\, m_{3}^{2}\right)+\\ &-\tilde{R}_{12}^{2}F\left(m_{3}^{2},\, m_{1}^{2}\right)-\tilde{R}_{13}^{2}F\left(m_{1}^{2},\, m_{2}^{2}\right)+3\sum_{j=1}^{3}\tilde{R}_{1j}^{2}\left[F\left(m_{Z}^{2},\, m_{j}^{2}\right)-F\left(m_{W}^{2},\, m_{j}^{2}\right)\right]+\\ &-3\left[F\left(m_{Z}^{2},\, m_{h_{SM}}^{2}\right)-F\left(m_{W}^{2},\, m_{h_{SM}}^{2}\right)\right]\Bigg\}\end{aligned} \tag{E.6}$$

$$\begin{aligned}U &= \frac{1}{24\pi}\Bigg\{\sum_{j=1}^{3}\left(1-\tilde{R}_{1j}^{2}\right)G\left(w_{+},\, w_{j}\right)-\left(s_{W}^{2}-c_{W}^{2}\right)^{2}G\left(z_{+},\, z_{+}\right)-\tilde{R}_{11}^{2}G\left(z_{2},\, z_{3}\right)+\\ &-\tilde{R}_{12}^{2}G\left(z_{3},\, z_{1}\right)-\tilde{R}_{13}^{2}G\left(z_{1},\, z_{2}\right)+\sum_{j=1}^{3}\tilde{R}_{1j}^{2}\left[\hat{G}\left(w_{j}\right)-\hat{G}\left(z_{j}\right)\right]-\hat{G}\left(w_{h_{SM}}\right)+\hat{G}\left(z_{h_{SM}}\right)\Bigg\}\end{aligned} \tag{E.7}$$

$$\begin{aligned}V &= \frac{1}{96\pi c_{W}^{2}s_{W}^{2}}\Big[\left(s_{W}^{2}-c_{W}^{2}\right)^{2}H\left(z_{+},\, z_{+}\right)+\tilde{R}_{11}^{2}H\left(z_{2},\, z_{3}\right)+\tilde{R}_{12}^{2}H\left(z_{3},\, z_{1}\right)+\tilde{R}_{13}^{2}H\left(z_{1},\, z_{2}\right)+\\ &+\sum_{j=1}^{3}\tilde{R}_{1j}^{2}\hat{H}\left(z_{j}\right)-\hat{H}\left(z_{h_{SM}}\right)\Big]\end{aligned} \tag{E.8}$$

$$W=\frac{1}{96\pi s_{W}^{2}}\left[\sum_{j=1}^{3}\left(1-\tilde{R}_{1j}^{2}\right)H\left(w_{+},\, w_{j}\right)+\sum_{j=1}^{3}\tilde{R}_{1j}^{2}\hat{H}\left(w_{j}\right)-\hat{H}\left(w_{h_{SM}}\right)\right] \tag{E.9}$$

$$X=\frac{c_{W}^{2}-s_{W}^{2}}{48\pi}G\left(z_{+},\, z_{+}\right) \tag{E.10}$$

where

$$F\left(x,\, y\right)=\begin{cases}\frac{x+y}{2}-\frac{xy}{x-y}\ln\frac{x}{y}, & x\neq y\\ 0, & x=y\end{cases} \tag{E.11}$$

$$\begin{aligned}G(x,\, y) &= -\frac{16}{3}+5(x+y)-2(x-y)^{2}+3\left[\frac{x^{2}+y^{2}}{x-y}-x^{2}+y^{2}+\frac{(x-y)^{3}}{3}\right]\ln\frac{x}{y}+\\ &+\left[1-2(x+y)+(x-y)^{2}\right]f\left(x+y-1,\, 1-2(x+y)+(x-y)^{2}\right)\end{aligned} \tag{E.12}$$

$$f\left(z,\,w\right)=\begin{cases}\sqrt{w}\ln\left|\frac{z-\sqrt{w}}{z+\sqrt{w}}\right|, & w>0\\ 0, & w=0\\ \sqrt{-w}\arctan\frac{\sqrt{-w}}{z}, & w<0\end{cases} \tag{E.13}$$

$$z_a=\frac{m_a^2}{m_Z^2},\;\; w_a=\frac{m_a^2}{m_W^2},\;\; a\in\{+,\,1,\,2,\,3,\,h_{SM}\} \tag{E.14}$$

$$\begin{aligned}H\left(x,\,y\right) &= 2-9(x+y)+6(x-y)^2+3\left[-\frac{x^2+y^2}{x-y}+2\left(x^2-y^2\right)-(x-y)^3\right]\ln\frac{x}{y}+\\ &\quad +3\left[x+y-(x-y)^2\right]f\left(x+y-1,\,1-2(x+y)+(x-y)^2\right)\end{aligned} \tag{E.15}$$

$$\begin{aligned}\hat{H}(x) &= 47-21x+6x^2+3\left(7-12x+5x^2-x^3-3\frac{x+1}{x-1}\right)\ln x+\\ &\quad +3\left(28-20x+7x^2-x^3\right)\frac{f\left(x,\,x^2-4x\right)}{x-4}\end{aligned} \tag{E.16}$$

F Electric dipole moments

As is discussed in [29], searches for EDMs of the electron, neutron, mercury and radium can be used to constrain the $\mathcal{CP}$ violating angles in 2HDMs. In particular, they constrain the angle α_b in the general basis (see Sec. 5.2.2) even though it might be better to constrain the actual physical $\mathcal{CP}$ violating angles α_1, α_2 and α_3 defined in Sec. 2.2.3. Everything below follows closely the material presented in [29].

The dipole moments are given by $\mathcal{T}$ and $\mathcal{P}$ violating low energy effective operators and the corresponding Lagrangian for fermions can be written

$$\mathcal{L}_f^{eff}=e\sum_f\frac{\delta_f}{\Lambda_{NP}^2}m_f\overline{f}i\gamma_5 f F^{\mu\nu} \tag{F.17}$$

where Λ_{NP} is the scale of new physics beyond the SM and δ_f is a rescaled version of a fermion EDM. δ_f can be calculated from 2-loop Barr-Zee diagrams (see fig. 21) and for the electron it is given by

$$\delta_e=(\delta_e)_t^{h\gamma\gamma}+(\delta_e)_t^{hZ\gamma}+(\delta_e)_W^{h\gamma\gamma}+(\delta_e)_W^{hZ\gamma}+(\delta_e)_{H^+}^{h\gamma\gamma}+(\delta_e)_{H^+}^{hZ\gamma}+(\delta_e)_{H^+}^{HW\gamma} \tag{F.18}$$

where, e.g., the top contribution in the $h\gamma\gamma$ channel is given by

$$(\delta_e)_t^{h\gamma\gamma}=-N_C Q_e Q_t e^2\frac{1}{64\pi^2}\sum_{i=1}^{3}\left[f\left(z_t^i\right)c_{t,i}\tilde{c}_{e,i}+g\left(z_t^i\right)\tilde{c}_{t,i}c_{e,i}\right] \tag{F.19}$$

and $c_{f,i}$ and $\tilde{c}_{f,i}$ are defined as in Sec. 5.2.2, $z_t^i=m_t^2/m_{h_i}^2$ and f as well as g are loop functions. Similar results hold for also other particles.

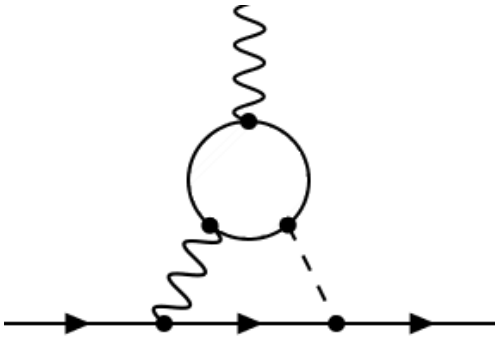

Figure 21: A Barr-Zee diagram.

References

[1] D. S. Gorbunov and V. A. Rubakov, *Introduction to the Theory of the Early Universe: Hot Big Bang Theory*. World Scientific, 2011.

[2] G. C. Dorsch, S. J. Huber and J. M. No, *A strong electroweak phase transition in the 2HDM after LHC8*, *JHEP* **10** (2013) 029, [hep-ph/1305.6610].

[3] CMS collaboration, S. Chatrchyan et al., *Observation of a new boson at a mass of 125 GeV with the CMS experiment at the LHC*, *Phys. Lett.* **B716** (2012) 30–61, [hep-ph/1207.7235].

[4] G. C. Branco, P. M. Ferreira, L. Lavoura, M. N. Rebelo, M. Sher and J. P. Silva, *Theory and phenomenology of two-Higgs-doublet models*, *Phys. Rept.* **516** (2012) 1–102, [hep-ph/1106.0034].

[5] D. E. Morrissey and M. J. Ramsey-Musolf, *Electroweak baryogenesis*, *New J. Phys.* **14** (2012) 125003, [hep-ph/1206.2942].

[6] G. D. Moore, *Measuring the broken phase sphaleron rate nonperturbatively*, *Phys. Rev.* **D59** (1999) 014503, [hep-ph/9805264].

[7] S. Davidson and H. E. Haber, *Basis-independent methods for the two-Higgs-doublet model*, *Phys. Rev.* **D72** (2005) 035004, [hep-ph/0504050].

[8] J. E. Camargo-Molina, B. O'Leary, W. Porod and F. Staub, `Vevacious`*: A Tool For Finding The Global Minima Of One-Loop Effective Potentials With Many Scalars*, *Eur. Phys. J.* **C73** (2013) 2588, [hep-ph/1307.1477].

[9] I. F. Ginzburg and M. Krawczyk, *Symmetries of two Higgs doublet model and CP violation*, *Phys. Rev.* **D72** (2005) 115013, [hep-ph/0408011].

[10] D. Fontes, J. C. Romão, R. Santos and J. P. Silva, *Large pseudoscalar Yukawa couplings in the complex 2HDM*, *JHEP* **06** (2015) 060, [hep-ph/1502.01720].

[11] A. W. El Kaffas, P. Osland and O. M. Ogreid, *CP violation, stability and unitarity of the two Higgs doublet model*, *Nonlin. Phenom. Complex Syst.* **10** (2007) 347–357, [hep-ph/0702097].

[12] J. F. Gunion and H. E. Haber, *The CP conserving two Higgs doublet model: The Approach to the decoupling limit*, *Phys. Rev.* **D67** (2003) 075019, [hep-ph/0207010].

[13] J. Bijnens, J. Lu and J. Rathsman, *Constraining General Two Higgs Doublet Models by the Evolution of Yukawa Couplings*, *JHEP* **05** (2012) 118, [hep-ph/1111.5760].

[14] S. L. Glashow and S. Weinberg, *Natural conservation laws for neutral currents*, *Phys. Rev. D* **15** (1977) 1958–1965.

[15] M. E. Peskin and D. V. Schroeder, *An Introduction to Quantum Field Theory*. Westview Press, 1995.

[16] M. Quiros, *Finite temperature field theory and phase transitions*, in *High energy physics and cosmology. Proceedings, Summer School, Trieste, Italy, June 29-July 17, 1998*, pp. 187–259, 1999. hep-ph/9901312.

[17] J. M. Cline, K. Kainulainen and M. Trott, *Electroweak Baryogenesis in Two Higgs Doublet Models and B meson anomalies*, *JHEP* **11** (2011) 089, [hep-ph/1107.3559].

[18] S. P. Martin, *Two loop effective potential for a general renormalizable theory and softly broken supersymmetry*, *Phys. Rev.* **D65** (2002) 116003, [hep-ph/0111209].

[19] M. Maniatis, A. von Manteuffel, O. Nachtmann and F. Nagel, *Stability and symmetry breaking in the general two-Higgs-doublet model*, *Eur. Phys. J.* **C48** (2006) 805–823, [hep-ph/0605184].

[20] I. P. Ivanov and J. P. Silva, *Tree-level metastability bounds for the most general two Higgs doublet model*, *Phys. Rev.* **D92** (2015) 055017, [hep-ph/1507.05100].

[21] I. P. Ivanov, *Minkowski space structure of the Higgs potential in 2HDM*, *Phys. Rev.* **D75** (2007) 035001, [hep-ph/0609018].

[22] I. F. Ginzburg and I. P. Ivanov, *Tree-level unitarity constraints in the most general 2HDM*, *Phys. Rev.* **D72** (2005) 115010, [hep-ph/0508020].

[23] D. Eriksson, J. Rathsman and O. Stal, 2HDMC*: Two-Higgs-Doublet Model Calculator Physics and Manual*, *Comput. Phys. Commun.* **181** (2010) 189–205, [hep-ph/0902.0851].

[24] H. E. Haber and D. O'Neil, *Basis-independent methods for the two-Higgs-doublet model. II. The Significance of tan beta*, *Phys. Rev.* **D74** (2006) 015018, [hep-ph/0602242].

[25] Particle Data Group collaboration, K. A. Olive et al., *Review of Particle Physics*, *Chin. Phys.* **C38** (2014) 090001.

[26] W. Grimus, L. Lavoura, O. M. Ogreid and P. Osland, *The Oblique parameters in multi-Higgs-doublet models*, *Nucl. Phys.* **B801** (2008) 81–96, [hep-ph/0802.4353].

[27] R. Enberg, J. Rathsman and G. Wouda, *Higgs phenomenology in the Stealth Doublet Model*, *Phys. Rev.* **D91** (2015) 095002, [hep-ph/1311.4367].

[28] F. Mahmoudi and O. Stal, *Flavor constraints on the two-Higgs-doublet model with general Yukawa couplings*, *Phys. Rev.* **D81** (2010) 035016, [hep-ph/0907.1791].

[29] S. Inoue, M. J. Ramsey-Musolf and Y. Zhang, *CP-violating phenomenology of flavor conserving two Higgs doublet models*, *Phys. Rev.* **D89** (2014) 115023, [hep-ph/1403.4257].

[30] ACME collaboration, J. Baron et al., *Order of Magnitude Smaller Limit on the Electric Dipole Moment of the Electron*, *Science* **343** (2014) 269–272, [physics.atom-ph/1310.7534].

[31] P. Z. Skands et al., *SUSY Les Houches accord: Interfacing SUSY spectrum calculators, decay packages, and event generators*, *JHEP* **07** (2004) 036, [hep-ph/0311123].

[32] F. Staub, SARAH, hep-ph/0806.0538.

[33] P. Bechtle, O. Brein, S. Heinemeyer, G. Weiglein and K. E. Williams, HiggsBounds*: Confronting Arbitrary Higgs Sectors with Exclusion Bounds from LEP and the Tevatron*, *Comput. Phys. Commun.* **181** (2010) 138–167, [hep-ph/0811.4169].

[34] P. Bechtle, S. Heinemeyer, O. Stål, T. Stefaniak and G. Weiglein, HiggsSignals*: Confronting arbitrary Higgs sectors with measurements at the Tevatron and the LHC*, *Eur. Phys. J.* **C74** (2014) 2711, [hep-ph/1305.1933].

[35] I. Antcheva et al., ROOT*: A C++ framework for petabyte data storage, statistical analysis and visualization*, *Comput. Phys. Commun.* **180** (2009) 2499–2512, [physics.data-an/1508.07749].

[36] H. E. Haber and O. Stål, *New LHC benchmarks for the $\mathcal{CP}$ -conserving two-Higgs-doublet model*, *Eur. Phys. J.* **C75** (2015) 491, [hep-ph/1507.04281].

[37] C. D. Froggatt, *The Fermion mass problem*, in *Perspectives in particle physics '94. Proceedings, 7th Adriatic Meeting, Brijuni, Croatia, September 13-20, 1994*, 1994. hep-ph/9504323.